Institut für Nutzpflanzenwissenschaften und Ressourcenschutz (INRES)
Fachbereich Pflanzen- und Gartenbauwissenschaften

Potential of fluorescence techniques with special reference to fluorescence lifetime determination for sensing and differentiating biotic and abiotic stresses in *Triticum aestivum* L.

I n a u g u r a l - D i s s e r t a t i o n

zur

Erlangung des Grades

Doktor der Agrarwissenschaften

(Dr. agr.)

der

Hohen Landwirtschaftlichen Fakultät

der

Rheinischen Friedrich-Wilhelms-Universität

zu Bonn

vorgelegt am 09.12.2010

von

Dipl.-Ing. agr. Kathrin Bürling

aus

Bonn-Bad Godesberg

Referent:	Prof. Dr. Georg Noga
Korreferent 1:	PD Dr. Erich-Christian Oerke
Korreferent 2:	PD Dr. Uwe Rascher
Tag der mündlichen Prüfung:	07.07.2011
Erscheinungsjahr:	2011

Potential of fluorescence techniques with special reference to fluorescence lifetime determination for sensing and differentiating biotic and abiotic stresses in *Triticum aestivum* L.

The key objective of the present thesis was to early assess physiological modifications of wheat plants due to biotic and abiotic stresses by means of non-destructive fluorescence measurement techniques. Experiments at leaf level were conducted under laboratory conditions, whereupon two economical important biotrophic fungi in wheat production, *Puccinia triticina* and *Blumeria graminis*, as well as nitrogen deficiency as the most significant factor in terms of nutrient management, were selected for representative studies. The first chapter addressed the hypothesis that the PAM-fluorescence imaging technique enables a discrimination of susceptible and resistant wheat (*Triticum aestivum* L.) cultivars to the leaf rust pathogen *P. triticina*. Two inoculation methods under consideration of the spore density were tested in order to evaluate the responses of the genotypes on the basis of fluorescence readings. Furthermore, the masking effect of fungal inoculum on chlorophyll fluorescence parameters was assessed. With the purpose of cultivar differentiation, the UV-induced fluorescence spectra between 350 and 820 nm and the lifetime of fluorophores at selected wavelengths were examined. Similar studies aiming at the early detection and differentiation of genotypes having distinct resistance degrees to powdery mildew (*B. graminis*) were conducted. In a last step, the challenge of the differentiation between stresses caused by pathogen infection (*P. triticina* or *B. graminis*) and N-deficiency occurring simultaneously was highlighted by UV-induced fluorescence spectral measurements. The results obtained and outlined in the single chapters can be summarized as follows:

1. Experiments with the PAM-imaging system showed that the quantum yield of non-regulated energy dissipation in PSII (Y(NO)) is the most promising parameter for screening wheat plants for leaf rust resistance. Measurements revealed a stronger pathogen-triggered increase of the Y(NO) values in the susceptible than in the resistant cultivar. Thereby, the most appropriate time for a reliable differentiation between was two days after inoculation. Preliminary experiments with densities of up to 20 000 spores per ml in case of fast fluorescence kinetic parameters, and up to 100 000 spores per ml in case of slow kinetic parameters, revealed that changes in the fluorescence signals were not related to physical masking.

2. The assessment of fluorescence lifetime and UV-induced spectra were adopted for the detection of leaf rust (*Puccinia triticina*) in three resistant in comparison to four susceptible cultivars. A combination of spectral and lifetime characteristics revealed pre-symptomatic alterations of fluorescence indicating changes in the content of chlorophyll and secondary metabolites. The determination of the B/G amplitude ratio seemed to be the most appropriate parameter for early detection of fungal infection. Discrimination between resistant and susceptible cultivars to the leaf rust pathogen might be feasible by monitoring the amplitude ratio of B/R fluorescence at three days after inoculation. In addition, mean lifetime at 440, 500 and 530 nm should be considered; these parameters revealed a more pronounced difference between control and inoculated leaves in the resistant cultivars.

3. UV-induced spectral signature as well as mean fluorescence lifetimes are suitable approaches for sensing powdery mildew (*Blumeria graminis*) as early as one day after inoculation. The decreased amplitude ratio B/G as well as the increased G/R and G/FR half-bandwidth ratios in inoculated as compared to control leaves, were appropriate parameters to detect fungal development. In addition, the increased mean lifetime in inoculated leaves in the wavelength range of 500-620 nm may enable a distinction between healthy and diseased leaves. Additional experiments revealed an increased mean lifetime of the green fluorescence as early as ten to twelve hours after the first host-pathogen interaction.

4. Fluorescence intensity measured between 370 and 800 nm provided to be a useful tool to address the challenge of discrimination between nitrogen deficiency and fungal diseases. Precisely, the amplitude ratio R/FR was suited for early detection, and gives a basis for discrimination between N-full-supply, N-deficiency, N-full-supply + pathogen and N-deficiency + pathogen. In addition, the blue-green fluorescence yielded important information targeting a possible discrimination between the evaluated multiple stress factors. Besides, several more fluorescence amplitude ratios and half-bandwidth ratios for leaf rust as well as half-bandwidth ratios for powdery mildew were found to be applicable for early detection of both leaf rust and powdery mildew infection, irrespective of the nitrogen status of the plants.

Potenzial von Fluoreszenztechniken unter besonderer Berücksichtigung der Fluoreszenzlebenszeit-Bestimmung zur Erfassung und Differenzierung biotischen und abiotischen Stresses in *Triticum aestivum* L.

Zielsetzung dieser Arbeit war es, mittels Fluoreszenz-Messtechniken am Beispiel von Weizenpflanzen die durch biotischen und abiotischen Stresss induzierten physiologischen Veränderungen zu ermitteln. Die Versuche wurden unter Laborbedingungen auf Blattebene durchgeführt, wobei zum einen zwei ökonomisch bedeutende biotrophe, pilzliche Erreger des Weizenanbaus, *Puccina triticina* und *Blumeria graminis*, sowie zum anderen Stickstoffmangel als bedeutendster Vertreter des Nährstoffmanagements, für repräsentative Studien ausgewählt wurden. Das erste Kapitel adressiert die Hypothese, dass mit der PAM-Fluoreszenz-Imaging Technik eine Unterscheidung zwischen Braunrost (*P. triticina*)-anfälligen und -resistenten Weizensorten (*Triticum aestivum* L.) möglich ist. Unter Berücksichtigung der Sporendichte wurden hierzu zwei Inokulationsmethoden mit der Zielsetzung getestet, eine Differenzierung der Genotypen auf Basis der gewonnenen Fluoreszenzdaten vorzunehmen. Des Weiteren wurde ein möglicher maskierender Effekt des pilzlichen Inokulums auf die Chlorophyllfluoreszenz-Parameter geprüft. Mit dem Ziel der Sortenunterscheidung wurden UV-induzierte Fluoreszenz-Spektren (FS) von 350-820 nm sowie die Fluoreszenz-Lebenszeit (FL) bei ausgewählten Wellenlängen bewertet. Vergleichbare Studien wurden zur frühzeitigen Erkennung und Differenzierung von Genotypen mit unterschiedlichen Resistenzgraden gegenüber Echtem Mehltau (*B. graminis*) durchgeführt. Eine Herausforderung stellte letztlich die Differenzierung zwischen zeitgleichem Auftreten eines Pathogenbefalls (*P. triticina* oder *B. graminis*) und einem Stickstoffmangel auf der Grundlage spektraler Messungen der UV-induzierten Fluoreszenz dar. Die erzielten und in den einzelnen Kapiteln dargestellten Ergebnisse können wie folgt zusammengefasst werden:

1. Die Versuche unter Einsatz des PAM-Imaging Systems ergaben, dass die Quantenausbeute der nicht regulierten Energieabgabe in Photosystem II (Y(NO)) der vielversprechendste Parameter für das Screening von gegenüber Braunrost resistenten Weizenpflanzen ist. Die Messungen dokumentieren, dass der Pathogen-induzierte Anstieg von Y(NO) in der anfälligen Sorte stärker ausgeprägt war als in der resistenten Sorte. Der geeignetste Zeitpunkt für eine verlässliche Differenzierung war zwei Tage nach der Inokulation (dai). Vorangegangene Versuche mit Sporendichten von 20.000 Sporen/ml im Falle von Parametern der schnellen und von 100.000 Sporen/ml bei Parametern der langsamen Fluoreszenzkinetik haben gezeigt, dass die Änderungen in den Fluoreszenzsignalen nicht auf eine physikalische Maskierung zurückzuführen waren.

2. Die Erfassung der FL und UV-induzierten Spektren wurde für die Erkennung von Braunrost (*P. triticina*) bei drei resistenten im Vergleich zu vier anfälligen Sorten eingesetzt. Eine Kombination von spektralen und zeitlich aufgelösten Charakteristika lieferte prä-symptomatische Änderungen der Fluoreszenz, die auf Änderungen im Chlorophyllgehalt sowie sekundären Metaboliten hinwiesen. Die Erfassung des B/G-Amplituden-Verhältnisses scheint der geeignetste Parameter zur Früherkennung einer pilzlichen Infektion zu sein. Eine Unterscheidung zwischen gegenüber Braunrost-sensitiven und -resistenten Sorten erscheint mittels Erfassung des B/R Amplituden-Verhältnisses 3 dai möglich. Dabei sollte allerdings eine zusätzliche Aufnahme der mittleren FL bei 440, 500 und 530 nm Berücksichtigung finden; diese Parameter zeigten nämlich bei den resistenten Sorten ausgeprägtere Unterschiede zwischen Kontroll- und inokulierten Blättern.

3. UV-induzierte spektrale Signaturen sowie die Mittlere FL sind geeignete Ansätze zur Erfassung von Echtem Mehltau (*B. graminis*) bereits einen Tag nach Inokulation. Das erniedrigte B/G-Amplituden-Verhältnis sowie die erhöhten G/R- und G/FR-Halbwertsbreiten-Verhältnisse, in inokulierten im Vergleich zu Kontroll-Blättern, waren probate Parameter zur Erkennung des Pilzbefalls. Des Weiteren scheint die erhöhte Mittlere FL in inokulierten Blättern im Wellenlängenbereich von 500-620 nm eine Unterscheidung zwischen gesunden und erkrankten Blättern zu ermöglichen. Zusätzliche Versuche ließen eine erhöhte mittlere Lebenszeit der Grün-Fluoreszenz bereits zehn Stunden nach der ersten Wirt-Pathogen-Interaktion erkennen.

4. Die Fluoreszenzintensität, gemessen zwischen 370 und 800 nm, stellt einen geeigneten Parameter für eine Diskriminierung zwischen Stickstoffmangel und pilzlicher Erkrankung dar. Das Amplituden-Verhältnis R/FR repräsentiert eine gute Grundlage sowohl für die Früherkennung als auch für eine Differenzierung zwischen N-Vollversorgung, N-Mangel, N-Vollversorgung+Pathogen und N-Mangel+Pathogen. Weitere vielversprechende Ansätze für eine mögliche Diskriminierung zwischen den evaluierten multiplen Stressfaktoren lieferte die Blau-Grün-Fluoreszenz. Darüber hinaus wurden mehrere Amplituden- und Halbwertsbreiten-Verhältnisse für eine Früherkennung der Pathogeninfektion, unabhängig vom Stickstoffversorgungsgrad der Pflanze, als geeignet befunden.

Table of Contents

List of abbreviations

A	absorbance
ANOVA	analysis of variance
aoi	area of interest
AOTF	acusto-optic tunable filter
ATP	adenosine triphosphate
B	blue
B. graminis	*Blumeria graminis*
BGF	blue-green fluorescence
c	control
ca.	circa
$Ca(NO_3)_2$	calcium nitrate
CCD	charge-coupled device
ChlF	chlorophyll fluorescence
Chl*t*	total chlorophyll
cm^2	square centimetre
CO_2	carbon dioxide
cv(s)	cultivar(s)
°	degree
°C	degree Celsius
dai	day(s) after inoculation
DCMU	3-(3,4-dichlorophenyl)-1,1-dimethylurea
DMSO	dimethyl sulfoxide
ETR	electron transport rate
Eq.	equation
$\triangle E$	energy difference
F	fluorescence (emission from dark-adapted leaf)
F’	fluorescence emission from light-adapted leaf
f. sp.	forma specialis
Fig.	figure
F_m	maximum fluorescence from dark-adapted leaf
F_m’	maximum fluorescence from light-adapted leaf
F_o	ground/minimal fluorescence from dark-adapted leaf
F_o’	ground/minimal fluorescence from light-adapted leaf
F_q’	difference in fluorescence between F_m’ and F’
F_q’/F_m’	photosystem II operating efficiency
FR	far-red
FW	fresh weight
G	green
g	gram
h	hour
h	Planck quantum
H_2O	water
ha	hectare
hai	hours after inoculation
hbw	half-bandwidth
HR	hypersensitive reaction
Hz	Hertz

i	inoculated
l	litre
KCl	potassium chloride
KH_2PO_4	potassium dihydrogen phosphate
KNO_3	potassium nitrate
L.	Linné
LF	lifetime
LHCII	light harvesting complex II
LIF	laser induced fluorescence
Ln	natural logarithm
LR	leaf rust
Lr	leaf rust gene
M	molar
m	metre
min	minutes
ml	millilitre
mm	millimetre
ms	millisecond
µJ	micro joule
µl	micro litre
µm	micro metre
µmol	micromole
N	nitrogen
N-	nitrogen-deficiency
N+	nitrogen-full-supply
n	number of replications
NADPH	nicotinamide adenine dinucleotide phosphate
$(NH_4)H_2PO_4$	ammonium dihydrogen phosphate
$(NH_4)_2SO_4$	ammonium sulphate
nm	nanometre
NPQ	nonphotochemical quenching
ns	nanosecond
%	percent
P. triticina	*Puccinia triticina*
pp.	pages
p	probability of error
PAM	pulse-amplitude-modulated
PAR	photosynthetic active radiation
PM	powdery mildew
PMT	photomultiplier
PPFD	photosynthetically active photon flux density
PR	pathogenesis related
PSII	photosystem II
Q_A	quinone acceptor
q_L	fraction of PSII centres that are ‘open’
R	red
R^2	coefficient of determination
r^2	Pearson’s correlation coefficient
RD	resistance degree
rel.	relative

RH	relative humidity
s	second
S_o	ground electronic singlet state
S_1	first electronic excited singlet state
S_2	second electronic excited singlet state
S_n	n electronic excited singlet state
SD	standard deviation
SE	standard error of the mean
SPEC	spectra
SVM	support vector machines
t	time
τ	mean fluorescence lifetime
UV	ultra-violet
UV-VIS	ultra-violet-visible
V	volt
v	volume
ν	frequency of radiation
w	weight
Y(NO)	quantum yield of non-regulated energy dissipation in PSII

A Introduction

1 Demand for sensors in precise agriculture and plant breeding

Nowadays wheat is cultivated on over 240 million ha, more land area than any other commercial crop. Annual global production of wheat exceeds 0.6 billion tons (Dixon *et al*. 2009). As every plant wheat is often affected by stresses that can stem from biotic or abiotic factors. In order to ensure high yields, farmers have to apply pesticides to prevent excessive losses due to pathogens. Similarly, the application of fertilizers is a pre-requisite for the economical viability of the production. The common way to determine pathogen infections and nutrient deficiency is by on-site visual observations. By this, impairment of the crops is detected in a late stage when plants are already aggrieved. Effective detection systems that identify plant stresses at earlier stages would be of enormous advantage and allow more effective applications.

In addition to the precise and timely application of agrochemicals and fertilizers, the use of cultivars which are resistant against specific stress situations, is of fundamental importance. As part of breeding programs, the resistance of new cultivars to pathogens is tested over several years in field experiments, requiring a high input of time and money (Schnabel *et al*. 1998). However, the exact experimental conditions are not reproducible, and the evaluation is somehow subjective. Therefore the question arises, if other techniques are available to support the assessment of the resistance degree to stresses in breeding programmes. Thus, it is generally agreed that there is a great demand for a rapid, automated and objective screening method as breeders are under a permanent pressure to release cultivars with improved resistance (Scholes and Rolfe 2009).

Biotic and abiotic stress factors can change leaf optical properties in different ways, and several approaches have been established to evaluate the occurrence of stress non-destructively (West *et al*. 2003). The output of several research activities indicates that three types of detectors - reflectance, fluorescence and thermal sensing - are suited for this purpose. Reflectance measurements reveal information about pigment content and leaf area (Mahlein *et al*. 2010) and might be used for the non-destructive estimation of the efficiency of photosynthetic light use (Rascher *et al*. 2007). The principle of thermography is based on differences of temperature. Hence, stress-induced stomatal closure results in increased leaf temperature which can be detected especially by imaging systems (Lindenthal *et al*. 2005). The third technique, fluorescence spectroscopy, is a versatile analytical technique widely used

to examine *in vivo* autofluorescence (Kumke and Löhmannsröben 2009). Besides particularities, advantages and disadvantages of each method, we focused on fluorescence techniques in the present study.

The fluorescence of plant tissue can be successfully used to evaluate the photosynthetic capacity, chlorophyll content and also quantitative modifications of plant secondary metabolites fluorescing between 350 and 620 nm (Buschmann *et al*. 2009). Over the years, for detection of nitrogen deficiency, field capable sensors based on reflectance as well as fluorescence readings, became commercially available. Thereby, nitrogen deficiency leads to changes in chlorophyll content as well as content of plant secondary metabolites (Cartelat *et al*. 2005). Further developments in optical technology enable a differentiation between healthy and diseased areas of the crop, so that several research groups provided results of a successful recognition of pathogens (e.g. Bodria *et al*. 2002; Bravo *et al*. 2004; Chaerle *et al*. 2004; Kuckenberg *et al*. 2009a; Lüdeker *et al*. 1996; West *et al*. 2003). Thereby, the detection of fungal infection before the occurrence of visual symptoms is of major importance and has to be further optimized. In experiments under controlled conditions, the effect of compatible and incompatible pathogen-plant interaction of *Phytophthora infestans* (Koch *et al*. 1994), *Blumeria graminis* (Swarbrick *et al*. 2006), *Cercospora beticola* (Chaerle *et al*. 2004, 2007a), and tobacco mosaic virus (Chaerle *et al*. 2007c) was evaluated. Upon contact of fungal spores with the leaf surface, changes in metabolic pathways are initiated very rapidly (Berger *et al*. 2007; Yarwood 1967). Thereby, the response of susceptible and resistant genotypes might vary in speed, as well as the amount and type of substances which are modified, accumulated, or synthesized. Moreover, photosynthetic rate or electron transport chains are also affected during early host-pathogen interaction (Swarbrick *et al*. 2006).

Under real field conditions it is not exceptional that more than one stress factor influences simultaneously the plant physiology. So far, one of the major fields to be addressed in sensor application is to distinguish between different concomitant stressors. In this context, evaluation of fluorescence characteristics showed to open a way for objective information about extent and nature of the impact of stress factors. When targeting at the early detection of disease and nutrient deficiency, fluorescence readings proved to provide a higher potential than other non-destructive sensor techniques (Chaerle *et al*. 2007b).

2 Biotic and abiotic constrains for wheat production

2.1 Fungal pathogens as biotic stress factors and relevance of host plant resistance

Fungal pathogens cause more economic damage in crop plants than any other microorganisms (Horbach *et al*. 2010). Pathogens have many effects on plant physiological functions like photosynthesis, translocation of water and nutrients in the host plant, host plant respiration, plant growth, etc. (Agrios 2005). Pathogens in general affect photosynthetic electron transport or the downstream metabolic reactions but very often, chlorophyll content is reduced whereas the photosynthetic activity of the remaining chlorophyll seems to remain unaffected (Agrios 2005). Generally, two major types of resistance in pathogen-host interaction can be distinguished. On the one hand, pathogen resistance due to physiological races that can overcome resistance gene (combination) in the host, can occur, and on the other hand the host or non-host plant resistance. If the pathogen is compatible (virulent) to the host, it can spread in a susceptible cultivar. Plants produce a large variety of secondary products including phenolic compounds which play a key role in early stages of infection (Marschner 2002) and may serve as defence compounds (Kruger *et al*. 2002; Taiz and Zeiger 2007). For example, accumulation of phenolic compounds in the walls of epidermal cells that are in close contact with the invading fungal hyphae have been observed (Cerovic 1999). The content of phenolics is often high in N deficient plants whereas its content and thereby the fungistatic effect can decrease in case of large nitrogen supply (Marschner 2002). By this, resistance expression in plants might be active or passive, where the phenolic compound is present in the plant and is not further metabolized but may be changed by the pathogen in the latter case. In case of the active system, a preformed substance is degraded or metabolized to a different compound by the host directly after pathogen attack (Vermerris and Nicholson 2006). Moreover, cultivar resistance can vary, as “active resistance comprises a series of interconnected processes which, following recognition, are induced in the host cell through its continuous irritation by structures or products of the pathogen and which results in exclusion, inhibition or elimination of the pathogen” (Heitefuss 1997b). At the genetic level, resistance can be controlled by one (monogenetic), a few major or minor genes (oligogenetic) or by a series of minor genes (polygenetic). Moreover it can be effective against some (race-specific, qualitative, vertical) or against all (race-nonspecific, quantitative, horizontal) races of the pathogen. Thereby, one has to distinguish between seedling-, adult plant-, complete-, and partial resistance. Preformed structural and chemical barriers (e.g. phenolics), cell wall modifications in relation to resistance (e.g. papilla formation), the hypersensitive resistance

reaction (rapid, local cell death), pre- or post-haustorial resistance, durable resistance and induced resistance are well known resistance types (Heitefuss 1997b).

Resistant cultivars are often the only way to prevent losses due to diseases (Heitefuss 2001); so far, progress in breeding for disease resistance of wheat was very effective against mildew and rusts (Hartleb *et al*. 1997).

2.1.1 *Puccinia triticina*

The following information is based on the book edited by Obst und Gehring (2002). *Puccinia triticina,* with a huge amount of physiological races, belongs to the class of Basidiomycotina. As an obligate parasite it overwinters on living host tissue in form of mycelia or urediospores. These urediospores are deposited by wind or rain on new host plants. After germination of the urediospores, 4-8 h after contact with host leaf surface and optimum environmental conditions (Bolton *et al*. 2008), the germ tube searches for a stomatal opening (Fig. 1A). There it produces an appressorium and out of it, a thin penetration peg in the substomatal cavity of the stomata. Following, a substomatal vesicle, infection hyphae and haustorial mother cells enter the neighbouring mesophyll cells. Haustoria form within leaf mesophyll cells as the major feeding structure through which nutrients are taken to support fungal colonization without killing the host cells (Bolton *et al*. 2008). Infectious hyphae are spreading in intercellular spaces till the mycelia compacts to uredia. Within 8-10 days after infection, urediospores rupture the epidermis (Fig. 1B and C), and the typical reddish-brownish pustules can be seen at the leaf surface. In addition, chlorotic spots become apparent around these pustules. Wind and rain can now disperse again the spores and initiate new infection.

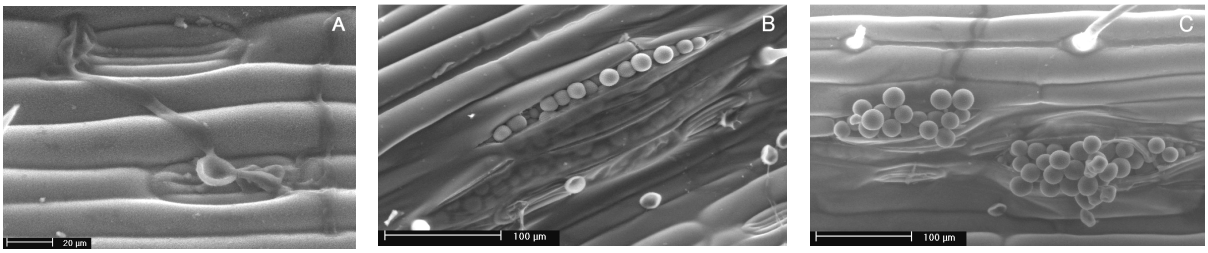

Fig. 1. Environmental scanning electron microscopy (ESEM) pictures of leaf rust (*Puccinia triticina*) infection on wheat leaves. **A)** Spore germination and penetration of stomatal cavity; **B)** and **C)** Leaf rust pustules rupture the leaf epidermis. (Bürling, unpublished observations).

The development of a rust epidemic is strongly influenced by the resistances present in the field and by environmental factors. The following temperatures and relative humidity are optimal for the respective developmental phase (Kluge *et al*. 1999) of the leaf rust pathogen: germination of urediospores 15-21°C (threshold 2-32°C), infection 15-18°C (threshold 4-25°C) and 100% relative humidity > 4 h, mycelia growth 20-26°C (threshold 2-35°C), total development 15-25°C. During summer, several cycles of infection can proceed.

At the end of vegetation period, sexual lifecycle of the pathogen begins, which is indicated by teliospores that appear on the abaxial leaf side. In spring, these teliospores produce basidia and basidiospores which are reliant on the alternate host *Thalictrum flavum* (*Ranunculaceae*). Aecidiospores that are created trough recombination of genetic information are able to infect the wheat host plants.

Leaf rust occurs in all growing areas, especially in warm areas and on late maturing cultivars, and is the most important rust variety worldwide (Kolmer *et al*. 2009). The tremendous genetic variation for virulence and the wind-dissemination of the pathogen makes breeding for stable leaf rust resistance a continually challenging task. In addition to race-specific resistance, the development of cultivars carrying non-specific resistance genes to provide effective durable resistance is of main interest in wheat research (Kolmer *et al*. 2009). So far, a huge number of *Lr* genes are known (Bolton *et al*. 2008). Resistance response to leaf rust is characterized by small uredinia surrounded by chlorosis or necrosis or by a batch of hypersensitive flecks produced in response to the infection (race-specific resistance). Non-hypersensitive resistance on the other hand is characterized by fewer and small uredinia with no or varying amounts of chlorosis or necrosis compared to a susceptible response (Bolton *et al*. 2008). Moreover, haustoria fail to develop or develop at a slower rate. In this context, abortion of infection structures and reduction of mycelium growth due to partial resistance (Jacobs 1990) as well as relatively more collapsed substomatal vesicles and collapsed primary infection hyphae in tissue of a resistant line (Hu and Rijkenberg 1998) have been observed. Moreover, a smaller number of haustorial mother cells in hypersensitive and partially resistant genotypes (Jacobs and Buurlage 1990) due to high percentage of infection units aborted early (Martinez *et al*. 2004) and a prevention of haustoria formation by the fungus and papilla formation from prehaustorial resistance (Anker and Niks 2001) have been reported in comparison to susceptible cultivars. New races of wheat rusts have recently emerged worldwide which makes the efforts to develop rust resistant cultivars more challenging.

2.1.2 *Blumeria graminis*

A second economically important and worldwide spread wheat pathogen is the causal fungus of powdery mildew, *Blumeria graminis* f. sp. *tritici* (Huang and Röder 2004). The following information is based on the book edited by Obst und Gehring (2002). *Blumeria graminis* belongs to the class of Ascomycotina and is an obligate ecto-parasite. By wind, conidio- or ascospores of the fungus reach emerging winter corn. There they germinate during 2 h after contact with the leaf surface (Eichmann and Hückelhoven 2008) and produce a short hypha with an appressorium at its end. Out of this structure, the infection hypha directly penetrates through the leaf surface into the epidermis where it develops a finger-like haustorium. These feeding structures export nutrients to the leaf surface where new haustoria are developed. Conidiophores with around eight tightly together adhering conidiospores develop on narrow branched hyphae that are closely arranged besides each other. The respectively mature tip-spore is disconnected by wind. By this, up to eight infection cycles during cereal vegetation period can take place. Typical symptoms to be seen macroscopically are the whitish mycelia structures on the leaf surface. At the end of the vegetation period male and female sexual organs are formed in old mycelia. After sexual combination, so called cleistothecia occur, in which up to 25 tubes (asci) with eight ascospores each mature. These structures can outlive hot summer and after-harvest periods. In humid autumn conditions they can rip, and ascospores are expelled actively to reach emerging winter corn where the fungus overwinters in form of mycelia or cleistothecia (Börner 1990).

Following temperatures and relative humidity are optimal for the respective developmental phase of the fungus (Kluge *et al*. 1999): conidia germination 5-20°C (threshold 0-30°C), infection 20-25°C (threshold 0-30°C) with relative humidity > 95%, pustule growth 15-20°C (threshold 4-31°C), sporulation 15-20°C (threshold -30°C) with relative humidity > 95%, overall development, 15-20°C.

Extensive plant damage to susceptible cultivars can occur under climatic conditions favourable to the pathogen. *Blumeria graminis* f. sp. *tritici* has acquired a high degree of specialization with races attacking specific cultivars. The use of host resistance is the most effective, economical and environmentally safe method of management (Bennett 1984), whereas emphasis must be placed on methods identifying durable host-plant resistance (Marshall 2009). By now, a huge number of *Pm* genes is known (Hsam and Zeller 2002; Marshall 2009), whereupon breeding for partial and race-nonspecific resistance, polygenetically controlled, is of major interest. Blocking the penetration or reducing the size

of haustoria and thus limiting the growth and sporulation of colonies are typical effects (Bushnell 2002; Gustafson and Shaner 1982; Lin and Edwards 1974). In race-specific resistance, mainly more or less plant cells undergo hypersensitive cell death (Bennett 1984; Bushnell 2002). Also, larger and earlier papillae are produced at attempted penetration sites (Skou *et al*. 1984), whereas speed of papilla formation plays an important role in non-race specific resistance (von Röpenack *et al*. 1998). Thereby, lignin and other phenolic compounds in the papillae and haloes, established in response to the pathogen attack, have been detected (Heitefuss 1997a; Thordal-Christensen 2000).

2.1.3 Fungal inoculation for experiments under controlled conditions

As indicated for leaf rust and powdery mildew, fungal pathogens have specific environmental requirements for distinct development stages of their infection cycle. This has to be considered when planning and conducting experiments to ensure optimal conditions for disease development. Further practical aspects include the in-time production of inoculum to inoculate the experimental plants.

Powdery mildew spores are applied to whole plants or plant organs as dry inoculum or in suspension (Nicot *et al*. 2002). Thereby, shaking or blowing conidia from infected plants (Liu *et al*. 1999) or more convenient by using settling towers (von Röpenack 1998) are sometimes coupled with prior spraying of the target plants with water. Leaf-to-leaf contact of infected and target plant is one of the most simple methods (Reifschneider and Boiteux 1988). Contradictory results on spore germination rate have been reported when preparing suspension in order to calibrate their concentration and to avoid formation of clumps (Nicot *et al*. 2002). To get a more precise local deposition, small paint brushes have been used to remove conidia from infected plant organs in order to deposit them on target plants (Edwards and Allen 1966). Advantages are given especially when locally restricted examinations are aimed at since the inoculation site is easily to be identified, which is hardly possible in the previously described approaches. Leaf fixation prior to inoculation procedure is often employed for further optimization (Sander and Heitefuss 1998). After inoculation plants are usually kept under controlled conditions of 15-20°C.

Similarly, several inoculation methods might be adopted for inoculation of single leaf rust isolates or pathotype mixtures. Freshly harvested urediospores from infected host plants are used for inoculation, but spores can also be stored under defined conditions up to several years (Roelfs *et al*. 1992). Atomization with water or mineral oil as spore carrier with or

without regulation of air pressure is a widely used approach (Kloppers and Pretorius 1997). Determination and adjustment of the spore density with a counting chamber is a very common procedure (Kloppers and Pretorius 1997). However, application of a defined weight of spores through a settling tower (Anker and Niks 2001; Jacobs 1990; Martinez *et al*. 2001) with downstreamed moisturization (Zhang and Dickinson 2001) is also practiced. In the latter case, often talc (Southerton and Deverall 1990) or *Lycopodium* spores are added (Anker and Niks 2001; Jacobs 1990; Martinez *et al*. 2001). Localized application can be achieved by using a camel hair brush (Southerton and Deverall 1990) with a sequential moisturizing of the leaves (Zhang *et al*. 2003). Settling towers provide little control of inoculum density but also spraying of spore solution can result in a modification of predefined concentration due to junction of droplets and spray run-off. In order to examine spatially resolved changes in plant tissue a highly precise and accurate inoculation is required. Thus, uniform and reproducible inoculation is necessary for quantitative evaluation, which is extremely important in breeding plants for disease resistance (Reifschneider and Boiteux 1988). Therefore, the application of monodroplets with defined spore density seems to be ideal. In this context the surfactant 'Tween' is used to enable application of spore suspension to very hydrophobic surfaces. Leaf fixation prior to inoculation is used to avoid effects of leaf inclination and gravity on the distribution of spores inside the droplet spread area. After application of droplets to the leaf surface, plants are kept for 16-24 h under 80-100% relative humidity at 15-20°C to ensure maximum spore germination.

2.2 Nitrogen management as abiotic factor

Regarding all mineral nutrients, nitrogen is quantitatively the most important for plant growth (Amberger 1996) and grain yield in wheat (Halse *et al*. 1969). As highlighted by Cassman,

> "the global challenge of meeting increased food demand and protecting environmental quality will be won or lost in cropping systems that produce maize, rice, and wheat. Achieving synchrony between N supply and crop demand without excess or deficiency is the key to optimizing tradeoffs amongst yield, profit, and environmental protection" (Cassman *et al*. 2002).

The main functions of nitrogen in the plant are their constituency of amino acids, amides, proteins, nucleic acids, nucleotides coenzymes, chlorophyll and cell walls (Taiz and Zeiger 2007). Except drought, no deficiency is as dramatic in its effects as nitrogen deficiency (Epstein and Bloom 2005). Due to chloroplast degradation and dislocation in the youngest tissues, the older leaves may get completely yellow (Schilling 2000). The chlorophyll content of wheat leaves and leaf N are closely related as the photosynthetic machinery accounts for more than half of the N in a leaf (Evans 1983). Besides the knowledge that leaf chlorophyll is low under N shortage and increases with N supply (Peng *et al*. 1996), the N supply influences also the synthesis of proteins and polyphenolics (Herrmann and Weaver 1999). Nitrogen influences carbohydrate source size by leaf growth and leaf area duration and also the photosynthetic rate per unit leaf area and thereby source activity. Moreover, the sink capacity in form of size and number of vegetative and generative storage organs is affected (Engels and Marschner 1995). On the other hand, excessive supply of nitrogen leads to N losses and thus negative impacts on the environment (Cartelat *et al*. 2005), and can decrease the quality of the harvested product or reduce plant growth and yield due to enzyme deficiency (Schilling 2000). Moreover, losses due to fungal infection (e.g. *Puccinia triticina, Blumeria graminis*) might be increased when pathogens are able to penetrate, multiply and develop more rapidly in succulent tissue due to an excessive nitrogen supply.

3 Fluorescence

3.1 Principle of the fluorescence

Upon excitation with light of distinct wavelength, several molecules absorb energy which they emit after a time difference (lifetime) as radiation energy. As a rule, the resonance condition has to be fulfilled for absorption to take place: $\triangle E = hv$, with $\triangle$E, energy difference between ground and excited state; *h*, Planck quantum; and *v*, frequency of radiation (Kumke and Löhmannsröben 2009). At room temperature, molecules have a low energy level in the so called ground electronic singlet state (S_o) and thereby usually in the lowest vibrational level (Noomnarm and Clegg 2009). When absorbing a photon, excitation of a molecule from S_o takes place in $< 10^{-15}$ s and raises the molecule mostly to many different vibrational levels of the first electronic excited singlet state S_1 (Fig. 2), depending on the distribution of the excitation light. Molecules can also be transferred to higher energy levels (S_2,…$_n$) from where they relax to the highest vibrational level of the S_1 electronic state via rapid internal conversion and then to the lowest vibrational level of the S_1 state (10^{-12} s). From

the metastable S_1 level where the molecule remains at most 10^{-8} s, it returns to the ground state through one of many pathways. If the molecule emits a photon, the molecule will usually relax to one of many different higher vibrational levels of the S_o, which results in a broad fluorescence spectrum. Also here, the energy of the emitted photon must equal the change in the energy levels.

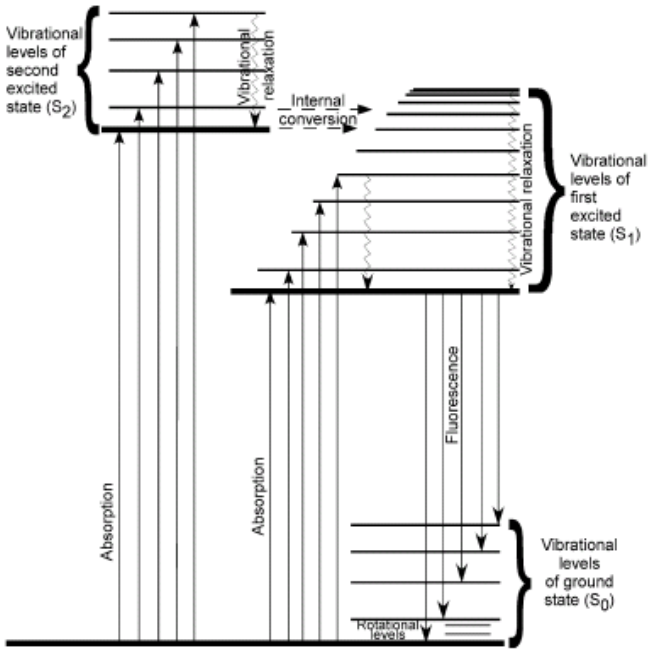

Fig. 2. Perrin-Jablonski diagram indicating the energy levels of the ground (unexcited) and excited states in a molecule, and the possible photophysical processes in molecular systems (source: Noomnarm and Clegg 2009).

Every fluorescing substance is characterized by its specific excitation and emission spectra as well as the average time the molecules remain in the excited state. The latter is the so-called fluorescence lifetime. By definition, the fluorescence lifetime τ is the time span after short-pulsed excitation when the number of molecules in the excited state has declined from the initial maximum to 1/e. This results from the exponential decay law $I(t) = e^{-t/\tau}$ (I = intensity, t = time), when setting $t = \tau$ (Lakowicz 2006). However, when the fluorophores are in complex biological samples, the fluorescence response is typically not a simple single-exponential decay but may follow more complex rules, e.g. a sum of exponential terms with different amplitudes and lifetimes. This is because the fluorophores are located in disparate locations and a sum of different fluorescing species is contributing to the total fluorescence signal. The single fluorescing species are characterized by their specific lifetimes and the percentage or fraction with which they contribute to the total signal. The occurrence of new

compounds might result in elongation or shortening of the mean lifetime, depending on the lifetime of the new substances. Time-resolved measurements turn out that much of the molecular information available from fluorescence is lost during the time averaging process (Lakowicz 2006).

Because of fluorescence emission is, in contrast to reflection, of longer wavelength than that of the absorbed light (stoke shift), the choice of excitation light determines the fluorescence information which is obtained. There is a number of irradiation/excitation light sources and detectors for the estimation of fluorescence emission properties (Cerovic *et al*. 1999; Lenk *et al*. 2007). In general, excitation of a leaf with blue or red light allows the determination of chlorophyll fluorescence, whereas the UV excitation enables the additional detection of blue and green fluorescence. Therefore, when excited with UV light, commonly four fluorescence peaks can be determined: the blue peak (~ 450 nm), the green shoulder (~ 530 nm) and the two chlorophyll peaks at ~ 690 and ~ 730 nm as presented in Fig. 3.

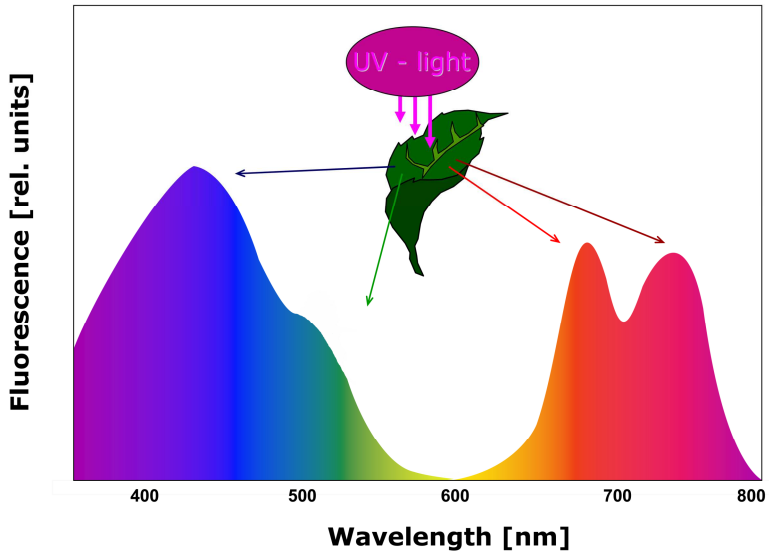

Fig. 3. Typical UV light-induced fluorescence emission spectrum of a green leaf (modified after Buschmann *et al*. 2000).

Possible light sources for fluorescence excitation are lasers, lamps (xenon, halogen) and LEDs. Pulse-modulated light sources have the advantage of possibly eliminating background signals. Also, the extremely short time scales of fluorescence decay curves (lifetime) can only be measured with short-pulsed lasers or LEDs. The electronic systems needed for measuring nanosecond decay curves is complex. An acusto-optic tunable filter (AOTF) can be used as emission monochromator. It transmits light in a narrow bandwidth

only. The choice of the transmitted wavelength is determined by a variable frequency of an electric signal that induces a diffraction grating in the AOTF-crystal. After blocking the undiffracted light, the fluorescence can be detected selectively at the desired wavelength. The variety of potential detectors includes photomultipliers, photodiodes, diode-arrays and CCD cameras whereupon the latter provides additional information of the spatial resolution in contrast to the other mentioned point measurements. In order to resolve nanosecond fluorescence lifetime information, the detector's signal needs to be analyzed with an ultrafast digitizer or with highly resolving gating techniques. Therefore, by using a gated integrator, sequentially delaying of the gate position enables to sample the fluorescence signal with a very high resolution and to acquire highly resolved fluorescence decay curves.

When measuring fluorescence signals several important influencing factors have to be considered. At first, the fluorescence intensity is directly proportional to the intensity of the excitation radiation, at least at first approximation. Moreover, with increasing temperature, the possibility of deactivation of molecules in the excited state is increased, resulting in a decreased fluorescence intensity and lifetime. Furthermore, the intensity of the excitation radiation and of the fluorescence emission decreases with increasing distance of the light source and sensing optics from the sample (Fig. 4).

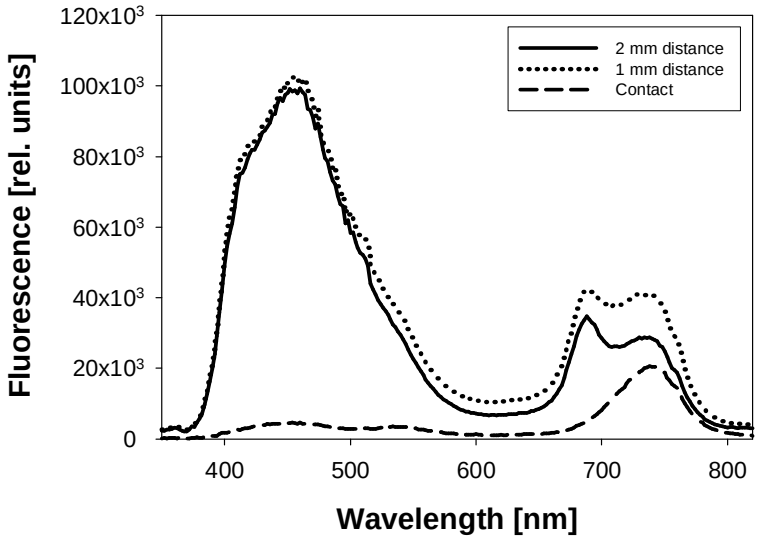

Fig. 4. Influence of the distance (2 mm, 1 mm or contact) between sample surface and probe on the fluorescence emission spectra of a wheat leaf excited with a pulsed N_2-laser at 337 nm wavelength (Bürling, unpublished observations).

Therefore, several commercial systems such as the PAM-series of the Heinz-Walz company (Effeltrich, Germany) are designed with a sample holder in order to set the distance between sample and sensor to provide optimum measuring conditions.

3.2 Chlorophyll fluorescence

Plant leaves contain pigments such as chlorophyll, phenols, carotenoids, and cell wall components which emit fluorescence at different wavelengths. In this context, chlorophyll *a* fluorescence of leaves is a non-destructive probe of photosynthetic efficiency which can reflect the impact of environmental factors on a plant (Cerovic *et al*. 1999; Schurr *et al*. 2006). Since several abiotic and biotic factors can lead to modification of the photosynthetic apparatus, specific chlorophyll fluorescence signatures have been identified as indicative of plant stress (Lichtenthaler and Miehé 1997). This is explained by the fact that the three processes, photochemistry, heat dissipation, and chlorophyll fluorescence, are in competition with each other, when light energy is absorbed by chlorophyll molecules (Maxwell and Johnson 2000). If photochemistry is reduced, fluorescence and heat increases; therefore chlorophyll fluorescence can be used as indicator for the exposure to and intensity of stress.

In the process of photosynthesis numerous pigments in combined action (e.g. chlorophylls and carotenoids) serve as antenna (light harvesting complex), collecting light and transferring its energy to the reaction centres, where by chemical reactions part of the energy is being stored by transferring electrons from a chlorophyll pigment to an electron acceptor molecule (Taiz and Zeiger 2007). An electron donor then reduces the chlorophyll again. Under normal conditions more than 80% of the captured photons are used in the photosynthetic light reaction and the associated electron transport to build-up ATP and NADPH, which are the essential substances for further CO_2 assimilation in the Calvin cycle (Lichtenthaler *et al*. 2005). Nevertheless, 1-2% of the absorbed light is dissipated as non-radiative heat and red fluorescence light during energy transduction (Maxwell and Johnson 2000). Thereby, fluorescence is of longer wavelength than the excitation light, and at room temperature more than 90% of the chlorophyll fluorescence comes from PSII (Gitelson *et al*. 1998). When leaves are kept under dark conditions, primary quinone acceptor of PSII (Q_A) becomes maximally oxidized and the PSII reaction centres are open, which means that they are capable of performing photochemical reduction of Q_A (Baker 2008). Hence, photochemical quenching is maximal and nonphotochemical quenching minimal (Schreiber 2004). If dark-adapted leaves are then exposed to a weak modulated and nonactinic

photosynthetically active photon flux density (PPFD) of ca. 0.1 µmol m^{-2} s^{-1}, not driving photosynthesis measuring beam, a minimal level of fluorescence, F_o, can be measured. F_o thereby originates exclusively from light harvesting complex II (LHCII) (Lichtenthaler 2005). If thereafter a short pulse of actinic light characterized by high PPFD of several thousand µmol m^{-2} s^{-1} and usually less than 1s is given, maximal fluorescence level F_m is reached due to maximal reduced Q_A, and both LHCII and the reaction centres of PSII are involved (Govindjee 2004). PSII reaction centres with reduced Q_A are termed as 'closed' and are unable to perform photochemistry. The ratio F_m-F_o/F_m, estimates the maximum quantum yield of Q_A reduction which is related to the PSII photochemistry. After the fluorescence rise from F_o to F_m, chlorophyll fluorescence declines to a low steady state level due to full activation of photochemical quantum conversion which includes also non-photochemical processes (Lichtenthaler *et al*. 2005). If under this situation a leaf is exposed to continuous actinic light, the fluorescence level F' can be measured. By applying brief saturating light pulses that maximally reduce Q_A such that photochemical quenching is completely suppressed (Schreiber 2004), F' rises to the maximal fluorescence level F_m'. The difference between F_m' and F' is referred to F_q' and is a result of F_m' quenching by PSII photochemistry. Thereby, F_q'/F_m' is proportional to quantum yield of PSII photochemistry before application of the saturating light pulse. Determination of F_q'/F_m' can be used for the estimation of non-cyclic electron transport rate through PSII (ETR).

In addition to the previously described chlorophyll fluorescence induction kinetic, several more chlorophyll fluorescence parameters, ratios, and quenching coefficients can be determined. All indices provide information on the functionality of the PSII and the photosynthetic apparatus (see Baker 2008; Lichtenthaler *et al*. 2005); particular chlorophyll fluorescence ratios are indicators of specific aspects of the photosynthetic apparatus (Buschmann 1999).

In fact, different approaches can be used to induce and measure chlorophyll fluorescence under laboratory conditions. One procedure is used to evaluate as above described the fluorescence induction kinetic as point or imaging measurements. This approach is called pulse-amplitude-modulated (PAM) chlorophyll fluorescence, and a typical result of a chlorophyll fluorescence quenching analysis is shown in Fig. 5. Another way is to determine the chlorophyll fluorescence emission spectra and generate the ratio between two chlorophyll peaks as indicator for chlorophyll content (Buschmann 2007). Particular for this system is the determination of two maxima, in the red region at 685-690 nm and far-red region at 730-740 nm. At higher chlorophyll concentrations, with increasing chlorophyll concentrations the

chlorophyll fluorescence increases and is mainly detected in the range of 730-740 nm, whereas in the range of 685-690 nm fluorescence decreases after a while due to re-absorption of the emitted red fluorescence by the chlorophyll absorption bands. As result, lower fluorescence is recorded at 685-690 nm with increasing chlorophyll content. The phenomenon of re-absorption is caused by the overlapping of the red fluorescence emission spectrum with the far-red fluorescence absorption spectrum.

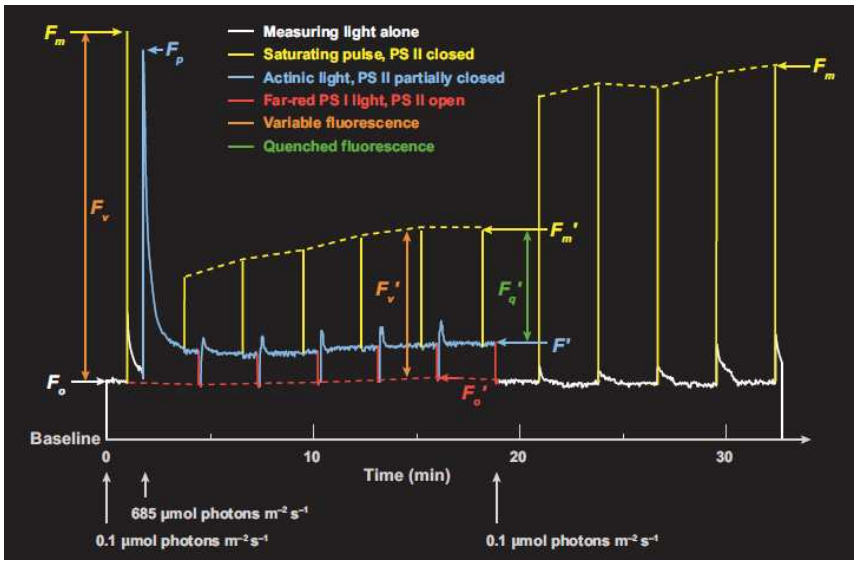

Fig. 5. Typical result of a fluorescence quenching analysis on healthy leaves using modulated fluorescence (source: Baker 2008).

3.3 Blue-green fluorescence

Whereas the red and far-red fluorescence emanates only from chlorophyll *a* located in guard cells chloroplasts in the epidermis and chloroplasts in palisade and spongy parenchyma cells, several other compounds located in the cuticle, epidermis and vascular bundles contribute to the emission of the blue-green fluorescence (Goodwin 1953; Lang *et al*. 1991; Rost 1995). Thereby, ferulic acid is the main fluorescing compound but also other products of the plant secondary metabolism can significantly contribute (Lichtenthaler and Schweiger 1998). These products comprise hydroxycinamic acids, stilbenes, coumarins, flavonols, phenolic acids, and many more. Coming from the shikimate pathway, they are biosynthetically related and are generally named plant phenolics (Cerovic *et al*. 1999). However, their contribution to fluorescence depends on the concentration of the fluorophore, its' localization in the leaf, its absorption and emission spectrum, the fluorescence quantum yield as well as the fluorophore's environment (temperature, pH, polarity, etc.). As absolute

fluorescence signals are strongly affected by distance (Fig. 4) and leaf geometry, ratios between fluorescence maxima are more reliable than absolute intensities, and proved to be suited for characterization of plant-stress (Buschmann *et al*. 2009). Thereby, ratios of blue or green fluorescence to red and far-red fluorescence as well as blue to green fluorescence can be calculated.

As shown, the stress-induced accumulation of pre-existing or new synthesized secondary metabolites in the epidermis can increase the blue and/or green fluorescence intensity (Lichtenthaler and Miehé 1997) and change the fluorescence lifetimes. However, the presence of compounds in the epidermis with high UV absorbtivity attenuates the UV excitation of chlorophyll molecules in the mesophyll (Chaerle and Van der Straeten 2000). As a consequence, the UV-induced chlorophyll fluorescence is decreased, resulting in a lower ratio of blue-green to chlorophyll fluorescence. Moreover, by this the presence of green fluorescence reabsorbing compounds can increase the blue-to-green fluorescence ratio, whereas the re-absorption of the blue-green fluorescence by chlorophyll molecules can also influence the respective ratios (Lang *et al*. 1991). In addition to pre-existing, accumulated and newly synthesized blue-green fluorescing compounds in the leaf tissue, also some biotic stressors themselves, like fungi or bacteria, may emit autofluorescence (Rost 1995; Zhang and Dickinson 2001). Furthermore, during plant-pathogen interaction, phenolic compounds proved to play an important role in plant defence mechanisms (Nicholson and Hammerschmidt 1992; Vermerris and Nicholson 2006) in susceptible as well as resistant cultivars. Thereby, several identified substances accumulate or are newly synthesized in response to pathogen attack. As observed by means of fluorescence microscopy, leaf rust infection can cause lignification of stomata surrounding cells (Fig. 6).

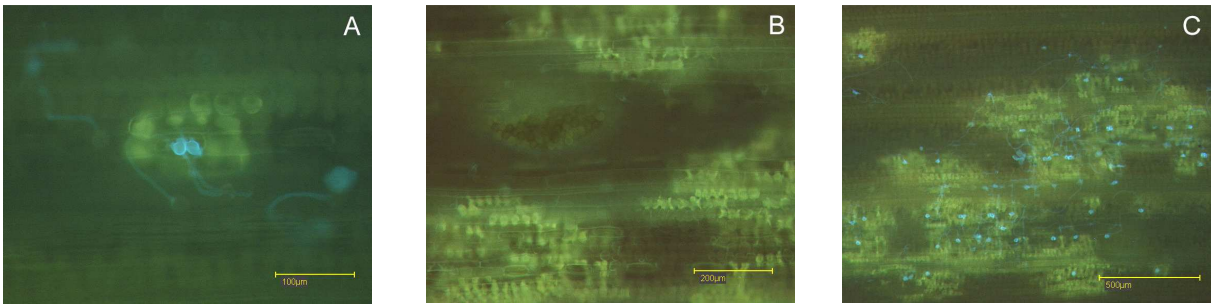

Fig. 6. Fluorescence microscopic examinations of wheat leaves infected with *Puccinia triticina*. **A)** Lignification (yellow) of stomata surrounding cells due to pathogen attack (blue); **B)** Leaf rust pustules rupture the epidermis; **C)** Distribution of pathogen structures (blue) and lignified tissue (yellow). (Bürling, unpublished observations).

As representative for abiotic stressors, high levels of nitrate increase the chlorophyll concentration but reduce phenol and lignin production (Brown *et al*. 1984), resulting in changes of the fluorescence signature.

3.4 Data processing

The common approach for processing fluorescence spectra is to determine the peak amplitudes for calculation of fluorescence ratios (Lichtenthaler and Miehé 1997). Nevertheless, the half-bandwidth of a peak can also be an indicator for modification of amount and composition of fluorescing substances, and changes might lead to modifications of the ratios amongst the peaks. Usually, a non-linear curve-fit like the Gaussian fit can be used to define position, amplitude and the half-bandwidth of the fluorescence peaks.

Furthermore, recording of the fluorescence lifetime is a suitable method in plant stress evaluation (Cerovic *et al*. 1999). Fluorescence lifetime data have to be processed by non-linear curve fitting and a deconvolution process based on specific algorithms like the Levenberg-Marquard (Kress *et al*. 2003). As outcome, fluorescence lifetimes, their percentage contribution to the mean lifetime, and the mean lifetime itself are obtained. As shown by other authors, up to four lifetimes with a fast, medium, a slow, and a very slow component have been detected *in vivo* (Goulas *et al*. 1990; Holzwarth 1986).

In contrast, data processing of fluorescence images is a more complex topic. Usually, commercial imaging systems have their specific software which allows a pixel by pixel or region of interest calculation, and analysis of fluorescence parameters. However, a number of general and more specific image processing software tools are available (Lenk *et al*. 2007). Nevertheless, calculation of mean value and standard deviation of the whole image or of regions of interest are the tools restricting image analysis. Meanwhile, image processing methods have been extended and automated algorithms should make image analysis more comfortable and accurate (Lenk *et al*. 2007).

3.5 Fluorescence spectra and lifetime and the use of imaging technique for evaluation of the physiological status of plant tissues

As mentioned above, several amplitude ratios between various peaks proved to be sensitive for stress detection. Some abiotic stress situations like nutrient deficiencies and water stress (Chappelle *et al*. 1984a, 1984b; Subhash and Mohanan 1997) are detectable by means of fluorescence spectra. The use of laser induced fluorescence (LIF) spectra for rapid

detection of nitrogen deficiency (Tartachnyk and Rademacher 2003) as well as cadmium- (Mishra and Gopal 2005) and nickel-induced (Mishra and Gopal 2008) stress in wheat plants are well known examples. Similarly, early recognition of nematodes in sugar beet (Schmitz *et al*. 2006) and the detection of fungal infection of different plants by LIF (Belasque *et al*. 2008; Lüdeker *et al*. 1996) have been successfully accomplished. Working with wheat, Tartachnyk and co-workers have shown that LIF is also suited for the differentiation between nitrogen deficiency and pathogen infestation (Tartachnyk *et al*. 2006).

In addition to the assessment of spectral signatures, the determination of lifetime of fluorescing constituents is an important tool to understand the plant reaction to impacting stresses. Nevertheless, only little information on stress-induced changes on chlorophyll- as well as blue-green fluorescence lifetime is available in the literature. Early decay-time measurements taken after application of the herbicide DCMU showed a strong increase of the slowest of four chlorophyll fluorescence lifetime components (Schmuck *et al*. 1991). Moreover, water stress (Schmuck *et al*. 1992) and iron deficiency (Morales *et al*. 1994) caused distinct changes in fluorescence lifetimes, amongst others due to flavin accumulation (Morales *et al*. 1994). Experiments on the effect of fungal metabolites on leaves as detected by chlorophyll fluorescence suggest that decay-time measurements have significant potential as non-intrusive probe of leaf damage by fungal metabolites (Kshirsagar *et al*. 2001). Hence, further work is needed to examine application possibilities for evaluations of distinct impairment of plant health status.

In general, the use of imaging techniques provides additional information, especially the spatial and temporal changes of stress intensity during plant development (see e.g. Chaerle and Van der Straeten 2000; Sankaran *et al*. 2010; Scholes and Rolfe 2009). The response of plants to several adverse situations like drought, freezing, salinity, chilling, high temperature and irradiation, nutrition, and herbicide application have been studied employing chlorophyll fluorescence imaging (Baker and Rosenqvist 2004; Buschmann and Lichtenthaler 1998; Heisel *et al*. 1996; Jansen *et al*. 2009; Kuckenberg *et al*. 2007; Lichtenthaler *et al*. 1997). Considering biotic stress factors, Chaerle *et al*. (2007b) confirmed the suitability of imaging chlorophyll fluorescence for early detection of magnesium deficiency and *Botrytis cinerea* infection in common bean, as compared to thermal and video camera detection. In studies with wheat, a foliar disease could be detected in field experiments (Bravo *et al*. 2004). Moreover, PAM chlorophyll fluorescence imaging allowed the early detection of leaf rust and powdery mildew on winter wheat leaves, respectively, three and two days prior to appearance of visual symptoms (Kuckenberg *et al*. 2009a). Furthermore, the potential of fluorescence

measurements for discrimination between nitrogen deficiency and pathogen infections was shown (Kuckenberg *et al*. 2009b). Fluorescence ratio images calculated from images of the blue, green, red, and far-red spectral region have been demonstrated for several types of stress (for review see e.g. Buschmann *et al*. 2000, 2009). Furthermore, the early detection of the hypersensitive reaction to tobacco mosaic virus as biotic stress factor (Chaerle *et al*. 2007c) has been accomplished by multicolour fluorescence imaging. This technique displayed the power to monitor the accumulation of secondary compounds synthesized by the plants upon stress (Lenk *et al*. 2007). Whereas imaging of fluorescence intensity is an established tool in plant stress detection, imaging of fluorescence lifetime on macroscopic level for such purposes is rudimental. In contrast to lifetime evaluation at microscopic level, no commercial system is available.

4 Objectives of the study

Nitrogen management as well as the control of leaf rust and powdery mildew are cultivation methods of major significance in wheat production. In this context breeding of new cultivars that are resistant to specific abiotic and biotic stresses has received more attention. Therefore, detection of plant stress, differentiation between compatible and incompatible pathogen-plant interaction as well as discrimination between biotic and abiotic stress is essential. In this context, non-destructive, optical, sensor based systems for evaluation of plant physiological status have been developed and adopted. However, several challenges are still remaining, and existing approaches need to be improved and their potential further exploited. In this study the Pulse-Amplitude-Modulated (PAM) fluorescence imaging and the Laser-Induced-Fluorescence (LIF) technique were used to elucidate temporal and spatial modifications in fluorescence signals upon stress events in wheat (*Triticum aestivum* L.) genotypes cultivated under controlled conditions. The influence of economically important pathogens (*Blumeria graminis* and *Puccinia triticina*) and N-deficiency as representative biotic and abiotic stresses affecting plant photosynthesis and quantitative changes in plant secondary metabolism was thereby investigated.

Aim of the study was to elucidate the following hypotheses:

1. Wheat (*Triticum aestivum*) cultivars with distinct levels of resistance to leaf rust (*Puccinia triticina*) can be discriminated between by imaging chlorophyll

fluorescence. As basis for these experiments, the impact of inoculum density in a multi-temporal approach on the characteristic fluorescence readings of sensitive and resistant genotypes was examined. As there is a lack of information, we addressed the question of whether there is a physical masking effect due to spore layer and density on absolute and relative chlorophyll fluorescence parameters.

2. Assuming pathogen induced changes in the characteristic spectral fluorescence signature between 350 and 820 nm, we hypothesized that fluorescence spectroscopy is a suitable method to early detect leaf rust (*Puccinia triticina*) on wheat. Based on the specificity of pathogen-plant interactions, we postulated that determination of fluorescence ratios and mean lifetime of fluorophores enables a reliable discrimination between susceptible and resistant wheat cultivars to leaf rust.

3. In a following study we hypothesized that the combined information of UV-induced fluorescence spectra and fluorescence lifetime enables the detection of powdery mildew (*Blumeria graminis*) infection on wheat plants shortly after inoculation. We furthermore claimed that discrimination among wheat genotypes that are either resistant or susceptible to powdery mildew is feasible.

4. Finally, we hypothesized that differentiation between the physiological reaction of wheat plants to N-deficiency and leaf rust (*Puccinia triticina*) as well as N-deficiency and powdery mildew (*Blumeria graminis*) might be accomplished by means of UV-induced fluorescence spectral measurements in the blue, green and yellow range (370 to 620 nm) in addition to the chlorophyll fluorescence (640 to 800 nm). Thereby we focused on a slight N-deficiency and the early stages of pathogen infection, justifying the need of sensors to detect pre-symptomatic stress-induced modifications.

5 References

Agrios GN (2005) Plant Pathology. New Delhi: Elsevier Academic Press, 922 pp.

Amberger A (1996) Pflanzenernährung. Stuttgart: Ulmer, 235 pp.

Anker CC and Niks RE (2001) Prehaustorial resistance to the wheat leaf rust fungus, *Puccinia triticina*, in *Triticum monococcum* (s.s.). Euphytica 117:209-215

Baker NR and Rosenqvist E (2004) Application of chlorophyll fluorescence can improve crop

production strategies: an examination of future possibilities. Journal of Experimental Botany 55:1607-1621

Baker N (2008) Chlorophyll fluorescence: a probe of photosynthesis *in vivo*. Annual Review of Plant Biology 59:89-113

Belasque Jr J, Gasparoto MCG, Marcassa LG (2008) Detection of mechanical and disease stresses in citrus plants by fluorescence spectroscopy. Applied Optics 47:1922-1926

Bennett F (1984) Resistance to powdery mildew in wheat: a review of its use in agriculture and breeding programmes. Plant Pathology 33:279-300

Berger S, Sinha AK, Roitsch T (2007) Plant physiology meets phytopathology: plant primary metabolism and plant-pathogen interactions. Journal of Experimental Botany 58:4019-4026

Bodria L, Fiala M, Oberti R, Naldi E (2002) Chlorophyll fluorescence sensing for early detection of crop´s diseases symptoms. In: Proceedings ASAE Annual International Meeting and CIGR XVth World Congress, 2002, (pp. 1-15). St. Joseph, Michigan: American Society of Agricultural and Biological Engineers

Bolton MD, Kolmer JA, Garvin DF (2008) Wheat leaf rust caused by *Puccinia triticina*. Molecular Plant Pathology 9:563-575

Börner H (1990) Pflanzenkrankheiten und Pflanzenschutz. Stuttgart: Ulmer, 464 pp.

Bravo C, Moshou D, Oberti R, West J, McCartney A, Bodria L, Ramon H (2004) Foliar disease detection in the field using optical sensor fusion. Agricultural Engineering International: the CIGR Journal of Scientific Research and Development, 6

Brown P, Graham R, Nicholas D (1984) The effects of managanese and nitrate supply on the levels of phenolics and lignin in young wheat plants. Plant and Soil 81:437-440

Buschmann C (1999) Photochemical and non-photochemical quenching coefficients of the chlorophyll fluorescence: comparison of variation and limits. Photosynthetica 37:217-224

Buschmann C (2007) Variability and application of the chlorophyll fluorescence emission ratio red/far-red of leaves. Photosynthesis Research 92:261-271

Buschmann C, Langsdorf G, Lichtenthaler HK (2000) Imaging of the blue, green, and red fluorescence emission of plants: an overview. Photosynthetica 38:483-491

Buschmann C, Langsdorf G, Lichtenthaler HK (2009) Fluorescence: the blue, green, red and far-red fluorescence signatures of plant tissues, their multicolour fluorescence imaging and application for agrofood assessment. In: Optical monitoring of fresh and processed agricultural crops, Zude M (Ed.). Boca Raton: CRS Press, Taylor & Francis

Group, 272-319

Buschmann C and Lichtenthaler HK (1998) Principles and characteristics of multi-colour fluorescence imaging of plants. Journal of Plant Physiology 152:297-314

Bushnell W (2002) The role of powdery mildew research in understanding host-parasite interaction: past, present and future. In: The powdery mildews. A comprehensive treatise, Bélanger R, Bushnell W, Dik A, Carver T (Eds.). St. Paul, Minnesota: APS Press, 1-12

Cartelat A, Cerovic ZG, Goulas Y, Meyer S, Lelarge C, Prioul J, Barbottin A, Jeuffroy M, Gate P, Agati G (2005) Optically assessed contents of leaf polyphenolics and chlorophyll as indicators of nitrogen deficiency in wheat (*Triticum aestivum* L.). Field Crops Research 91:35-49

Cassman K, Dobermann A, Walters D (2002) Agroecosystems, nitrogen-use efficiency, and nitrogen management. Ambio 31:132-140

Cerovic ZG, Samson G, Morales F, Tremblay N, Moya I (1999) Ultraviolet-induced fluorescence for plant monitoring: present state and prospects. Agronomie 19:543-578

Chaerle L, Hagenbeek D, De Bruyne E, Valcke R, Van der Straeten D (2004) Thermal and chlorophyll-fluorescence imaging distinguish plant-pathogen interactions at an early stage. Plant Cell Physiology 45:887-896

Chaerle L, Hagenbeek D, De Bruyne E, Van Der Straeten D (2007a) Chlorophyll fluorescence imaging for disease-resistance screening of sugar beet. Plant Cell, Tissue and Organ Culture 91:97-106

Chaerle L, Hagenbeek D, Vanrobaeys X, Van der Straeten D (2007b) Early detection of nutrient and biotic stress in *Phaseolus vulgaris*. International Journal of Remote Sensing 28:3479-3492

Chaerle L, Lenk S, Hagenbeek D, Buschmann C, Van Der Straeten D (2007c) Multicolour fluorescence imaging for early detection of the hypersensitive reaction to tobacco mosaic virus. Journal of Plant Physiology 164:253-262

Chaerle L and Van Der Straeten D (2000) Imaging techniques and the early detection of plant stress. Trends in Plant Science 5:495-501

Chappelle EW, McMurtrey III JE, Wood Jr FM, Newcomb WW (1984a) Laser-induced fluorescence of green plants. 2: LIF caused by nitrient deficiencies in corn. Applied Optics 23:139-142

Chappelle EW, Wood Jr FM, McMurtrey III JE, Newcomb WW (1984b) Laser-induced fluorescence of green plants. 1: A technique for the remote detection of plant stress

and species differentiation. Applied Optics 23:134-138

Dixon J, Braun H-J, Kosina P, Crouch J (2009) Wheat facts and futures 2009. Mexico: CIMMYT, 95 pp.

Edwards H and Allen P (1966) Distribution of the products of photosynthesis between powdery mildew and barley. Plant Physiology 41:683-688

Eichmann R and Hückelhoven R (2008) Accommodation of powdery mildew fungi in intact plant cells. Journal of Plant Physiology 165:5-18

Engels C and Marschner H (1995) Plant uptake and utilization of nitrogen. In: Nitrogen fertilization in the environment, Bacon P (Ed.). New York: Marcel Dekker, Inc., 41-81

Epstein E and Bloom AJ (2005) Mineral nutrition of plants: principles and perspectives. Sunderland, Massachusetts: Sinauer Associates, Inc., 400 pp.

Evans J (1983) Nitrogen and photosynthesis in the flag leaf of wheat (*Triticum aestivum* L.). Plant Physiology 72:297-302

Gitelson A, Buschmann C, Lichtenthaler HK (1998) Leaf chlorophyll fluorescence corrected for re-absorption by means of absorption and reflectance measurements. Journal of Plant Physiology 152:283-296

Goodwin R (1953) Fluorescent substances in plants. Annual Review of Plant Physiology 4:283-304

Goulas Y, Moya I, Schmuck G (1990) Time-resolved spectroscopy of the blue fluorescence of spinach leaves. Photosynthesis Research 25:299-307

Govindjee (2004) Chlorophyll a fluorescence: a bit of basics and history. In: Chlorophyll a Fluorescence: A signature of photosynthesis, Papageorgiou GC and Govindjee (Eds.). Dordrecht: Springer, 1-42

Gustafson G and Shaner G (1982) Influence of plant age on the expression of slow-mildewing resistance in wheat. Phytopathology 72:746-749

Halse N, Greenwood E, Lapins P, Boundy C (1969) An analysis of the effects of nitrogen deficiency on the growth and yield of a Western Australian wheat crop. Australian Journal of Agricultural Research 20:987-998

Hartleb H, Heitefuss R, Hoppe H-H (1997) Utilisation of resistant cultivars as components of integrated crop protection. In: Resistance of crop plants against fungi, Hartleb H, Heitefuss R, Hoppe H-H (Eds.). Jena: Gustav Fischer, 449-469

Heisel F, Sowinska M, Miehé JA, Lang M, Lichtenthaler HK (1996) Detection of nutrient deficiencies of maize by laser induced fluorescence imaging. Journal of Plant Physiology 148:622-631

Heitefuss R (1997a) Cell wall modification in relation to resistance. In: Resistance of crop plants against fungi, Hartleb H, Heitefuss R, Hoppe H-H (Eds.). Jena: Gustav Fischer, 100-125

Heitefuss R (1997b) General principles of host-parasite interactions. In: Resistance of crop plants against fungi, Hartleb H, Heitefuss R, Hoppe H-H (Eds.). Jena: Gustav Fischer, 19-32

Heitefuss R (2001) Defence reactions of plants to fungal pathogens: principles and perspectives, using powdery mildew on cereals as an example. Naturwissenschaften 88:273-283

Herrmann K and Weaver L (1999) The shikimate pathway. Annual Review of Plant Physiology and Plant Molecular Biology 50:473-503

Holzwarth A (1986) Fluorescence lifetimes in photosynthetic systems. Photochemistry and Photobiology 43:707-725

Horbach R, Navarro-Quesada A, Knogge W, Deising H (2010) When and how to kill a plant cell: Infection strategies of plant pathogenic fungi. Journal of Plant Physiology 168:51-62

Hsam S and Zeller F (2002) Breeding for powdery mildew resistance in common wheat (*Triticum aestivum* L.). In: The powdery mildews. A comprehensive treatise, Bélanger R, Bushnell W, Dik A, Carver T (Eds.). St. Paul, Minnesota: APS Press, 219-238

Hu G and Rijkenberg FHJ (1998) Scanning electron microscopy of early infection structure formation by *Puccinia recondita* f. sp. *tritici* on and in susceptible and resistant wheat lines. Mycological Research 102:391-399

Huang X and Röder M (2004) Molecular mapping of powdery mildew resistance genes in wheat: a review. Euphytica 137:203-223

Jacobs T (1990) Abortion of infection structures of wheat leaf rust in susceptible and partially resistant wheat genotypes. Euphytica 45:81-86

Jacobs T and Buurlage MB (1990) Growth of wheat leaf rust colonies in susceptible and partially resistant spring wheats. Euphytica 45:71-80

Jansen M, Gilmer F, Biskup B, Nagel K, Rascher U, Fischbach A, Briem S, Dreissen G, Tittmann S, Braun S, De Jaeger I, Metzlaff M, Schurr U, Scharr H, Walter A (2009) Simultaneous phenotyping of leaf growth and chlorophyll fluorescence via GROWSCREEN FLUORO allows detection of stress tolerance in *Arabidopsis thaliana* and other rosette plants. Functional Plant Biology 36:902-914

Kloppers F and Pretorius Z (1997) Effects of combinations amongst genes *Lr13*, *Lr34* and

Lr37 on components of resistance in wheat to leaf rust. Plant Pathology 46:737-750

Kluge E, Enzian S, Gutsche V (1999) Befallsatlas: Atlas der potentiellen Befallsgefährdung durch wichtige Schadorganismen im Ackerbau Deutschlands. Ribbesbüttel: Saphir Verlag, 160 pp.

Koch C, Noga G, Strittmatter G (1994) Photosynthetic electron transport is differentially affected during early stages of cultivar/race-specific interactions between potato and *Phytophthora infestans*. Planta 193:551-557

Kolmer J, Chen X, Jin J (2009) Diseases which challenge global wheat production - the wheat rusts. In: Wheat: science and trade, Carver B (Ed.). Ames: Wiley-Blackwell, 89-124

Kress M, Meier T, Steiner R, Dolp F, Erdmann R, Ortmann U, Rück A (2003) Time-resolved microspectrofluorometry and fluorescence lifetime imaging of photosensitizers using picosecond pulsed diode lasers in laser scanning microscopes. Journal of Biomedical Optics 8:26-32

Kruger W, Carver T, Zeyen R (2002) Effects of inhibiting phenolic biosynthesis on penetration resistance of barley isolines containing seven powdery mildew resistance genes or alleles. Physiological and Molecular Plant Pathology 61:41-51

Kshirsagar A, Reid AJ, McColl SM, Saunders VA, Whalley JS, Evans EH (2001) The effect of fungal metabolites on leaves as detected by chlorophyll fluorescence. New Phytologist 151:451-457

Kuckenberg J, Tartachnyk I, Schmitz-Eiberger M, Noga G (2007) UV-B induced damage and recovery processes in apple leaves as assessed by LIF and PAM fluorescence techniques. Journal of Applied Botany and Food Quality 81:77-85

Kuckenberg J, Tartachnyk I, Noga G (2009a) Temporal and spatial changes of chlorophyll fluorescence as a basis for early and precise detection of leaf rust and powdery mildew infections in wheat leaves. Precision Agriculture 10:34-44

Kuckenberg J, Tartachnyk I, Noga G (2009b) Detection and differentiation of nitrogen-deficiency, powdery mildew and leaf rust at wheat leaf and canopy level by laser-induced chlorophyll fluorescence. Biosystems Engineering 103:121-128

Kumke M and Löhmannsröben H-G (2009) Fluorescence - Introduction. In: Optical monitoring of fresh and processed agricultural crops, Zude M (Ed.). Boca Raton: CRS Press, Taylor & Francis Group, 253-271

Lakowicz JR (2006) Principles of fluorescence spectroscopy. New York: Springer Science + Business Media, 954 pp.

Lang M, Stober F, Lichtenthaler HK (1991) Fluorescence emission spectra of plant leaves and

plant constituents. Radiation and Environmental Biophysics 30:333-347

Lenk S, Chaerle L, Pfündel EE, Langsdorf G, Hagenbeek D, Lichtenthaler HK, Van Der Straeten D, Buschmann C (2007) Multispectral fluorescence and reflectance imaging at the leaf level and its possible applications. Journal of Experimental Botany 58:807-814

Lichtenthaler HK, Buschmann C, Knapp M (2005) How to correctly determine the different chlorophyll fluorescence parameters and the chlorophyll fluorescence decrease ratio R_{Fd} of leaves with the PAM fluorometer. Photosynthetica 43:379-393

Lichtenthaler HK and Miehé JA (1997) Fluorescence imaging as a diagnostic tool for plant stress. Trends in Plant Science 2:316-320

Lichtenthaler H and Schweiger J (1998) Cell wall bound ferulic acid, the major substance of the blue-green fluorescence emission of plants. Journal of Plant Physiology 152:272-282

Lichtenthaler HK, Subhash N, Wenzel O, Miehé JA (1997) Laser-induced imaging of blue/red and blue/far-red fluorescence ratios, F440/F690 and F440/F740, as a means of early stress detection in plants. Geoscience and Remote Sensing, 1997. IGARSS '97. Remote Sensing - A Scientific Vision for Sustainable Development, 1997 IEEE International 4:1799-1801

Lin M and Edwards H (1974) Primary penetration process in powdery mildewed barley related to host cell age, cell type, and occurrence of basic staining material. New Phytologist 73:131-137

Lindenthal M, Steiner U, Dehne H-W, Oerke E-C (2005) Effect of downy mildew development on transpiration of cucumber leaves visualized by digital infrared thermography. Phytopathology 95:233-240

Liu Z, Sun Q, Ni Z, Yang T (1999) Development of SCAR markers linked to the *Pm10* gene conferring resistance to powdery mildew in common wheat. Plant Breeding 118:215-219

Lüdeker W, Dahn H-G, Günther KP (1996) Detection of fungal infection of plants by laser-induced fluorescence: an attempt to use remote sensing. Journal of Plant Physiology 148:579-585

Mahlein A-K, Steiner U, Dehne H-W, Oerke E-C (2010) Spectral signatures of sugar beet leaves for the detection and differentiation of diseases. Precision Agriculture 11:413-431

Marschner H (2002) Mineral nutrition of plants. London, San Diego (California): Elsevier

Academic Press, 889 pp.

Marshall D (2009) Diseases which challenge global wheat production - powdery mildew and leaf and head blights. In: Wheat: science and trade, Carver B (Ed.). Ames: Wiley-Blackwell, 155-169

Martinez F, Niks R, Singh R, Rubiales D (2001) Characterization of *Lr46*, a gene conferring partial resistance to wheat leaf rust. Hereditas 135:111-114

Martinez F, Sillero JC, Rubiales C (2004) Effect of host plant resistance on haustorium formation in cereal rust fungi. Journal of Phytopathology 152:381-382

Maxwell K and Johnson GN (2000) Chlorophyll fluorescence - a practical guide. Journal of Experimental Botany 51:659-668

Mishra KB, Gopal R (2005) Study of laser-induced fluorescence signatures from leaves of wheat seedlings growing under cadmium stress. General and Applied Plant Physiology 31:181-196

Mishra KB, Gopal R (2008) Detection of nickel-induced stress using laser-induced fluorescence signatures from leaves of wheat seedlings. International Journal of Remote Sensing 29:157-173

Morales F, Cerovic ZG, Moya I (1994) Characterization of blue-green fluorescence in the mesophyll of sugar beet (*Beta vulgaris* L.) leaves affected by iron deficiency. Plant Physiology 106:127-133

Nicholson R and Hammerschmidt R (1992) Phenolic compounds and their role in disease resistance. Annual Review of Phytopathology 30:369-389

Nicot P, Bardin M, Dik A (2002) Basic methods for epidemiological studies of powdery mildews: culture and preservation of isolates, production and delivery of inoculum, and disease assessment. In: The powdery mildews. A comprehensive treatise, Bélanger R, Bushnell W, Dik A, Carver T (Eds.). St. Paul, Minnesota: APS Press, 83-99

Noomnarm U and Clegg R (2009) Fluorescence lifetimes: fundamentals and interpretations. Photosynthesis Research 101:181-194

Obst A and Gehring K (2002) Getreide: Krankheiten, Schädlinge, Unkräuter. Gelsenkirchen: Verlag Th Mann, 256 pp.

Peng S, Garcia F, Laza R, Sanico A, Visperas R, Cassman K (1996) Increased N-use efficiency using a chlorophyll meter on high-yielding irrigated rice. Field Crops Research 47:243-252

Rascher U, Nichol C, Small C, Hendricks L (2007) Monitoring spatio-temporal dynamics of

photosynthesis with a portable hyperspectral imaging system. Photogrammetric Engineering and Remote Sensing 73:45-56

Reifschneider F and Boiteux L (1988) A vacuum-operated settling tower for inoculation of powdery mildew fungi. Phytopathology 78:1463-1465

Roelfs AP, Singh RP, Saari EE (1992) Rust diseases of wheat: concepts and methods of disease management. Mexico, DF: CIMMYT, 81 pp.

Rost FWD (1995) Autofluorescence in plants, fungi and bacteria. In: Fluorescence microscopy, Volume II, Rost FWD (Ed.). Cambridge, New York, Melbourne: Cambridge University Press, 16-39

Sander J and Heitefuss R (1998) Suceptibility to *Erysiphe graminis* f. sp *tritici* and phenolic acid content of wheat as influenced by different levels of nitrogen fertilization. Journal of Phytopathology 146:495-507

Sankaran S, Mishra A, Ehsani R, Davis C (2010) A review of advanced techniques for detecting plant diseases. Computers and Electronics in Agriculture 72:1-13

Schilling G (2000) Pflanzenernährung und Düngung. Stuttgart: Ulmer, 464 pp.

Schmitz A, Tartachnyk I, Kiewnick S, Sikora R, Kühbauch W (2006) Detection of *Heterodera schachtii* infestation in sugar beet by means of laser-induced and pulse amplitude modulated chlorophyll fluorescence. Nematology 8:273-286

Schmuck G, Moya I, Pedrini A, van der Linde D, Lichtenthaler HK, Stober F, Schindler C, Goulas Y (1992) Chlorophyll fluorescence lifetime determination of water stressed C3- and C4-plants. Radiation and Environmental Biophysics 31:141-151

Schmuck G, Verdebout J, Koechler C, Moya I, Goulas Y (1991) Laser-induced time-resolved fluorescence of vegetation. Geoscience and Remote Sensing, IEEE Transactions on 29:674-678

Schnabel G, Strittmatter G, Noga G (1998) Changes in photosynthetic electron transport in potato cultivars with different field resistance after infection with *Phytophthora infestans*. Journal of Phytopatholgy 146:205-210

Scholes JD and Rolfe SA (2009) Chlorophyll fluorescence imaging as tool for understanding the impact of fungal diseases on plant performance: a phenomics perspective. Functional Plant Biology 36:880-892

Schreiber U (2004) Pulse-Amplitude-Modulation (PAM) fluorometry and saturation pulse method: an overview. In: Chlorophyll a fluorescence: a signature of photosynthesis, Papageorgiou GC and Govindjee (Eds.). Dordrecht: Springer, 279-319

Schurr U, Walter A, Rascher U (2006) Functional dynamics of plant growth and

photosynthesis - from steady state to dynamics - from homogeneity to heterogeneity. Plant, Cell and Environment 29:340-352

Skou J, Jorgensen J, Lilholt U (1984) Comparative studies on callose formation in powdery mildew compatible and incompatible barley. Journal of Phytopathology 109:147-168

Southerton SG and Deverall BJ (1990) Histochemical and chemical evidence for lignin accumulation during the expression of resistance to leaf rust fungi in wheat. Physiological and Molecular Plant Pathology 36:483-494

Subhash N and Mohanan C (1994) Laser-induced red chlorophyll fluorescence signatures as nutrient stress indicator in rice plants. Remote Sensing of Environment 47:45-50

Swarbrick PJ, Schulze-Lefert P, Scholes JD (2006) Metabolic consequences of susceptibility and resistance (race specific and broad spectrum) in barley leaves challenged with powdery mildew. Plant, Cell and Environment 29:1061-1076

Taiz L and Zeiger E (2007) Plant Physiology. Berlin, Heidelberg: Springer, 770 pp.

Tartachnyk I and Rademacher I (2003) Estimation of nitrogen deficiency of sugar beet and wheat using parameters of laser induced and pulse amplitude modulated chlorophyll fluorescence. Journal of Applied Botany 77:61-67

Tartachnyk I, Rademacher I, Kühbauch W (2006) Distinguishing nitrogen deficiency and fungal infection of winter wheat by laser-induced fluorescence. Precision Agriculture 7:281-293

Thordal-Christensen H, Gregersen PL, Messmer M (2000) The barley/*Blumeria* (Syn. Erysiphe) *graminis* interaction. In: Mechanisms of resistance to plant diseases, Slusarenko AJ, Fraser RSS, van Loon LC (Eds.). Dordrecht: Kluwer Academic Publishers, 77-100

Vermerris W and Nicholson R (2006) The role of phenols in plant defence. In: Phenolic compound biochemistry, Vermerris W and Nicholson R (Eds.). Dordrecht: Springer, 222-234

von Röpenack E, Parr A, Schulze-Lefert P (1998) Structural analysis and dynamics of soluble and cell wall-bound phenolics in a broad spectrum resistance to the powdery mildew fungus in barley. The Journal of Biological Chemistry 273:9013-9022

West J, Bravo C, Oberti R, Lemaire D, Moshou D, McCartney HA (2003) The potential of optical canopy measurement for targeted control of field crop diseases. Annual Review of Phytopathology 41:593-614

Yarwood C (1967) Response to parasites. Annual Review of Plant Physiology 18:419-438

Zhang L and Dickinson M (2001) Fluorescence from rust fungi: a simple and effective

method to monitor the dynamics of fungal growth *in planta*. Physiological and Molecular Plant Pathology 59:137-141

Zhang L, Meakin H, Dickinson M (2003) Isolation of genes expressed during compatible interactions between leaf rust (*Puccinia triticina*) and wheat using cDNA AFLP. Molecular Plant Pathology 4:469-477

B Quantum yield of non-regulated energy dissipation in PSII (Y(NO)) for early detection of leaf rust (*Puccinia triticina*) infection in susceptible and resistant wheat (*Triticum aestivum* L.) cultivars

1 Introduction

In the context of precision agriculture, accurate *in situ* detection and differentiation of stress symptoms resulting from pathogen infection, for example, are essential for starting appropriate prevention measures such as the timely application of pesticides. One aim of precision agriculture is to develop techniques for site-specific fertilizer application as well as weed and disease control (Auernhammer 2001; Pierce and Nowak 1999). Specifically, several approaches such as hyperspectral measurements and laser-induced chlorophyll fluorescence (LIF) have been tested, developed and optimized under laboratory and field conditions to enable more precise evaluation of a plant's nutritional status and development of diseases (Kuckenberg *et al*. 2009a, 2009b; Li *et al*. 2010; Mahlein *et al*. 2010). In this context noticeable progress of the 'so called' nitrogen sensors enable the *in situ* detection of N-deficiency in cereals and *on-line* variable-rate application of fertilizers (Steiner *et al*. 2008; Tremblay *et al*. 2009). However, the development of non-invasive and non-destructive technologies requires a good understanding of the physiological status that underlies the measured signals in living tissues (Buschmann and Lichtenthaler 1998).

On the other hand, preliminary measures that assist accurate site-specific procedures are of increasing importance (Lütticken 2000), for example the selection of resistant cultivars to specific stresses such as those caused by pathogens, are an integral component of modern and precise agriculture (Auernhammer 2001; Doll *et al*. 1994). In this context, appropriate genotypes may contribute to reducing variability in the crop and that due to diseases, both of which are important factors in precision agriculture (Zhang *et al*. 2002). In breeding programs, the resistance of new cultivars is tested over several years in field experiments that require high inputs of time and money (Schnabel *et al*. 1998). In general, the severity of plant disease is assessed visually with ordinal rating scales. This time-consuming, qualitative evaluation can be subjective and does not indicate invisible damage to the photosynthetic mechanism of the plant. Furthermore, the rapid advances of genetic engineering and tailored plant breeding, with their potential impact on precision agriculture (Auernhammer 2001), underline the demand for rapid, objective and more precise methods of screening to quantify resistance to stress (Scholes and Rolfe 2009; Steiner *et al*. 2008).

Recently, chlorophyll fluorescence devices have been used to evaluate plant resistance to different abiotic stress situations such as chilling, freezing, ice cover, heat and high light intensity (Petkova *et al*. 2007; Schapendonk *et al*. 1989; Smillie and Hetherington 1983), as well as salinity (Belkhodja *et al*. 1994; Hunsche *et al*. 2010). Furthermore, Schnabel *et al*. (1998) used an imaging chlorophyll fluorescence system to estimate the resistance to stress from infection by *Phytophthora infestans* on leaf disks of potato cultivars. It is rare for entire leaves to be affected at once by pathogen attacks (Lichtenthaler and Miehé 1997). Therefore, changes in plant physiology may be suitably recorded by imaging fluorescence systems that provide spatially resolved information. On this basis, the responses of susceptible and resistant barley leaves infected with powdery mildew have been assessed by electron transport rate (ETR), non-photochemical quenching (NPQ) and effective PSII quantum yield (Y(II)) (Swarbrick *et al*. 2006). However, this work focused on the observation of metabolic consequences and started with the occurrence of visual symptoms. Similarly, Chaerle *et al*. (2007) assessed the plant-fungus interaction of *Cercospora beticola* on attached leaves, leaf stripes and leaf disc assays of sugar-beet cultivars with different levels of resistance using imaging chlorophyll fluorescence and thermal and video cameras.

Regardless of the extensive use of the PAM technology in physiological surveys, the potential of chlorophyll fluorescence imaging for the early detection of leaf rust as well as the discrimination between wheat genotypes based on their level of resistance has been neglected. Wheat is one of the three most cultivated cereal species worldwide, and leaf rust is one of its most common and widespread diseases. Yield losses reflect mainly the periodic occurrence of the disease and susceptibility of cultivars (Devadas *et al*. 2008). One plausible alternative for maximizing the yield is to select wheat genotypes that have adequate resistance to leaf rust (Kolmer *et al*. 2007). In addition to the usual approach for the evaluation of genotypes and new cultivars, we hypothesize that wheat (*Triticum aestivum*) cultivars with distinct levels of resistance to leaf rust (*P. triticina*) can be discriminated between by imaging chlorophyll fluorescence. Screening of genotypes under controlled conditions ensures the reproducibility of the timing of infection and minimizes to a large extent the possibility of simultaneous occurrence of other stresses (Huang *et al*. 2005; Pawelec *et al*. 2006). Furthermore, we studied the impact of inoculum density in a multi-temporal approach on the characteristic fluorescence readings of sensitive and resistant genotypes. It is well known that specific pigments in the cuticle or epidermal cells, such as anthocyanins, may mask the fluorescence signal from chlorophyll molecules in the deeper cell layers (Lichtenthaler *et al*. 1986). As there is a lack of information on the impact of fungal spore suspension density on

fluorescence imaging readings, we addressed the question of whether there is a physical masking effect due to spore density on absolute and relative chlorophyll fluorescence parameters.

2 Materials and Methods

2.1 Plant material and growth conditions

Experiments were conducted in a controlled-environment cabinet under a 14 h photoperiod and 200 µmol m^{-2} s^{-1} photosynthetic active radiation (PAR; Philips PL-L 36 W fluorescent lamps, Hamburg, Germany), day/night temperature regimes of 20/15 ± 2°C and relative humidity of 75/80 ± 10%. Seeds of winter wheat (*Triticum aestivum* L. emend. Fiori. et Paol.) were sown in 0.44 l square Teku-Pots (Pöppelmann GmbH & Co. KG, Lohne, Germany) filled with perlite, at the rate of 5 seeds per pot. Selection of cultivars was based on the resistance degree (RD) given by the German Federal Plant Variety Office [Bundessortenamt] (2008) on a scale ranging from one to nine. The rust-susceptible cultivar Dekan (RD = 8) and the rust-resistant cultivar Retro (RD = 3) were chosen. Emerging plants were provided with a Hoagland nutrient solution every two days. Twenty days after sowing, when plants had reached the three-leaf stage, the youngest fully expanded leaf of one plant per pot was selected for inoculation with leaf rust.

2.2 Chlorophyll fluorescence measurements

Readings of chlorophyll fluorescence were taken with a pulse amplitude modulated (PAM) imaging chlorophyll fluorometer (Heinz-Walz GmbH, Effeltrich, Germany). The light source for fluorescence excitation and actinic illumination contains 96 blue light diodes emitting at 470 nm. The fluorescence images were recorded by a black and white CCD (8.458 mm chip with 640 x 480 pixels) camera operated in 10-bit-mode at 30 frames per second. Daily measurements of the fast fluorescence parameters F_o (ground fluorescence), F_m (maximum fluorescence) and the slow fluorescence induction kinetic parameters were made on plants adapted to the dark for 60 min until the first small red-brown pustules appeared in the centre of chlorotic spots. Details of the measuring procedure, pathogen inoculation, as well as data evaluation and analysis are given below.

In general, parameters of the slow chlorophyll fluorescence kinetic are more sensitive in the early detection of stress (Schreiber 2004). Preliminary tests to evaluate both cultivars, Dekan and Retro, indicated reliable discrimination between control and infected leaves with

the fluorescence parameter Y(NO). The Y(NO) describes the quantum yield of non-regulated energy dissipation in photosystem II (PSII) and is calculated according to Kramer *et al*. (2004) by the equation:

$$Y(NO) = 1/(NPQ+1+q_L(F_m/F_o-1)), \quad (1)$$

where

$$NPQ = (F_m-F_m')/F_m' \quad (2)$$

and

$$q_L = (F_m'-F)/(F_m'-F_o') \times F_o'/F. \quad (3)$$

2.3 Experiments using undefined spore concentration

With this approach an undefined large amount of *P. triticina* spores (non-specific mixture of spores produced on wheat without known resistance genes) was applied with a fine-brush on a predefined area of horizontally fixed leaves to form a layer of spores. Following this, water was atomized above the leaves and the plastic micro chamber in which plants were allocated was closed for 24 h to reach a high relative humidity (RH > 98%). Thereafter, the visible spore coat was removed carefully using water and a fine-brush.

Fluorescence acquisition started with the determination of ground fluorescence (F_o; blue light excitation at an intensity of 0.5 µmol m^{-2} s^{-1} PAR) and maximum fluorescence (F_m; blue light saturation pulse of 2400 µmol m^{-2} s^{-1} PAR for 800 ms) before initializing the actinic illumination (265 µmol m^{-2} s^{-1} PAR) after a delay of 40 seconds. Thereafter, saturation pulses (2400 µmol m^{-2} s^{-1} PAR for 800 ms) were applied with repetition every 20 s for the whole recording time of 340 seconds. The last of 17 recorded images was analyzed by ImagingWin v2.21d (Heinz-Walz GmbH, Effeltrich, Germany), with *n* = 20 areas of interest (aoi). Digital pictures of the leaves and fluorescence images were used to interpret the results. Localized modifications in relative fluorescence values, seen by changes in colour (Fig. 1), were marked as circular areas of interest. Corresponding aois were set on the control leaves.

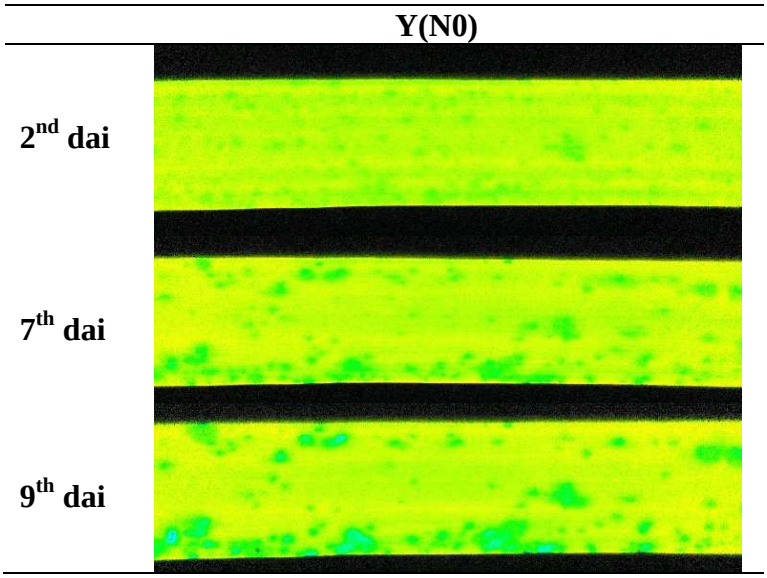

Fig. 1. Image of the impact of leaf rust on the spatial and temporal variation of the quantum yield of non-regulated energy dissipation in PSII, Y(NO), measured with a pulse amplitude modulated imaging chlorophyll fluorometer on the cultivar Retro.

2.4 Experiments using defined spore concentration

2.4.1 Optimization of spore density

Single droplets of spore suspensions were applied onto the wheat leaves to evaluate the extent of physical masking of *P. triticina* inoculum in relation to the spore density and its impact on absolute and relative chlorophyll fluorescence parameters. A non-specific mixture of dead and inactive spores of *P. triticina* was suspended in distilled water containing 0.01% (w/v) of Tween 20 (Merck-Schuchardt, Hohenbrunn, Germany). The spore concentration was estimated microscopically with a Fuchs-Rosenthal counting chamber, and subsequently diluted to the highest concentration required (1 000 000 spores per ml). From this suspension, dilutions of 1:25 (40 000), 1:50 (20 000), 1:75 (13 333), 1:3 (330 000) and 1:9 (111 111) were prepared and droplets applied immediately to predefined areas on the wheat leaves. Two areas per leaf (n = 6 leaves) were marked with a felt-tip pen in the middle of the adaxial leaf half, and within each of these zones a 6 µl droplet of the accordant spore solution or of distilled water + 0.01% Tween 20 (equates 0 spores per ml as control) was deposited gently after an initial fluorescence measurement. The F_o and F_m were determined as described above, followed by the actinic illumination (PAR of 265 µmol m^{-2} s^{-1}) after a delay-time of 30 seconds. Saturation pulses (2400 µmol m^{-2} s^{-1} PAR for 800 ms) during kinetic induction were applied repetitively every 45 s; the total duration of recording was 165 seconds.

Measurements were made when droplets had dried, one hour after application. The masking effect was quantified by setting a circular area of interest (aoi) in the images recorded before and after application of droplets containing *P. triticina* spores or water + Tween 20 solution as reference. The kinetic parameters of the last image, recorded after 165 s were analyzed. Maximal fluorescence (F_m) was selected to represent the absolute fluorescence parameters whereas for relative parameters the quantum yield of non-regulated energy dissipation in PSII (Y(NO)) was chosen.

2.4.2 Inoculum density for differentiation between susceptible and resistant cultivars

In these studies a non-specific mixture of *P. triticina* spores was suspended in distilled water + Tween 20 solution as described above, and subsequently diluted to 100 000 spores per millilitre. From this stock solution three dilutions were prepared using a dilution factor of 5, resulting in 20 000, 4000 and 800 spores per millilitre. Two 6 µl droplets were applied onto the adaxial leaf lamina in the middle of the leaf length, on one half (n = 6 leaves). Control plants were treated with droplets of distilled water + Tween 20. During the inoculation period of 24 h, plants were maintained in the climate chamber under a plastic cover at almost saturated relative humidity.

Fluorescence measurements were made as outlined above in the section 'Experiments using undefined spore concentration', whereas the biological assessment was made using the last of 17 images recorded 300 s after starting actinic illumination. If pathogen-induced changes within the droplet application site were observed, circular areas of interest (aoi) were marked on the infected points and one additional aoi was marked on the healthy tissue next to the application site to serve as reference. For the analysis, the aoi's within the droplet application site were regarded as 'modification of control'. If no changes were detected in response to the application, one aoi covering the whole application site and one aoi beside this circular area were marked.

2.5 Statistical analysis

The experimental data were analyzed by One-way ANOVA with SPSS (PASW statistics version 15.0, SPSS Inc., Chicago, USA). Graphs (mean ± SE) were designed with SigmaPlot 8.02 (Systat Software Inc., Richmond, CA, USA). In the masking experiment, fluorescence means before and after droplet application were compared by analysis of variance (ANOVA, $p \leq 0.05$). In the experiment on biological efficacy a regression analysis

was done for data recorded at 2 dai (days after infection) for each wheat cultivar, with the spore concentration (Ln) as a quantitative factor.

3 Results

3.1 Undefined spore concentration

With this method of inoculation, clear spatial and temporal differences in fungal development on the susceptible and resistant cultivars could be established. Visual evaluations of the pathogen development indicate the first chlorotic spots 4 dai in both cultivars (Fig. 2). In the susceptible cultivar, Dekan, the first small red-brown pustules appeared 6 dai; these became larger and more distinct in the following days. In the resistant cultivar, Retro, the chlorotic spots became progressively larger, conspicuous and were partially necrotic, and by the 7th dai a few pustules became apparent (Fig. 2). At the end of the experiment almost the whole leaf of Dekan showed leaf rust symptoms, whereas the resistant cultivar, Retro, showed an irregular distribution of infected spots on the leaf lamina.

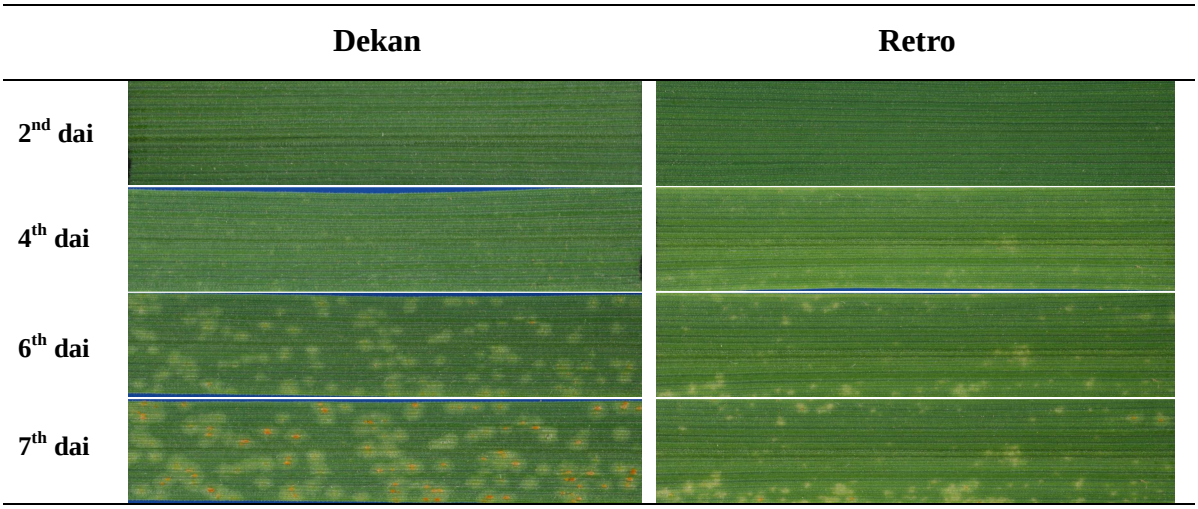

Fig. 2. Digital photographs showing the development of leaf rust on wheat leaves of the susceptible cultivar, Dekan (left) and the resistant cultivar, Retro (right) on the 2nd, 4th, 6th and 7th day after inoculation (dai) with *P. triticina*.

Measurements of chlorophyll fluorescence started 2 dai, when differences in Y(NO) values in infected leaves reached 12.7% compared to control leaves in the cultivar Dekan and 7.9% in leaves of the cultivar Retro (Fig. 3). During the following two days inoculated leaves of both cultivars Dekan and Retro showed significantly higher Y(NO) values than the

respective controls, but no difference between the cultivars was recorded. Thereafter, for Dekan values declined from 11.3% (5 dai) to 3.4% (6 dai), and they finally peaked at 21.5% at the end of the experiment. On the other hand, for Retro the sharp decline to 4.1% and the following increase occurred at 5 dai, which was one day earlier than for Dekan. In addition, evaluations from 5 to 7 dai indicated that differences between the control and inoculated leaves were statistically significant.

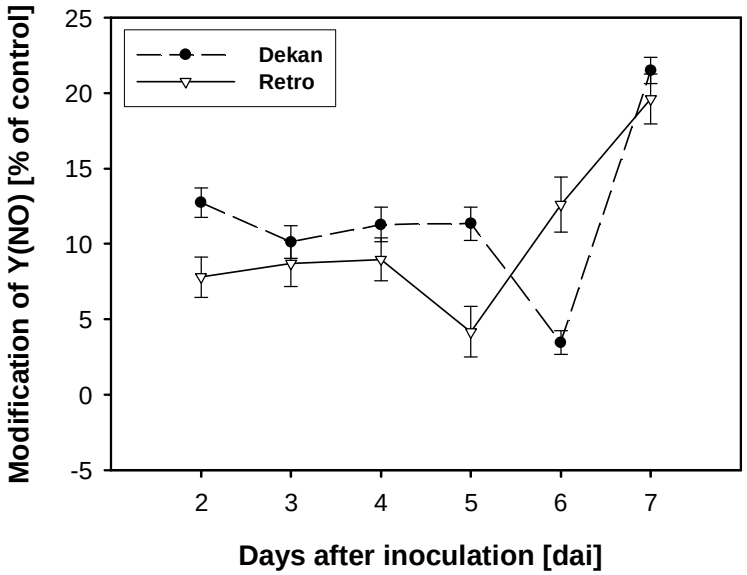

Fig. 3. Modification of the quantum yield of non-regulated energy dissipation in PSII (Y(NO)), given as % of control) in leaves of the susceptible wheat cultivar Dekan (circles, dashed line) and the resistant wheat cultivar Retro (triangles, solid line) inoculated with an undefined concentration of *P. triticina* spores (Mean ± SE). Adapted from Bürling *et al*. 2009.

Although leaf rust was detected successfully as early as 2 dai and both cultivars tested could be differentiated between, there is still some uncertainty because the spore density might have had a significant influence on pathogen infection and physiological responses of the plant. The method of inoculation used in this experiment does not enable spore density to be quantified and is, therefore, not reproducible in terms of applying the same spore amount per unit of area. This limitation accounts for the following experiments using the droplet application procedure with defined concentrations of spores.

3.2 Physical masking of fluorescence with *Puccinia triticina* spores

Our investigations showed that concentrations of both 40 000 and 1 000 000 spores per ml have a significant effect on the absolute fluorescence parameters, reducing F_m values from 0.7 to 0.64 and 0.69 to 0.23, respectively (Table 1). Similarly, light absorption was less at the highest spore concentration (*data not shown*). At densities of 20 000 and 13 333 spores per ml, no significant effect on the parameters evaluated was observed. On the other hand, the highest inoculum density (1 000 000 spores per ml) resulted in a significant increase of Y(NO) values (Table 1). It is noteworthy that in all other treatments no significant difference was recorded between Y(NO) values before and after droplet application.

Table 1. Maximal fluorescence (F_m) and quantum yield of non-regulated energy dissipation in PSII (Y(NO)) measured on wheat leaves before and after application of 6 µl single droplets with defined density of *P. triticina* spores. Measurements were done 1 h after droplet application.

Spore density [spores per ml]	F_m [rel. units]		Y(NO) [rel. units]	
	Before application	After application	Before application	After application
0	0.716 ± 0.005	0.714 ± 0.005	0.311 ± 0.010	0.336 ± 0.018
13 333	0.699 ± 0.009	0.682 ± 0.008	0.347 ± 0.027	0.319 ± 0.020
20 000	0.696 ± 0.007	0.692 ± 0.007	0.340 ± 0.027	0.304 ± 0.014
40 000	0.701 ± 0.007*	0.644 ± 0.008	0.365 ± 0.021	0.334 ± 0.025
1 000 000	0.698 ± 0.009*	0.237 ± 0.025	0.305 ± 0.024*	0.465 ± 0.039

* significant differences between values measured before and after application according to ANOVA, $p \leq 0.05$; Mean ± SE.

In additional experiments inoculum densities of 333 333 and 111 111 spores per ml, which are between the two highest levels of the previous experiment, were chosen. For these, no statistical change in the measured fluorescence parameters was observed. Based on these results, it was decided not to exceed 100 000 spores per ml for assessing the physiological response of plants.

3.3 Biological assessment of leaf rust on susceptible and resistant cultivars

3.3.1 Evaluation of visual symptoms

Visual assessment of leaf rust confirmed the distinct effect of the inoculum concentration for disease establishment and fungal development (*not shown*). In this context, plants of the cultivar Dekan inoculated with 100 000 or 20 000 spores per ml had their first chlorotic spots at five days after inoculation. These spots became larger and more distinct during the next day, and by the 7th dai small red-brown pustules were observed at the centre of these lesions. Plants treated with 4000 spores per ml had chlorotic spots one day later (6 dai). For these plants, pustules also appeared on the 7th dai but to a lesser extent than at the higher spore densities. Plants inoculated with 800 spores per ml showed no visible symptoms until the end of experiment.

The effect of spore density was also confirmed for the cultivar Retro (*not shown*). Here, plants inoculated with 100 000 or 20 000 spores per ml showed their first chlorotic spots one day later than the susceptible cultivar Dekan (6 dai), and they became larger and more distinct within the next 24 hours. In contrast, as observed for Dekan, the spots had a necrotic appearance. At 7 dai, the first pustules appeared on plants inoculated with 20 000 spores per ml, whereas plants inoculated with 4000 or 800 spores per ml remained healthy until the end of the experiment.

3.3.2 Quantum yield of non-regulated energy dissipation (Y(NO))

During the pathogen-plant interaction assessed on the two wheat cultivars, Y(NO) showed changes in plant physiology earlier and with greater robustness than others such as NPQ or Y(II). Similarly, as in the experiment with undefined amounts of spores, physiological changes were detected in infected leaves of both susceptible and resistant cultivars on the first date of measurement (2 dai). However, the degree of modification in Y(NO) clearly depended on the inoculum density. As shown in the regression curves (Fig. 4), the cultivars tested have distinct models when inoculated with low or high densities of spores. Accordingly, the resistant cultivar, Retro, shows only minor changes compared to the control, whereas the susceptible cultivar, Dekan, shows significant differences with increasing spore density.

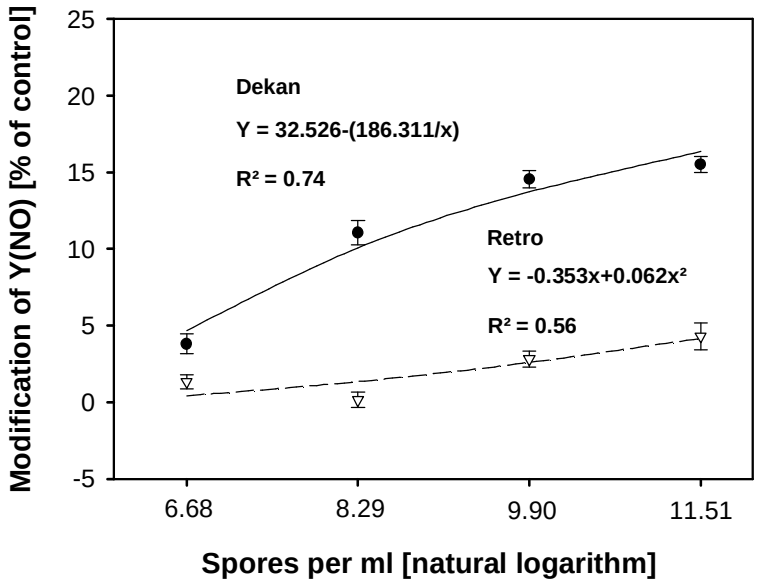

Fig. 4. Modification of the quantum yield of non-regulated energy dissipation in PSII (Y(NO)), given as % of control) in leaves of the susceptible wheat cultivar Dekan (filled circles, solid line) and the resistant wheat cultivar Retro (triangles, dashed line) two days after inoculation with *P. triticina*. Inoculation densities (spores per ml): 800 (Ln = 6.7), 4000 (Ln = 8.3), 20 000 (Ln = 9.9) and 100 000 (Ln = 11.5). Mean ± SE.

Plants of the susceptible cultivar Dekan inoculated with 20 000 or 100 000 spores per ml show a similar response during the whole evaluation period (Fig. 5A). Two days after inoculation, the modification in Y(NO) peaks at 15.5% and 14.5% in the 100 000 spores per ml and 20 000 spores per ml, respectively. In the following two days the values decrease to 9.2% and 8.7%, respectively. The values of Y(NO) increased up to the 7th dai and reached a modification of 14.8% and 14.1%, respectively. As shown in Fig. 5A, the dose of 4000 spores per ml induced changes in fluorescence, however to a lesser extent compared to 20 000 spores per millilitre. Furthermore, the lowest *P. triticina* spore density (800 spores per ml) induced a progressive decrease of Y(NO) values. In the cultivar Retro, densities of 4000 and 800 spores per ml show a similar response with a slight increase in the modification of Y(NO) at the 2nd dai, followed by a slight reduction in the percentage modification, which then remained constant until the end of the experiment. In contrast, the two higher doses of fungal inoculum, 20 000 and 100 000 spores per ml, induced significantly greater changes in Y(NO) values in the period of pre-visual symptoms (Fig. 5B). The former dose of inoculum initially induces a modification of about 3% which increases to 6.3% during the following 24 hours. At the end of the measurement period these values reach a level of 7.9% and 9.7% at the 6th and 7th dai,

respectively. An overall increase in modification of Y(NO) also occurs with a concentration of 100 000 spores per millilitre. In this case, the first two days of measurement show a modification of 4.3% and 4.6%, respectively, and this is almost double by the next day at up to 8.8%. Modifications of Y(NO) decrease to 6.3% until the 7th day after inoculation.

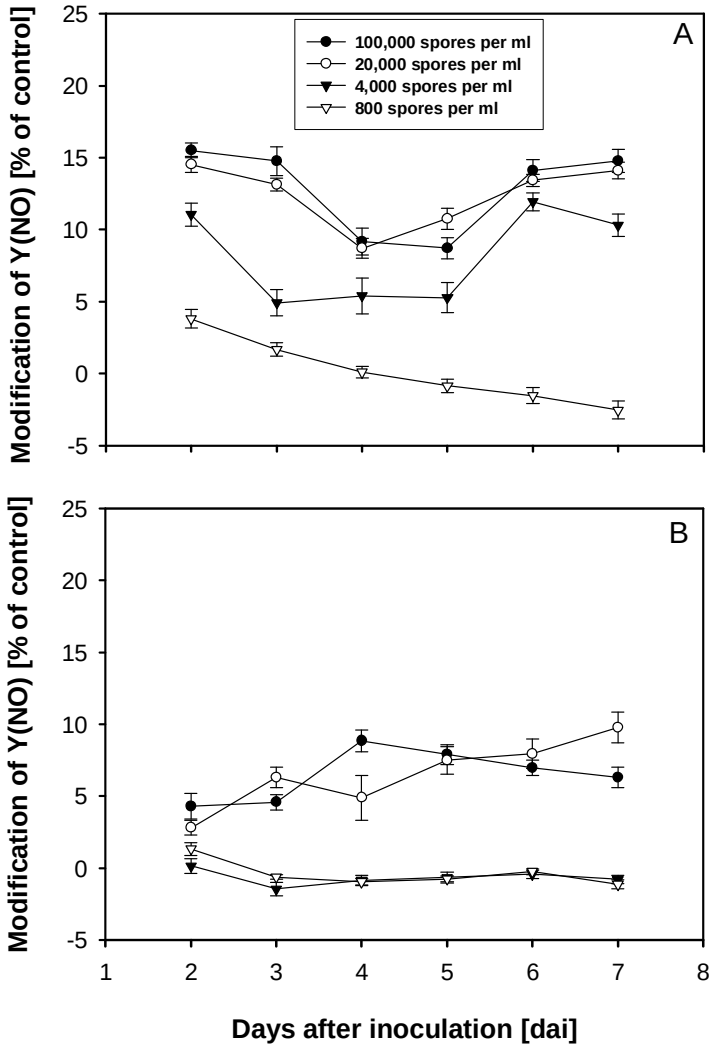

Fig. 5. Modification of the quantum yield of non-regulated energy dissipation in PSII (Y(NO)), given as % of control) in leaves of : **A)** the susceptible wheat cultivar Dekan and **B)** the resistant cultivar Retro inoculated with different densities of *P. triticina* spores during biological assessment (Mean ± SE). Solid circles 100 000 spores per ml, open circles 20 000 spores per ml, solid triangles 4 000 spores per ml and open triangles 800 spores per millilitre.

4 Discussion

In the present study, the suitability of imaging chlorophyll fluorescence was evaluated as a potential tool for screening wheat genotypes with different degrees of resistance to leaf rust. The common approach for screening genotypes for disease resistance is costly and time-consuming, and also prone to changing environmental conditions and the simultaneous occurrence of other undesirable biotic or abiotic stresses. Hence, the development of fast, accurate and objective evaluation protocols to detect stress supports a precision agriculture approach, by for example, enabling rapid screening with a high throughput of new genotypes that are more stable and less prone to the variability caused by pathogens in the field.

In our preliminary studies on the masking effect of the inoculum, the highest spore density of 1 000 000 spores per ml caused a significant increase in Y(NO) values (Table 1); this resulted from the strong decrease in F_o and F_m values that were used to calculate Y(NO) (Eq. 1). Kuckenberg *et al*. (2009a) described a strong reduction in F_o and F_m concomitant with the appearance of pustules on the leaf surface of wheat leaves because of the shielding of plant tissues from excitation light. Alternatively, the main parameters of slow induction kinetics of chlorophyll fluorescence have been discussed extensively in the literature, but information on the value of Y(NO) to assess host-pathogen interaction is lacking. As described by Klughammer and Schreiber (2008), Y(NO) reflects the fraction of energy that is dissipated passively as heat and fluorescence, mainly because of closed PSII reaction centres at saturating light intensity. In this context, large values of Y(NO) reflect a suboptimal capacity of photoprotective reactions.

The results of our experiments using either undefined or defined spore concentrations showed that at the beginning of pathogen infection the capacity of photoprotective reactions, indicated by increased values of Y(NO), was more affected in the susceptible cultivar Dekan than in the resistant one Retro (Figs. 3 and 5). Moreover, the cultivars showed differences in the temporal development of Y(NO) depending on the dose of inoculum (Fig. 4). With a high spore concentration, the larger values of Y(NO) in the susceptible cultivar at 2 dai were followed by a decrease, indicating a delayed onset of the defence mechanisms. At 6 dai, chlorosis was evident on the leaves of the cultivar Dekan, together with the strong decrease in Y(NO). Changes in leaf optical properties might be caused by, for example, the loss of chlorophyll or the development of pustules underneath the leaf surface as well as changes in plant or cell physiology resulting from the pathogen infection. One day earlier (5 dai) when chlorotic spots became necrotic in the resistant cultivar, values of Y(NO) also decreased. In

recent studies on leaf rust susceptible wheat cultivars, an increase in chlorophyll fluorescence after pathogen inoculation has been documented before symptoms appear (Bodria *et al*. 2002; Kuckenberg *et al*. 2009a), which has been attributed to chlorophyll breakdown within the chlorotic patches. As reported for sugar beet infected with *Cercospora beticola*, after an increase in chlorophyll fluorescence a decrease linked to cell death has been observed (Chaerle *et al*. 2007).

According to our results, the lowest density of spores did not induce any locally defined plant reactions as recorded by PAM-chlorophyll fluorescence imaging. The number of spores in a 6 µl droplet (theoretically an average of 4.8 spores) was probably not large enough to establish the disease. Considering the difference in response between the susceptible and resistant cultivars, genotype screening should be done using controlled inoculation densities of 20 000 or 100 000 spores per millilitre. As shown in Fig. 5, the larger the number of spores the stronger is the effect on photosynthetic disturbance in the susceptible cultivar. This resulted in a greater difference between the tested cultivars because the resistant one remained at a more or less continuous level. Hence, the results suggest that the resistant cultivar could avoid damage to PSII more effectively than the susceptible one.

In the past, several research programs adopted microscopic observations to analyse the development of *P. triticina* in susceptible, partially resistant and resistant wheat cultivars, and contributed to the elucidation of some of the resistance mechanisms (Jacobs 1989; Martínez *et al*. 2004; Poyntz *et al*. 1987). In this context, it was shown that the host-pathogen interaction, which depends on the genotype of both plant and fungus, determines the resistance to a great extent (Bolton *et al*. 2008; Kolmer 1997; McIntosh *et al*. 1995; Rubiales and Niks 1995). As already known, genes can increase the early abortion of sporelings as well as reduce the number of haustoria per sporeling and the rate of haustorium formation in the early stages of infection due to papilla formation or a low rate of intercellular hyphal development (Rubiales and Niks 1995). A reduction in the percentage germination of spores as well as cell collapse, cell disintegration and finally necrosis has also been observed (García-Lara *et al*. 2007).

In contrast to most studies on pathogen resistance with well-defined monospore strains, we chose a multispore inoculum. The spore inoculation led to differential pathogen development in the susceptible and resistant cultivars, and early changes in chlorophyll fluorescence values occurred (Fig. 3 and 5). Higher passively dissipated fluorescence and heat emission indicated a stronger disturbance of the PSII reaction centres. At the end of the test with undefined spore concentration, stronger chlorosis, rather necrosis, with just a few pustules in the resistant cultivar Retro indicated papilla formation and cell collapse. Analysis

of the genetic background of the two cultivars and microscopic observations can begin to elucidate the reasons for the higher Y(NO) values in the susceptible cultivar. Moreover, the need for an accurate inoculation protocol, including spore strains and spore density, should not be neglected.

5 Conclusions

Our results show that the quantum yield of non-regulated energy dissipation in PSII (Y(NO)) as measured by a PAM imaging fluorometer is valuable for screening wheat plants for leaf rust resistance. The susceptible cultivar Dekan showed a stronger modification of Y(NO) than the resistant cultivar Retro. The most appropriate time for a reliable differentiation between the cultivars is the 2nd dai, when differences are large and changes in leaf optical properties are negligible. This is also supported by the fact that both inoculation methods reveal the same trend for this point of time, even if differences in development over time (2 to 7 dai) were noticed. The use of spore densities of up to 20 000 spores per ml with fast fluorescence kinetic parameters and up to 100 000 spores per ml with slow fluorescence kinetic parameters are adequate without producing any physical masking. Nevertheless, to establish an accurate and reliable evaluation protocol, further assay optimization, essentially on symptom development, and a wider selection of cultivars need to be investigated. Therefore, several wheat genotypes known to differ in their reaction to *P. triticina* should be evaluated at the first stage to test the accuracy of the technique to differentiate compatible and incompatible pathogen-plant interaction. Following this a differentiation between genotypes with different levels of resistance or susceptibility should be determined. The adoption of screening protocols as suggested in this study will have a positive impact on precision agriculture both directly and indirectly. However, the use of such methods under field conditions requires the development of complex instrumentation for non-contact measurements. Other aspects of precision agriculture have shown that there is about ten years between the first research activities and the development of commercial sensors (Reyns *et al*. 2002). Our studies are in the initial phase of trying to understand physiological changes due to cultivar resistance. In the future, new mathematical algorithms and further developments in sensor technology could enable fast and robust determination of complex fluorescence parameters such as Y(NO) to be implemented in screening systems with a high throughput.

6 References

Auernhammer H (2001) Precision agriculture – the environmental challenge. Computers and Electronics in Agriculture 30:31-43

Belkhodja R, Morales F, Abadía A, Gómez-Aparisi J, Abadía J (1994) Chlorophyll fluorescence as a possible tool for salinity tolerance screening in barley (*Hordeum vulgare* L.). Plant Physiology 104:667-673

Bodria L, Fiala M, Oberti R, Naldi E (2002) Chlorophyll fluorescence sensing for early detection of crop´s diseases symptoms. In: Proceedings ASAE Annual International Meeting and CIGR XVth World Congress, 2002, (pp. 1-15). St. Joseph, Michigan: American Society of Agricultural and Biological Engineers

Bolton MD, Kolmer JA, Garvin DF (2008) Wheat leaf rust caused by *Puccinia triticina*. Molecular Plant Pathology 9:563-575

Buschmann C and Lichtenthaler HK (1998) Principles and characteristics of multi-colour fluorescence imaging of plants. Journal of Plant Physiology 152:297-314

Bürling K, Hunsche M, Noga G (2009) Early detection of *Puccinia triticina* infection in susceptible and resistant wheat cultivars by chlorophyll fluorescence imaging technique. In: Precision Agriculture ´09, van Henten EJ, Goense D, Lokhorst C (Eds.). Wageningen: Wageningen Academic Publishers, 243-249

Chaerle L, Hagenbeek D, De Bruyne E, Van Der Straeten D (2007) Chlorophyll fluorescence imaging for disease-resistance screening of sugar beet. Plant Cell, Tissue and Organ Culture 91:97-106

Devadas R, Lamb DW, Simpfendorfer S, Backhouse D (2008) Evaluating ten spectral vegetation indices for identifying rust infection in individual wheat leaves. Precision Agriculture 10:459-470

Doll H, Holm U, Sogaard B, Bay H (1994) Phenolic compounds in barley varieties with different degree of partial resistance against powdery mildew. Acta Horticulturae 381:576-582

García-Lara E, Leyva-Mir SG, Càrdenas-Soriano E, Huerta-Espino J, Sandoval-Islas JS, Villasenor-Mir E (2007) Infection process to wheat leaf rust (*Puccinia triticina* Erikson) in genotypes with partial resistance. Agrociencia 41:775-785

German Federal Plant Variety Office [Bundessortenamt] (2008) Beschreibende Sortenliste – Getreide, Mais, Ölfrüchte, Leguminosen und Hackfrüchte außer Kartoffeln. Hannover: Deutscher Landwirtschaftsverlag GmbH

Huang S, Vleeshouwers V, Visser RGF, Jacobsen E (2005) An accurate in vitro assay for high-throughput disease testing of *Phytophthora infestans* in potato. Plant Disease 89:1263–1267

Hunsche M, Bürling K, Saied AS, Schmitz-Eiberger M, Sohail M, Gebauer J, Noga G, Buerkert A (2010) Effects of NaCl on surface properties, chlorophyll fluorescence and light remission, and cellular compounds of *Grewia tenax* (Forssk.) Fiori and *Tamarindus indica* L. leaves. Plant Growth Regulation 61:253-263

Jacobs T (1989) Germination and appressorium formation of wheat leaf rust on susceptible, partially resistant and resistant wheat seedlings and on seedlings of other Gramineae. Netherlands Journal of Plant Pathology 95:65-71

Klughammer C and Schreiber U (2008) Complementary PS II quantum yields calculated from simple fluorescence parameters measured by PAM fluorometry and the saturation pulse method. PAM Application Notes 1:27-35

Kolmer JA (1997) Virulence in *Puccinia recondita* f. sp. *tritici* isolates from Canada to genes for adult-plant resistance to wheat leaf rust. Plant Disease 81:267-271

Kolmer JA, Long DL, Hughes ME (2007) Physiologic specialization of *Puccinia triticina* on wheat in the United States in 2005. Plant Disease 918:979-984

Kramer DM, Johnson G, Kiirats O, Edwards GE (2004) New fluorescence parameters for the determination of QA redox state and excitation energy fluxes. Photosynthesis Research 79:209-218

Kuckenberg J, Tartachnyk I, Noga G (2009a) Temporal and spatial changes of chlorophyll fluorescence as a basis for early and precise detection of leaf rust and powdery mildew infections in wheat leaves. Precision Agriculture 10:34-44

Kuckenberg J, Tartachnyk I, Noga G (2009b) Detection and differentiation of nitrogen-deficiency, powdery mildew and leaf rust at wheat leaf and canopy level by laser-induced chlorophyll fluorescence. Biosystems Engineering 103:121-128

Li F, Miao Y, Hennig SD, Gnyp ML, Chen X, Jia L, Bareth G (2010) Evaluating hyperspectral vegetation indices for estimating nitrogen concentration of winter wheat at different growth stages. Precision Agriculture 11:335-357

Lichtenthaler HK, Buschmann C, Rinderle U, Schmuck G (1986) Application of chlorophyll fluorescence in ecophysiology. Radiation and Environmental Biophysics 25:297-308

Lichtenthaler HK and Miehé JA (1997) Fluorescence imaging as a diagnostic tool for plant stress. Trends in Plant Science 2:316-320

Lütticken RE (2000) Automation and standardisation of site specific soil sampling. Precision

Agriculture 2:179-188.

Mahlein A-K, Steiner U, Dehne H-W, Oerke E-C (2010) Spectral signatures of sugar beet leaves for the detection and differentiation of diseases. Precision Agriculture 11:413-431

Martínez F, Sillero JC, Rubiales C (2004) Effect of host plant resistance on haustorium formation in cereal rust fungi. Journal of Phytopathology 152:381-382

McIntosh RA, Wellings CR, Park RF (1995) Wheat rusts: an atlas of resistance genes. Dordrecht: Kluwer Academic Publishers, 200 pp.

Pawelec A, Dubourg C, Briard M (2006) Evaluation of carrot resistance to alternaria leaf blight in controlled environments. Plant Pathology 55:68-72

Petkova V, Denev ID, Cholakov D, Porjazov I (2007) Field screening for heat tolerant common bean cultivars (*Phaseolus vulgaris* L.) by measuring of chlorophyll fluorescence induction parameters. Scientia Horticulturae-Amsterdam 111:101-106

Pierce FJ and Nowak P (1999) Aspects of precision agriculture. Advances in Agronomy 67:1-85

Poyntz B and Hide PM (1987) The expression of partial resistance of wheat to *Puccinia recondita*. Journal of Phytopathology 120:136-142

Reyns P, Missotten B, Ramon H, De Baerdemaeker J (2002) A review of combine sensors for precision farming. Precision Agriculture 3:169-182

Rubiales D and Niks RE (1995) Characterization of *LR34*, a major gene conferring nonhypersensitive resistance to wheat leaf rust. Plant Disease 79:1208-1212

Schapendonk AHCM, Dolstra O, Van Kooten O (1989) The use of chlorophyll fluorescence as a screening method for cold tolerance in maize. Photosynthesis Research 20:235-247

Schnabel G, Strittmatter G, Noga G (1998) Changes in photosynthetic electron transport in potatoe cultivars with different field resistance after infection with *Phytophthora infestans*. Journal of Phytopathology 146:205-210

Scholes JD and Rolfe SA (2009) Chlorophyll fluorescence imaging as tool for understanding the impact of fungal diseases on plant performance: a phenomics perspective. Functional Plant Biology 36:880-892

Schreiber U (2004) Pulse-Amplitude-Modulation (PAM) fluorometry and saturation pulse method: an overview. In: Chlorophyll a fluorescence: a signature of photosynthesis, Papageorgiou GC and Govinjee (Eds.). Dordrecht: Springer, 279-319

Smillie RM and Hetherington SE (1983) Stress tolerance and stress-induced injury in crop

plants measured by chlorophyll fluorescence *in vivo*. Plant Physiology 72:1043-1050

Steiner U, Bürling K, Oerke E-C (2008) Sensorik für einen präzisierten Pflanzenschutz. Gesunde Pflanzen 60:131–141

Swarbrick PJ, Schulze-Lefert P, Scholes JD (2006) Metabolic consequences of susceptibility and resistance (race-specific and broad-spectrum) in barley leaves challenged with powdery mildew. Plant Cell and Environment 29:1061-1076

Tremblay N, Wang Z, Ma B-L, Belec C, Vigneault P (2009) A comparison of crop data measured by two commercial sensors for variable-rate nitrogen application. Precision Agriculture 10:145–161

Zhang N, Wang M, Wang N (2002) Precision agriculture – a worldwide overview. Computers and Electronics in Agriculture 36:113-132

C UV-induced fluorescence spectra and lifetime determination for detection of leaf rust (*Puccinia triticina*) in susceptible and resistant wheat (*Triticum aestivum*) cultivars

1 Introduction

Cultivars resistant against specific stresses, such as pathogen infection, are integral components of modern agriculture. As a decisive step of breeding programs, the resistance of new cultivars is tested over several years in field experiments, requiring a high input of time and money (Schnabel *et al*. 1998). Since this approach is highly subjective and the results might depend on inoculum type and density as well as environmental conditions at the experimental plots, breeders are looking for rapid screening systems that enable to distinguish between compatible and incompatible pathogen-plant interactions, as they are in a permanent pressure to reveal cultivars with improved stress resistance (Scholes and Rolfe 2009). Considering the great demand for rapid and objective screening methods for stress resistance and the parallel development of non-invasive and non-destructive technologies for plant stress evaluation (Belasque *et al*. 2008; Jansen *et al*. 2009), the question arises, if the spectral and time-resolved fluorescence spectroscopy is suitable for detection of fungal diseases and discrimination of genotypes differing in the degree of pathogen resistance.

For many years, determination of fluorescence signals have proven to be a very sensitive tool for early stress indication reflecting changes in photosynthesis and plant secondary metabolism (Lichtenthaler 1996). Moreover, the non-destructive character allows monitoring of changes in tissue's health status over a long time. Excitation of green leaves with ultraviolet light (UV) induces two types of fluorescence signals: blue-green fluorescence (BGF) in the range of 400-630 nm and chlorophyll fluorescence (ChlF) in the range of 630-800 nm. While the latter is related to chlorophyll *a* molecules, blue-green fluorescence originates from several fluorophores, mainly polyphenols (lists of the most important fluorescing substances in plants are presented e.g. by Cerovic *et al*. 1999; Lang *et al*. 1991; Rost 1995). Since the absolute fluorescence intensities may vary between samples due to optical characteristics of the leaf tissue and the strong influence of external factors such as measurement setup, ratios between fluorescence peaks are calculated for reliable comparisons of treatments (Cerovic *et al*. 1999). The common approach of handling fluorescence spectral data is to determine the position of peaks and the peak amplitudes, on which basis, a number of fluorescence ratios is calculated. Furthermore, determination of half-bandwidth as well as

amplitude-to-half-bandwidth ratio could also reveal changes in plant tissue. As shown in earlier experiments, the F450/F530, F690/F740, F440/F690, and F440/F740 amplitude ratios are very sensitive to stress events and reflect the degradation of chlorophyll and accumulation of secondary metabolites which emit blue-green fluorescence (Buschmann *et al*. 2009; Cerovic *et al*. 1999; Lichtenthaler and Miehé 1997). Thereby, the ratio between the chlorophyll fluorescence peaks F690 and F740 is a good inverse indicator of the *in vivo* chlorophyll content (Buschmann 2007). Contrasting, there is lack of information about the usefulness of the green to red and green to far-red amplitude ratio for stress detection. When exposed to biotic stress, plants often accumulate specific compounds of the secondary metabolism as part of their defence mechanism. A large number of these compounds is known to emit fluorescence in the blue-green spectral range when excited with UV light (Chaerle and Van Der Straeten 2000). Moreover, fungi itself might show a specific autofluorescence as indicated by a UV light-induced bright blue fluorescence from fungal structures of wheat leaf rust (Zhang and Dickinson 2001).

Determination of the fluorescence lifetime provides an alternative method to the fluorescence ratios and yields valuable information on changes in plant metabolism (Cerovic *et al*. 1999). Single fluorophores exhibit specific lifetimes and the enhanced accumulation of one or more of them may lead to changes in their percentage fraction, whereas the synthesis of new compounds might result in elongation or shortening of the mean lifetime, depending on the lifetime of the synthesized substance. Nevertheless, modifications of the pH-value or the localization of substances in the cell/cell compartments can also cause changes in fluorescence lifetime (Cerovic *et al*. 1999). In this context, studies have shown that iron deficiency increased the contribution of the slow kinetic component of the BGF in sugar beets due to accumulation of green fluorescing flavins in the leaf mesophyll (Morales *et al*. 1994).

In terms of biotic stresses, the type and intensity of the plant response to fungal infection depends greatly on the specificity and compatibility of the pathogen-plant interaction. For example, plants might accumulate salicylic acid and phenylpropanoid compounds (e.g. cinnamic acid, stilbenes, coumarins and flavonoids), which are key substances in plant disease resistance. As shown by Chaerle and colleagues, the hypersensitive reaction (HR) of resistant tobacco plants to the tobacco mosaic virus was followed by pre-symptomatic changes of blue-green and chlorophyll fluorescence as a consequence of phenolic compounds i.e. scopoletin accumulation and of the breakdown of the photosynthetic system during HR, respectively (Chaerle *et al*. 2007). Other studies showed a hypersensitive reaction expressed by localized cell death leading to necrotic lesions, limiting

the further pathogen development (Jabs and Slusarenko 2000). In addition to papilla formation, lignification, suberin production, accumulation of phytoalexins, and induction of pathogenesis related proteins (PR-proteins) are common resistance mechanisms in pathogen defence. By comparing wheat cultivars, a stronger increase of the enzyme ß-1,3-glucanase concentration due to *Puccinia recondita* f.sp. *tritici* infection was detected in resistant plants than in susceptible plants (Hu and Rijkenberg 1998). Furthermore, linolenic acid and jasmonic acid play important roles in signal transduction for defence reactions (Berger *et al*. 2007; Somssich and Hahlbrock 1998). Several preformed defence substances, such as phenol derivates, lactones, saponines and stilbenes, are involved in various host pathogen interactions (Agrios 2005). However, phenolic compounds might be accumulated as a stress response even in susceptible cultivars (Lenk *et al*. 2007). As consequence of the pathogen-induced changes of amount and composition of fluorescing compounds in the affected tissue, in addition to the autofluorescence of the fungal structures, a pre-symptomatic increase of both blue and green fluorescence in wheat leaves due to leaf rust infection is expected.

Until now, the use of non-destructive laser-induced fluorescence for detecting pathogens focused on measurements at red and far-red wavelengths, and only limited information on pathogen-triggered changes of the blue-green spectral signature is available. Studies on the mean fluorescence lifetime are also missing in context of non-invasive fungal detection. Assuming pathogen induced changes in the characteristic spectral fluorescence signature between 350 and 820 nm, we hypothesized that fluorescence spectroscopy, is a suitable method to early detect leaf rust (*P. triticina*). For this purpose, a number of fluorescence ratios as well as decay at previously selected wavelengths were evaluated. Based on the specificity of pathogen-plant interactions, we postulated that fluorescence ratios and the mean lifetime of fluorophores enable a reliable discrimination between susceptible and resistant wheat cultivars to the leaf rust pathogen *P. triticina*. Hence, the time after pathogen inoculation was considered as important factor and therefore readings were taken in a time series.

2 Materials and Methods

2.1 Plant material and growth conditions

Experiments were conducted in a controlled-environment cabinet simulating a 14 h photoperiod with 200 µmol m^{-2} s^{-1} photosynthetic active radiation (PAR; Philips PL-L 36 W fluorescent lamps, Hamburg, Germany), day/night temperature of 20/15 ± 2°C and relative

humidity of 75/80 ± 10%. Winter wheat (*Triticum aestivum* L. emend. Fiori. et Paol.) seeds (*n* = 5 per pot) of each evaluated cultivar were sown in pots (0.44 l) filled with perlite. Selection of cultivars was based on the resistance degree (RD) according to the descriptive variety list of the German Federal Plant Variety Office [Bundessortenamt] (2008), in a scale ranging from one to nine. Following, the rust-susceptible cultivars Dekan (RD = 8), Ritmo (RD = 8), Skalmeje (RD = 7), and Aron (RD = 8) as well as the rust-resistant cultivars Retro (RD = 3), Esket (RD = 3), Mirage (RD = 2) were chosen. Emerging plants were provided with Hoagland nutrient solution. Twenty days after sowing, when plants had reached the second-leaf stage, seven pots of each cultivar (four for inoculation, three as control) were selected for the experiment. Leaf rust inoculation was done on the youngest fully expanded leaf of two plants per pot.

2.2 Inoculation with *Puccinia triticina*

Inoculation was accomplished with a non-specific mixture of *Puccinia triticina* spores produced on wheat without known resistance genes (INRES - Phytomedicine, University of Bonn). Before each experiment, fresh *P. triticina* spores were suspended in a solution of distilled water + Tween 20 (0.01% w/v; Merck-Schuchardt, Hohenbrunn, Germany). The spore concentration was estimated microscopically with a Fuchs-Rosenthal counting chamber and adjusted to 10 000 spores per millilitre. On each leaf, the middle of the leaf length was marked on the adaxial side with a felt tip pen, and seven 6 µl droplets of spore suspension were applied in a row, as shown in Fig. 1. Prior to the application, leaves were fixed horizontally on a sample holder to prevent droplet run-off.

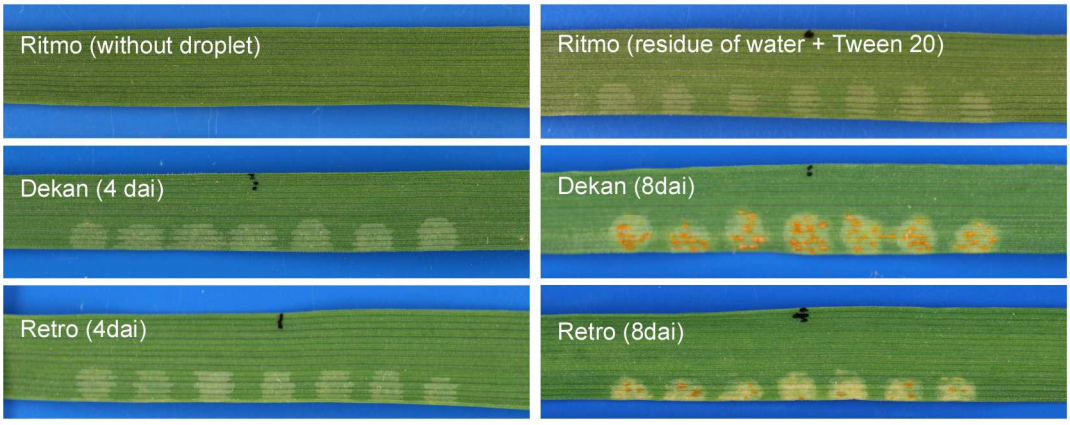

Fig. 1. Digital photographs of wheat leaves 4 and 8 days after inoculation (dai) with *P. triticina*. Bright spots visible at the surface of Ritmo as well as Dekan and Retro at 4 dai (and partially at 8 dai) originate from the droplets deposited for *P. triticina* inoculation.

Control plants were handled similarly but treated with droplets of distilled water + Tween 20 (0.01% w/v). During the inoculation period (22 h), plants were maintained in the climate chamber at an almost saturated atmosphere under a plastic cover. Thereafter, the plastic cover was removed and the leaves were released from their horizontal fixation. The development of disease spots was evaluated visually over the experimental period *in situ* and on digital photographs taken in parallel to the fluorescence readings. For both control and inoculated leaves, the central droplet was chosen for fluorescence measurements.

2.3 Fluorescence measurements

Fluorescence measurements were carried out using a compact fibre-optic fluorescence spectrometer with nanosecond time resolution by the boxcar technique (IOM GmbH, Berlin, Germany). A pulsed N_2-laser (MSG803-TD, LTB Lasertechnik Berlin GmbH, Berlin, Germany) with an emission wavelength of 337 nm and a repetition rate of 20 Hz served as the excitation source. The fibre-optic probe for detection of fluorescence signals consisted of a central excitation fibre and six surrounding emission fibres, each with a 200 µm diameter. The pulse energy at the probe exit was adjusted to be 1-2 µJ with a pulse length of approximately 1 ns resulting in a density of 5.5 x 10^{15} photons per cm^2 and impulse. Fluorescence was recorded with an acousto-optic tunable filter (AOTF) monochromator, which enables a minimal step width of 1 nm. A photomultiplier (PMT; H5783-01, Hamamatsu, Hamamatsu City, Japan) was used as the detector. The sensitivity of the PMT was adjusted in order to optimize the signal intensity during the spectral and lifetime measurements. Time resolution was accomplished using a gated integrator with a 2 ns half-width; the position of the gate could be set with an accuracy of 0.1 nanoseconds.

Fluorescence spectra and decay data were recorded from leaves fixed horizontally on a plate with integrated sample holder. The fibre-optic probe was positioned in a 90° angle to the leaf. Thereby, with help of a laser-based rangefinder (OptoNCDT 1300, Micro-Epsilon Messtechnik GmbH & Co. KG, Ortenburg, Germany) fixed beside the probe, the distance between leaf- and probe surface was detected and adjusted for the point of measurement. This alignment of correct distance was conducted to provide fluorescence intensities in a narrow data range to avoid signal minimum or saturation. Spectra and lifetime at selected wavelengths were measured at 21-23°C under ambient light conditions (about 18 µmol m^{-2} s^{-1} PAR) at two to four days after pathogen inoculation (dai) on the inoculation area as described

below. Before starting measurements, plants were adapted for 0.5 h to room light and temperature conditions.

For an optimal recording of fluorescence signals, the experimental settings were adjusted for spectral measurements (SPEC; 370-800 nm), lifetime 1 (LF 1; 410-530 nm), lifetime 2 (LF 2; 560-620 nm), and lifetime 3 (LF 3; 670-760 nm), respectively. Common to all measurements was a pulse count of 32, which is the number of laser pulses averaged for each single data point. Spectrally resolved measurements were accomplished at a gate position of 3 ns (in the temporal signal maximum), with a wavelength interval of 2 nm, a distance of 3.95 mm between the probe and sample, and a PMT gain of 600 Volt. Lifetime measurements (LF 1, LF 2, and LF 3) were performed within their respective range at multiple wavelengths with an interval of 30 nm (e.g. at 410, 440, 470, 500 and 530 nm for LF 1). The step width of the integrator gate was set to 0.2 nanoseconds. LF 1 and LF 3 had the same PMT gain of 600 V, while LF 2 was set to 800 Volt. The distance between the probe tip and sample was adjusted to 4.57 mm for LF 1, 5.82 mm for LF 2, and 2.08 mm for LF 3 to provide fluorescence intensities in a narrow signal range irrespective of the measured wavelength. In order to avoid a time-shift effect within the time-course of a single measuring day alternate measurements on inoculated and non-inoculated leaves were conducted.

2.4 Data processing and statistics

The measured UV-induced fluorescence spectra were processed by Gaussian curve fitting using a freeware portable command-line driven graphing utility (Gnuplot, version 4.2, patchlevel 4, (http://www.gnuplot.info) (Fig. S1, supplementary material of this chapter). Peak positions, amplitudes, and half-bandwidths were determined to calculate the ratios of peak amplitudes, half-bandwidths, and amplitudes-to-half-bandwidths. Before curve fitting, the raw data was corrected for the laser energy to remove possible data distortion due to fluctuations of the excitation energy. In order to analyse the fluorescence decay, the data was processed by performing a Levenberg-Marquardt fit using a deconvolution software (DC4 version 2.0.6.3, IOM GmbH, Berlin, Germany, 2008).

The processed experimental data was subjected to analysis of variance with a statistic software (PASW statistics version 15.0, SPSS Inc., Chicago, USA). For each day, cultivar and evaluation, the means of inoculated and healthy plants were compared by One-way ANOVA ($p \leq 0.05$). Graphs (Mean ± SD) were designed with graphic software (SigmaPlot 8.02, Systat

Software Inc., Richmond, CA, USA and OriginLab 7.1 SR2, OriginLab Cooperation, Northhampton, USA).

3 Results

3.1 Specificity of fluorescence spectra and lifetime of wheat leaves

After Gaussian curve fitting, the positions of the fluorescence peaks were determined at 451 nm for the blue peak (F451), 522 nm for the green shoulder (F522), and 687 nm (F687) and 736 nm (F736) for the chlorophyll peaks (Fig. S1). The fluorescence intensity was genotype dependent with higher blue and green peaks for cv Dekan and higher chlorophyll peaks for cv Retro. With exception of F687/F736, control leaves of Dekan showed higher amplitude ratios than control leaves of Retro, irrespective of measuring day. However, the senescence of leaves during the measuring time from 2 to 4 dai led to a decrease of the F451/F522, F451/F687, F451/F736, F522/F687, F522/F736 ratios (Table 1). The ratios between half-bandwidth amongst the four evaluated peaks indicate higher values of F451/F736, F522/F736 and F687/F736 for the cv Dekan and higher values of F451/F687 and F522/F687 for the cv Retro. The half-bandwidth ratio F451/F522 was similar for both cultivars (Table S1). In general, the half-bandwidth ratios were not appropriate to reveal clear senescence signs, whereupon the most pronounced modification (0.03 units) was observed for the parameter F451/F736 in both cultivars and for the parameter F522/F687 (0.05 units) in cv Dekan. Cultivar-specific signatures were also observed for the amplitude-to-half-bandwidth ratios, Dekan showing higher values of F451 and F522, and lower values of F687 and F736 as compared to Retro. Furthermore, the ratios of amplitude-to-half-bandwidth at the 451 nm (blue) and the 522 nm (green) peak in control leaves of both Dekan and Retro decreased in the time-course, while ratios of the chlorophyll peaks (F687 and F736) remained at the same level (Table S2).

In general, deconvolution of fluorescence decay data indicated that one mean fluorescence lifetime could be generated with greater robustness than multiple lifetimes. Nevertheless, variations of residuals indicated a bi-exponential development. Healthy control plants of both cultivars Dekan and Retro showed a similar pattern of fluorophore lifetimes over the selected wavelengths of the analyzed spectra. The mean lifetime increased from about 0.6-0.7 ns at 410 nm up to 1.1-1.2 ns between 530 and 560 nm and decreased to 0.9-1.0 ns at 620 nm (Fig. 2). The chlorophyll fluorescence also had a shorter lifetime of 0.7 ns at 670 nm and of ~0.65 ns over the range of 700-760 nm (*data not shown*).

Table 1. Ratio of amplitudes between fluorescence peaks (F451, F522, F687 and F736) measured on control (c) and inoculated (i) wheat leaves of the cultivars Dekan (RD = 8) and Retro (RD = 3) at 2, 3, and 4 days after inoculation (dai).

Fluorescence ratio	Wheat cultivar	2 dai		3 dai		4 dai	
		c	i	c	i	c	i
F451/F522	Dekan	4.14*	4.01	4.00*	3.83	3.91*	3.57
	Retro	3.98	3.93	3.79*	3.62	3.69*	3.48
F451/F687	Dekan	6.55	6.46	5.68	6.13	5.14	6.15
	Retro	3.30*	4.17	3.03*	4.19	2.76*	4.26
F451/F736	Dekan	6.97	7.10	5.97	6.72	5.41*	7.32
	Retro	3.72*	4.53	3.33*	4.94	3.02*	5.30
F522/F687	Dekan	1.59	1.61	1.42	1.60	1.31*	1.72
	Retro	0.83*	1.06	0.80*	1.16	0.75*	1.22
F522/F736	Dekan	1.69	1.77	1.49	1.75	1.38*	2.04
	Retro	0.93*	1.15	0.88*	1.36	0.82*	1.53
F687/F736	Dekan	1.07	1.09	1.05	1.09	1.05*	1.19
	Retro	1.14	1.09	1.11	1.18	1.10*	1.25

* Significant differences (ANOVA, $p \leq 0.05$) between control (c) and inoculated (i) leaves for each cultivar and measuring day ($n = 6$ for control plants; $n = 8$ for inoculated plants).

3.2 Detection of pathogen-triggered plant responses

In both cultivars, visual evaluations of the pathogen development indicated very small and loom chlorotic spots at 4 dai which were visible inside the residue area of the water + Tween 20 droplet (Fig. 1). In the susceptible cv Dekan, small red-brown pustules appeared two days later (6 dai), and became larger and more distinct in the following days. In the case of the resistant cv Retro, the chlorotic spots became larger and more conspicuous (necrotic), and only a few pustules were apparent. Typical disease symptoms on both Dekan and Retro cultivars at 4 and 8 dai are presented in Fig. 1.

Fluorescence recordings were stopped when the first visual symptoms appeared (4 dai) since the small and loom chlorotic spots in both cultivars induced clear modifications of fluorescence intensity over the entire spectral range. At this time, the ratios of amplitudes (Table 1) revealed a decrease of the F451/F522 ratio due to leaf rust infection, e.g. from 3.91 (control, c) to 3.57 (inoculated, i) (Dekan). In contrast, the values of all the other ratios increased in the inoculated as compared to the control leaves, e.g. from 5.41 (c) to 7.32 (i) for F451/F736 (Dekan) and from 1.10 (c) to 1.25 (i) (Retro) for F687/F736. Ratios of half-

bandwidth also showed significant changes due to pathogen-plant interactions (Table S1). Thereby, evaluations showed a decreased F451/F522 ratio and increased F451/F736 and F522/F736 ratios in the diseased leaves. The ratio between the chlorophyll peaks increased at similar magnitude in both cultivars. Changes in fluorescence for each single peak were determined by the amplitude-to-half-bandwidth ratios (Table S2), where a strong increase, e.g. from 348 (c) to 425 (i) for the green peak in Dekan, was observed. Moreover, the ratio of the two chlorophyll peaks decreased in both cultivars.

Summarizing, irrespective of wheat cultivar several fluorescence parameters can be used for detection of leaf rust four days after inoculation. Furthermore, differences between control and inoculated wheat leaves could be established as early as two days after inoculation (Table 1). As shown, the F451/F522 amplitude ratio decreased from 4.14 in control plants to 4.01 in inoculated leaves of Dekan. Moreover, significantly higher ratios of F451/F687, F451/F736, F522/F687, and F522/F736 were observed in Retro, whereupon measurements on Dekan leaves indicate a similar trend. In both cultivars, the half-bandwidth ratio of F451/F522 was decreased, while the F522/F736 ratio increased (Table S1). Moreover, amplitude-to-half-bandwidth ratio for both chlorophyll peaks decreased from e.g. 942 (c) to 718 (i) for F687 in Retro.

The pre-symptomatic detection of rust infection was also ensured by lifetime measurements. For both cultivars, recordings at 4 dai indicate a longer mean lifetime in leaves infected with *P. triticina* in the range between 560 and 620 nm (Fig. 2). It is important to note that position of the blue peak, the green shoulder and the both chlorophyll peaks remained unchanged in leaves infected with the pathogen as compared to control ones during three days of fluorescence measurements. Significant differences were observed already on the first measuring day. Thereby, longer mean lifetimes were measured in inoculated than in control leaves at wavelengths of 470, 500, 530, 560 and 590 nm (Fig. 2).

Finally, the rust-susceptible Ritmo (RD = 8), Skalmeje (RD = 7), and Aron (RD = 8) and the rust-resistant Esket (RD = 3) and Mirage (RD = 2) cultivars showed comparable results in terms of early detection of pathogen infection, especially for the spectral readings (Tables S3, S4, and S5). Thereby, several parameters instead of one single should be evaluated. In contrast, especially lifetime determinations at 470 nm indicated to be unspecific to the resistance degree of the cultivar. In general, chlorophyll fluorescence lifetime measurements revealed no clear differences between healthy and inoculated leaves. A tendency of lifetime elongation at 670 nm was noticed 3 and 4 dai in the susceptible cultivar, but results were statistically not significant and are not presented.

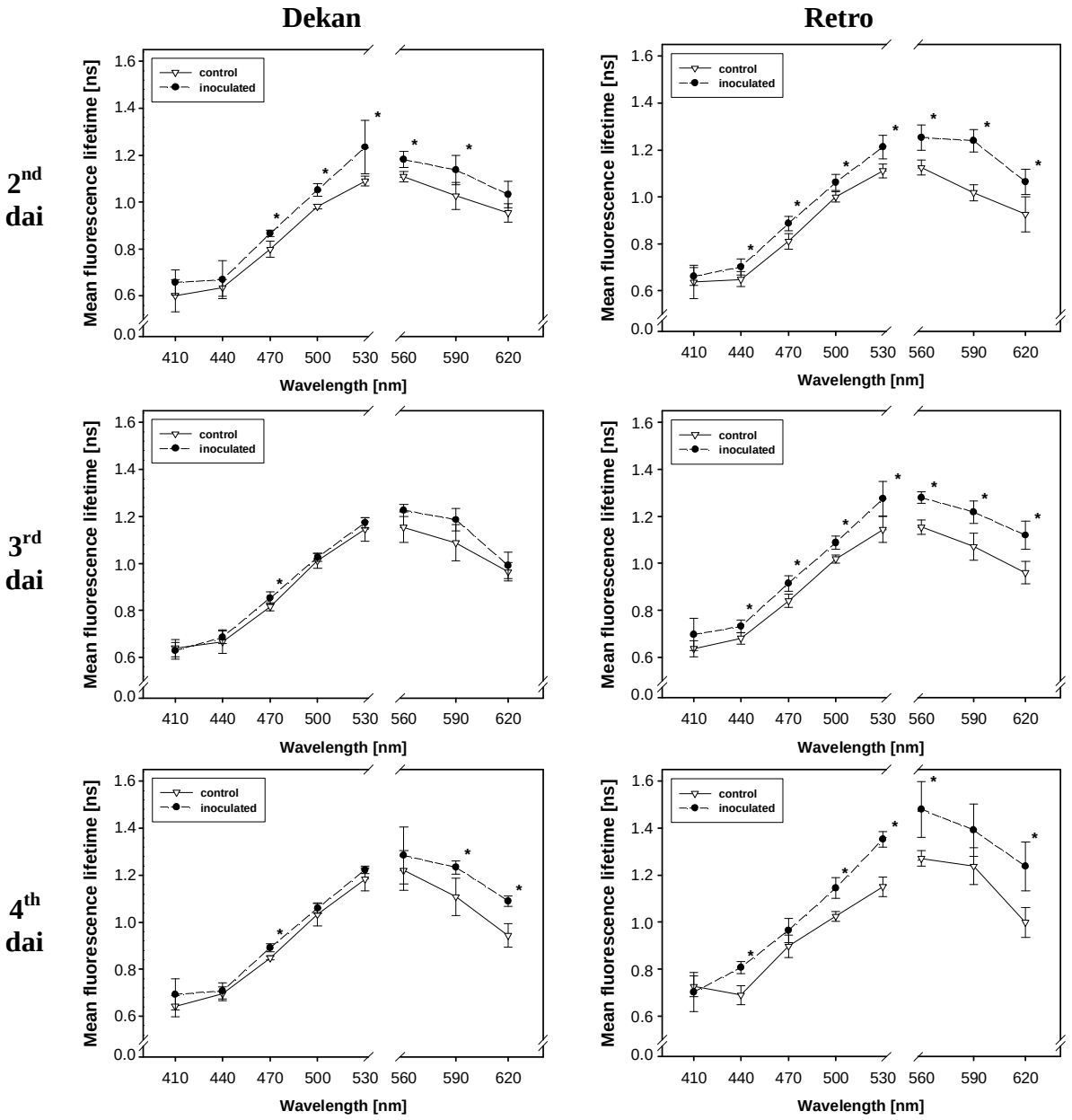

Fig. 2. Mean fluorescence lifetime at selected wavelengths of control and inoculated leaves from Dekan (left) and Retro (right) at 2, 3, and 4 days after inoculation (dai). Values indicate mean ± SD (n = 4 for control plants; n = 5 for inoculated plants). * Significant differences (ANOVA, $p \leq 0.05$) between control and inoculated leaves for each cultivar, wavelength, and measuring day. Measurements from 410-530 nm and from 560-620 nm were conducted with different settings as described in materials and methods.

3.3 Cultivar-specific responses to *Puccinia triticina* infection

In both, the susceptible (Dekan) and the resistant (Retro) cultivar, the fluorescence ratios and lifetime were influenced by pathogen development from two to four days after

inoculation. Thereby the affected parameters and intensity of changes were cultivar specific. Moreover, there was a clear difference between the susceptible and resistant cultivars concerning the temporal response to the leaf rust pathogen.

At 2 and 3 dai, the susceptible cultivar Dekan revealed significant differences only in the F451/F522 amplitude ratio; at 4 dai, changes were observed in all other ratios, except F451/F687 (Table 1). By contrast, the resistant cultivar Retro showed changes in the ratios F451/F687, F451/F736, F522/F687 and F522/F736 (2 dai), F451/F522 (3 dai) and F687/F736 (4 dai, Table 1). The observed modifications were partially based on the significant higher absolute blue and green fluorescence intensity in inoculated as compared to healthy leaves. Even if not statistically significant, fluorescence increase in both wavelengths was more pronounced in the resistant cultivar Retro (Fig. 3).

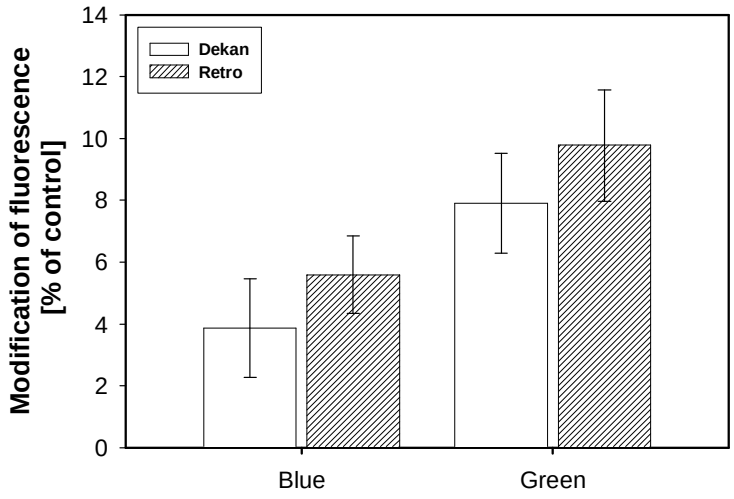

Fig. 3. Modification of the blue and green fluorescence intensity in inoculated leaves (as compared to control leaves) three days after inoculation. Vertical bars indicate the standard deviation.

Similar temporal differences were observed for the half-bandwidth ratios (Table S1) and the ratios amplitude-to-half-bandwidth (Table S2). At 3 dai, significant changes in the half-bandwidth ratios were only observed in the resistant cv Retro for F451/F522, F451/F736, F522/F687, F522/F736 and F687/F736. One day later, the F451/F736 and F522/F736 ratios were significantly higher in the susceptible cultivar (Table S1). In addition, evaluations in the red and far-red peaks indicate significant changes only in the resistant cultivar at two to four days after inoculation (Table S2). Based on our results and under consideration of the time after inoculation, more than one parameter could be adopted for discrimination between the both tested genotypes. In general, the trends observed for the cultivars Dekan and Retro were

also found in the other evaluated genotypes (Table S3-S6). Amongst the several previously selected parameters, robust results were obtained with the amplitude ratio F451/F687. Measurements revealed that the amplitude ratio F451/F687 at 3 dai in the resistant cvs Esket and Mirage increased (e.g. from 3.14 (c) to 3.83 (i) in Esket). At that point, of time, the susceptible cvs Ritmo, Skalmeje, and Aron showed only minor changes for this parameter. The pathogen-induced modification of the amplitude ratio F451/F687 three days after inoculation is presented for the seven evaluated cultivars in Fig. 4.

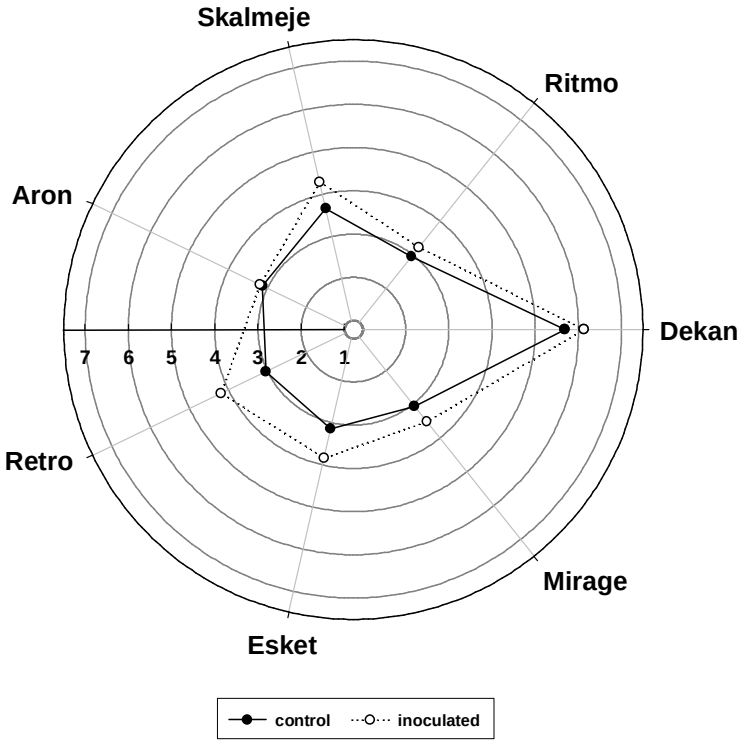

Fig. 4. Fluorescence amplitude ratio F451/F687 in control and diseased leaves, three days after pathogen inoculation.

Comparisons of the mean lifetime modification in Dekan and Retro revealed that only the resistant cultivar showed significant changes at 440 nm throughout the whole measurement period. At 3 and 4 dai, a clear elongation of lifetime was observed at 500 and 530 nm in the rust-resistant cv Retro, whereas the susceptible cv Dekan revealed no differences between control and inoculated leaves (Fig. 2). Similarly, at 3 dai inoculated leaves of Esket and Mirage had a significant longer mean lifetime at 500 and 530 nm. For example, the mean fluorescence lifetime of Esket leaves was elongated from 1.05 ns (c) to 1.09 ns (i) at 500 nm and from 1.13 ns (c) to 1.18 ns (i) at 530 nm. Differences between

inoculated and healthy leaves were recorded also one day later (4 dai) for Esket and Mirage, whereas no significant changes were detected in the susceptible cultivars (Ritmo, Skalmeje, and Aron), three and four days after inoculation. Therefore, comparisons of mean lifetime at 500 nm in inoculated and healthy leaves might be used for discrimination between susceptible and resistant wheat genotypes (Fig. 5). Moreover, at 440 nm, all of the resistant cultivars showed a more pronounced elongation of lifetime in leaves inoculated with leaf rust than the susceptible ones at two to four days after inoculation.

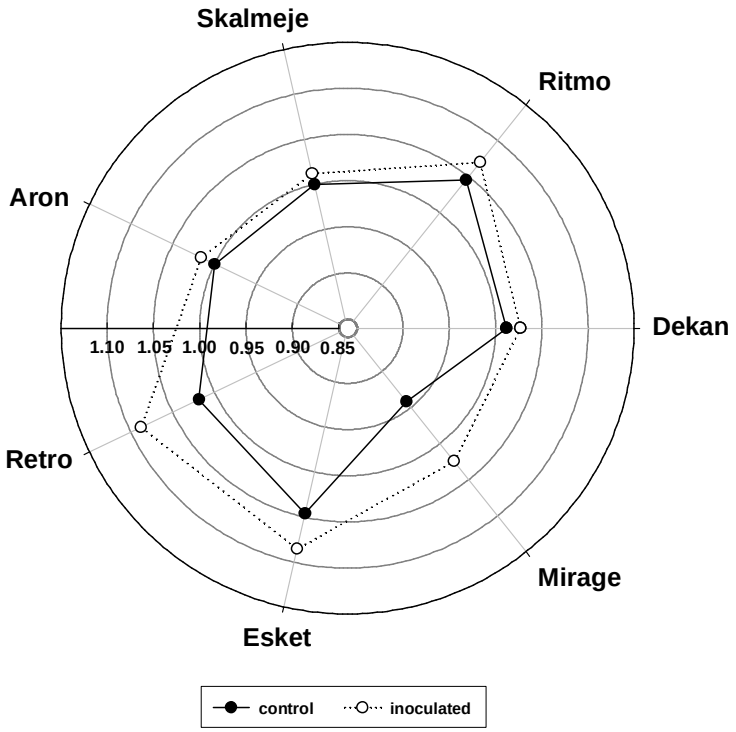

Fig. 5. Fluorescence mean lifetime [ns] measured at 500 nm on control and inoculated (3 dai) wheat leaves.

4 Discussion

It is well established that the early response of plants after interaction with pathogens is followed by accumulation of phenolic compounds at the infection site, whereupon the restricted pathogen development can be the outcome of rapid and hypersensitive cell death (Agrios 2005; Berger *et al*. 2007). Such alterations in plant secondary metabolism may result in changes of specific fluorescence intensities, thus fluorescence ratios, and also of fluorescence lifetime. In the blue-green spectral range a number of fluorophores emit fluorescence light, whereupon any change in the composition might affect the mean

fluorescence lifetime. Based on the results of our experiments, there is strong evidence that cultivar reactions due to pathogen infection might be detectable with UV-induced fluorescence spectroscopy. Moreover, spectral characteristics and the determination of fluorescence lifetime clearly demonstrated the potential for discriminating between highly susceptible and highly resistant wheat genotypes. Thereby, screening of genotypes under controlled conditions ensures the reproducibility of the timing of infection and minimizes to a large extent the possibility of simultaneous occurrence of other stresses, as reported elsewhere (Huang *et al*. 2005; Pawelec *et al*. 2006).

In the present study, the evaluated cultivars revealed lower F451/F522 amplitude ratios (Table 1). This is the consequence of a more pronounced raise of green fluorescence as compared to the increase in blue fluorescence (Fig. 3). The same assumption is declared for the ratio of the F451/F522 half-bandwidth. Our results are in accordance with observations of Lüdeker *et al*. (1996) who proposed that the increase of F520 is due to the blue/green fluorescence band of the fungi and due to the production of blue-green fluorescing intercellular substances. In fact, the observed increase in F522 in our experiments can not be attributed exclusively to fungal fluorescence or plant reaction. However, the ratios where F522 is involved could be therefore useful for the detection of fungal attack. In this context, the suitability for discrimination between resistant and sensitive cultivars is presumably influenced by the ability of the cultivars to limit fungi development.

In our experiments, the first modification of the F687/F736 amplitudes, expressed by increased amplitude ratio as consequence of the begin of chlorophyll degradation, was observed 4 dai in both susceptible and resistant cultivars. This change occurred one and two days after an increase of the corresponding half-bandwidth and decrease of the amplitude-to-half-bandwidth ratio, respectively (Tables S1 and S2). The ratio of the amplitude-to-half-bandwidth is an indicator of the relative concentration of a fluorescent substance (Komura and Itoh 2009), which is probably a reason for modifications of amplitude-to-half-bandwidth ratios in the chlorophyll fluorescence peaks. Moreover, the amplitude-to-half-bandwidth ratio (Table S2) of the green peak at 3 and 4 dai, and of the blue peak at 4 dai, increased significantly, presumably due to compound accumulation as well as fungal fluorescence. Morales *et al*. (1994) reported that most of the increased blue-green fluorescence with iron deficiency can be attributed to decreased chlorophyll and carotenoids. In our case, the amplitude ratio F687/F736, which is an inverse indicator for chlorophyll content, revealed only at 4 dai significant modifications. Hence, the observed higher F451/F687, F451/F736, F522/F687 and F522/F736 amplitude ratios (Table 1) seems to be related to a real

accumulation of blue-green fluorescing compounds, as UV light absorption and blue-green fluorescence re-absorption due to variable chlorophyll content can be neglected. These observations indicate a mixed effect of changes in chlorophyll concentration during further pathogen development, in addition to the accumulation of blue-green fluorescing compounds; the latter express predominantly their impact at early infection stages. Lüdeker *et al*. (1996) related the strong increase of the F440/F730 ratio due to pathogen infection to both a decrease of chlorophyll concentration and an increase of blue fluorescence. In summary, our results confirm the suitability of amplitude ratios - including the green to red and green to far-red ratios - for detection of pathogen infection. However, contrary to our expectations, the ratios of half-bandwidth as well as amplitude-to-half-bandwidth revealed less precise results.

In the case of the wheat-leaf rust interaction, an increased concentration of bound phenolic acids (ferulic acid, p-coumaric and syringic acids) after hypersensitive collapse of single or small groups of cells was reported (Southerton and Deverall 1990a). In our evaluations the susceptible cultivar Dekan showed a significant increase of the F451/F736, F522/F687, and F522/F736 ratios only at 4 dai; similar changes were detected in the resistant cultivar Retro two days earlier. Wheat cultivars resistant to *P. triticina* accumulate more lignin than susceptible ones (Southerton and Deverall 1990b), and a strict correlation between resistance and lignification has been demonstrated (Moerschbacher *et al*. 1990).

In our studies comprising spectral resolved fluorescence measurements on the cultivars Dekan and Retro, the amplitude ratio F451/F687 provided a reliable basis for the discrimination between susceptible and resistant cultivars. Measurements on further five susceptible or resistant wheat cultivars showed similar results. Here, evaluations at 3 dai showed a significantly higher increase of the F451/F687 amplitude ratio in the resistant cultivars than in the susceptible ones (Fig. 4). Thereby, the resistant cultivars displayed modifications in the blue and green amplitude-to-half-bandwidth ratios two days earlier than the susceptible ones.

The observation of a lifetime elongation is in accordance with the results of spectral measurements, as a slight and more distinct enhancement in the blue and green spectral range, respectively, were detected (Fig. 3). Our data revealed a general tendency of a longer mean lifetime in the leaf rust inoculated than in the control plants (Fig. 2). This is presumable related to the accumulation of existing compounds with a longer lifetime, or the synthesis of defence-related substances with a longer fluorescence lifetime as consequence of the pathogen attack.

Moreover, differences between rust-susceptible and -resistant cultivars at particular wavelengths were detected. At 440 nm, the lifetime elongation was significantly more pronounced in the resistant cultivar at two to four days after inoculation. Similar differences were also observed at 500 nm, 530 nm, and 560 nm at three and four days after inoculation. The additional studies with three rust-susceptible (Ritmo, Skalmeje and Aron) and two rust-resistant (Esket and Mirage) cultivars revealed similar fluorescence decay results as observed for Dekan and Retro. Specific wavelengths (440 nm, 500 nm, and 530 nm) indicated a more pronounced lifetime elongation and were therefore identified as suitable for differentiation of cultivars with distinct resistance degrees, as exemplarily shown for 500 nm in Fig. 5.

Hence, the proposed experimental design and especially the determination of fluorescence lifetime, ensures the detection of leaf rust and might support the discrimination between resistant and susceptible cultivars to the leaf rust pathogen. However, a minimum of two wavelengths is needed to provide robust and reliable information about the resistance degree of wheat cultivars.

Switching the excitation wavelength to red light could be an appropriate alternative to get more information on chlorophyll fluorescence lifetime. As we now assume, a more precise detection of pathogen-induced changes in PSII could be reached by exciting the chlorophyll molecules solely. Besides the usefulness of our measuring system, chlorophyll fluorescence excited with UV light source requires careful data interpretation since phenolics located in the cell wall have a strong absorption and shield the chloroplasts in the mesophyll against excitation (Cerovic *et al.* 1999). As a consequence, any change in the concentration of epidermally located phenolic compounds will cause a corresponding change in chlorophyll fluorescence even if the quantum yield of the chlorophyll fluorescence itself remains unaffected. Therefore, the ratio between chlorophyll fluorescence excited by UV and red light will provide additional information on accumulation of UV light absorbing compounds in the epidermis. In general, the ratios of blue-green fluorescence over chlorophyll fluorescence should be even more sensitive to detect changes in phenolics, since the numerator will increase and the denominator decrease with enhanced phenolics accumulation. In the context of pathogen infection and establishment, future investigations should try to elucidate the link between fluorescence emission and metabolite accumulation in the plant tissue.

5 Conclusions

Based on the fluorescence lifetime and UV-induced spectral measurements conducted on seven wheat cultivars, the pre-symptomatic detection of leaf rust infection was feasible two days after pathogen inoculation. As an innovative approach, resistant and susceptible cultivars to the leaf rust pathogen might be discriminated by monitoring the F451/F687 amplitude ratio (3 dai) and the lifetime at 440 nm, 500 nm and 530 nm. A combination of spectral characteristics and fluorescence lifetime could be an additional tool in plant breeding programs for a rapid and non-destructive evaluation of genotype susceptibility against leaf rust.

The results obtained in our experiments open new perspectives for developing automated, objective and precise high-throughput screening systems, similarly as the phenotyping and stress evaluation unit based on chlorophyll fluorescence (Jansen *et al*. 2009). Besides the success of the present studies, a scale covering genotypes with “intermediate” resistance degree in addition to those highly resistant or highly susceptible to the pathogen, remains to be developed. Another challenge would be to discriminate genotypes independently of measurements on control, healthy plants.

The following pages of this chapter display the supplementary figure (S1) and tables (S1-S6).

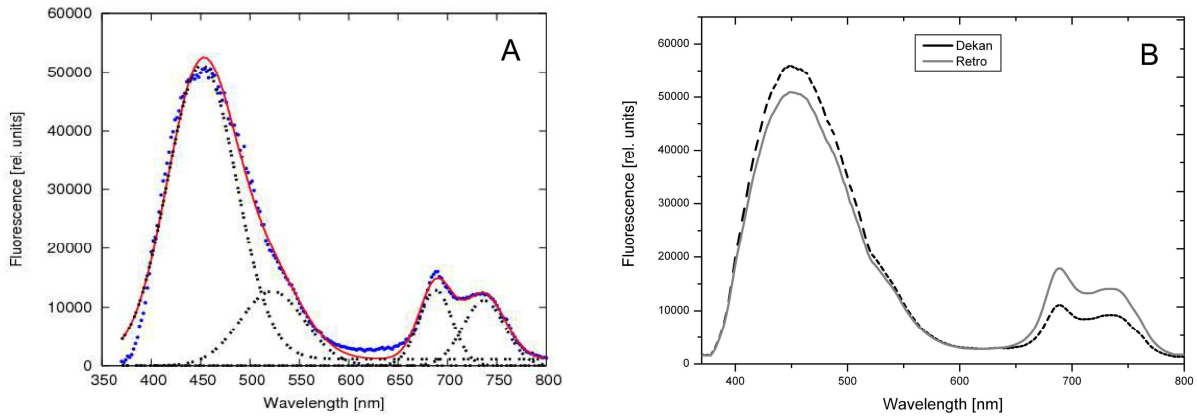

Fig. S1. A) Deconvolution in Gaussian spectral components. Blue dotted line: measured fluorescence emission spectrum (370-800 nm), black dotted lines: individual Gaussian spectral components of the fitted spectrum, red solid line: fitted spectrum. **B)** Characteristic fluorescence emission spectrum (370-800 nm, smoothed curves) of healthy wheat leaves (excitation at 337 nm) of the cultivars Dekan and Retro. The spectra were measured by means of a fluorescence spectrometer with nanosecond time resolution using a pulsed nitrogen laser as excitation source.

Table S1. Ratio of half-bandwidth between fluorescence peaks (F451, F522, F687 and F736) on control (c) and inoculated (i) wheat leaves of the cultivars Dekan (RD = 8) and Retro (RD = 3) at 2, 3, and 4 days after inoculation (dai).

Fluorescence ratio	Wheat cultivar	2 dai		3 dai		4 dai	
		c	i	c	i	c	i
F451/F522	Dekan	1.05	1.04	1.04	1.03	1.03	1.02
	Retro	1.05	1.03	1.05*	1.03	1.04*	1.01
F451/F687	Dekan	1.99	1.99	1.99	1.98	1.99	1.95
	Retro	2.07	2.06	2.06	2.05	2.05	2.03
F451/F736	Dekan	1.67	1.67	1.65	1.66	1.64*	1.66
	Retro	1.64	1.65	1.62*	1.65	1.61*	1.64
F522/F687	Dekan	1.89	1.91	1.92	1.91	1.94	1.92
	Retro	1.97	1.99	1.96*	2.00	1.98*	2.01
F522/F736	Dekan	1.59	1.61	1.59	1.61	1.60*	1.63
	Retro	1.56	1.60	1.55*	1.61	1.56*	1.63
F687/F736	Dekan	0.84	0.84	0.83	0.84	0.83	0.85
	Retro	0.79	0.80	0.79*	0.80	0.79*	0.81

* Significant differences (ANOVA, $p \leq 0.05$) between control (c) and inoculated (i) leaves for each cultivar and measuring day ($n = 6$ for control plants; $n = 8$ for inoculated plants).

Table S2. Ratio of amplitude-to-half-bandwidth from fluorescence (F451, F522, F687 and F736) on control (c) and inoculated (i) wheat leaves of the cultivars Dekan (RD = 8) and Retro (RD = 3) at 2, 3, and 4 days after inoculation (dai).

Fluorescence peak	Wheat cultivar	2 dai		3 dai		4 dai	
		c	i	c	i	c	i
F451	Dekan	1607	1585	1397	1454	1326*	1490
	Retro	1433	1423	1288	1355	1188*	1370
F522	Dekan	407	410	363*	393	348*	425
	Retro	378	375	356*	384	334*	399
F687	Dekan	503	493	503	480	528	486
	Retro	942*	718	906*	683	913*	681
F736	Dekan	394	382	397	372	413	349
	Retro	647*	528	640*	463	648*	439

* Significant differences (ANOVA, $p \leq 0.05$) between control (c) and inoculated (i) leaves for each cultivar and measuring day ($n = 6$ for control plants; $n = 8$ for inoculated plants).

Table S3. Ratio of amplitudes between fluorescence peaks (F451, F522, F687, and F736) measured on control (c) and inoculated (i) wheat leaves of the cultivars Ritmo (RD = 8), Skalmeje (RD = 7), Aron (RD = 8), Esket (RD = 3), and Mirage (RD = 2) at 2, 3, and 4 days after inoculation (dai).

Fluorescence ratio	Wheat cultivar	2 dai		3 dai		4 dai	
		c	i	c	i	c	i
F451/F522	Ritmo	3.86	3.78	3.89*	3.77	3.84*	3.58
	Skalmeje	4.10*	3.97	4.02*	3.84	3.97	3.64
	Aron	-	-	3.36	3.30	-	-
	Esket	4.13*	4.00	3.97*	3.77	3.85*	3.65
	Mirage	-	-	3.58*	3.36	-	-
F451/F687	Ritmo	2.89	3.07	2.94	3.22	2.78*	3.33
	Skalmeje	3.85	4.39	3.66	4.29	3.46*	4.29
	Aron	-	-	3.12	3.19	-	-
	Esket	3.27	3.65	3.14*	3.83	2.92*	3.73
	Mirage	-	-	3.06	3.51	-	-
F451/F736	Ritmo	2.80	3.06	2.83*	3.2	2.64*	3.34
	Skalmeje	4.18	4.85	3.84*	4.66	3.56*	4.86
	Aron	-	-	3.32	3.41	-	-
	Esket	3.39	3.98	3.14*	4.39	2.91*	4.48
	Mirage	-	-	3.14	3.81	-	-
F522/F687	Ritmo	0.75	0.81	0.76*	0.85	0.73*	0.90
	Skalmeje	0.94	1.10	0.91*	1.16	0.87*	1.18
	Aron	-	-	0.93	0.97	-	-
	Esket	0.79	0.91	0.79*	1.02	0.76*	1.02
	Mirage	-	-	0.85	1.05	-	-
F522/F736	Ritmo	0.73	0.81	0.73*	0.8	0.69*	0.93
	Skalmeje	1.02*	1.22	0.96*	1.21	0.90*	1.33
	Aron	-	-	0.99	1.03	-	-
	Esket	0.82	0.99	0.79*	1.17	0.75*	1.23
	Mirage	-	-	0.88*	1.14	-	-
F687/F736	Ritmo	0.97*	1.00	0.96*	1.01	0.95*	1.03
	Skalmeje	1.09	1.11	1.05	1.09	1.03*	1.13
	Aron	-	-	1.06	1.07	-	-
	Esket	1.04*	1.09	1.00*	1.14	0.99*	1.19
	Mirage	-	-	1.03*	1.09	-	-

* Significant differences (ANOVA, $p \leq 0.05$) between control (c) and inoculated (i) leaves for each cultivar and measuring day ($n = 6$ for control plants; $n = 8$ for inoculated plants).

Table S4. Ratio of half-bandwidth between fluorescence peaks (F451, F522, F687, and F736) on control (c) and inoculated (i) wheat leaves of the cultivars Ritmo (RD = 8), Skalmeje (RD = 7), Aron (RD = 8), Esket (RD = 3), and Mirage (RD = 3) at 2, 3, and 4 days after inoculation (dai).

Fluorescence ratio	Wheat cultivar	2 dai		3 dai		4 dai	
		c	i	c	i	c	i
F451/F522	Ritmo	1.05*	1.03	1.04	1.03	1.04*	1.03
	Skalmeje	1.05	1.04	1.04	1.03	1.03*	1.02
	Aron	-	-	1.04	1.04	-	-
	Esket	1.05	1.05	1.05*	1.03	1.04*	1.02
	Mirage	-	-	1.03*	1.02	-	-
F451/F687	Ritmo	2.06	2.06	2.05	2.05	2.06	2.05
	Skalmeje	2.08	2.07	2.07	2.06	2.07	2.04
	Aron	-	-	2.02	2.03	-	-
	Esket	2.11	2.09	2.09	2.08	2.09	2.08
	Mirage	-	-	2.04	2.03	-	-
F451/F736	Ritmo	1.62*	1.63	1.62	1.62	1.62*	1.62
	Skalmeje	1.64*	1.66	1.64*	1.65	1.63	1.64
	Aron	-	-	1.61	1.62	-	-
	Esket	1.65	1.65	1.64*	1.65	1.64	1.65
	Mirage	-	-	1.61	1.62	-	-
F522/F687	Ritmo	1.96*	2.00	1.97*	1.99	1.98	1.99
	Skalmeje	1.98	1.99	2.00	1.99	2.00	2.00
	Aron	-	-	1.95	1.96	-	-
	Esket	2.01	2.00	2.00	2.01	2.01	2.03
	Mirage	-	-	1.97	1.99	-	-
F522/F736	Ritmo	1.54*	1.58	1.55*	1.57	1.55*	1.58
	Skalmeje	1.56*	1.59	1.58	1.59	1.58	1.61
	Aron	-	-	1.55	1.56	-	-
	Esket	1.57	1.57	1.56*	1.60	1.57	1.61
	Mirage	-	-	1.56*	1.59	-	-
F687/F736	Ritmo	0.78*	0.78	0.79	0.79	0.79*	0.79
	Skalmeje	0.79*	0.80	0.79*	0.80	0.79*	0.81
	Aron	-	-	0.80	0.80	-	-
	Esket	0.78	0.79	0.78	0.79	0.78	0.79
	Mirage	-	-	0.79	0.80	-	-

* Significant differences (ANOVA, $p \leq 0.05$) between control (c) and inoculated (i) leaves for each cultivar and measuring day ($n = 6$ for control plants; $n = 8$ for inoculated plants).

Table S5. Ratio of amplitude-to-half-bandwidth from fluorescence (F451, F522, F687, and F736) on control (c) and inoculated (i) wheat leaves of the cultivars Ritmo (RD = 8), Skalmeje (RD = 7), Aron (RD = 8), Esket (RD = 3), and Mirage (RD = 3) at 2, 3, and 4 days after inoculation (dai).

Fluorescence peak	Wheat cultivar	2 dai		3 dai		4 dai	
		c	i	c	i	c	i
F451	Ritmo	1280	1261	1338	1366	1251*	1354
	Skalmeje	1173	1202	1131	1162	1031	1155
	Aron	-	-	1324	1423	-	-
	Esket	1061*	1132	1030*	1204	958*	112
	Mirage	-	-	1430	1564	-	-
F522	Ritmo	332	334	344	362	326*	379
	Skalmeje	301	315	292	314	269*	324
	Aron	-	-	409	447	-	-
	Esket	270*	297	272*	330	258*	316
	Mirage	-	-	413	477	-	-
F687	Ritmo	881	827	908	858	902	843
	Skalmeje	644	578	650	568	621	557
	Aron	-	-	860	918	-	-
	Esket	697	663	695	666	692	648
	Mirage	-	-	965	918	-	-
F736	Ritmo	715	655	746*	671	749*	648
	Skalmeje	465	416	486*	417	477*	396
	Aron	-	-	643	684	-	-
	Esket	526	482	545	465	546*	435
	Mirage	-	-	741	672	-	-

* Significant differences (ANOVA, $p \leq 0.05$) between control (c) and inoculated (i) leaves for each cultivar and measuring day ($n = 6$ for control plants; $n = 8$ for inoculated plants).

Table S6. Mean fluorescence lifetime at selected wavelength of control (c) and inoculated (i) leaves of cvs Ritmo (RD = 8), Skalmeje (RD = 7), Aron (RD = 8), Esket (RD = 3), and Mirage (RD = 2) at 2, 3, and 4 days after inoculation (dai).

Wavelength [nm]	Wheat cultivar	2 dai		3 dai		4 dai	
		c	i	c	i	c	i
410	Ritmo	0.63	0.66	0.65	0.63	0.65	0.64
	Skalmeje	-	-	-	-	-	-
	Aron	-	-	-	-	-	-
	Esket	-	-	-	-	-	-
	Mirage	-	-	-	-	-	-
440	Ritmo	0.67	0.70	0.70	0.70	0.66	0.67
	Skalmeje	-	-	-	-	-	-
	Aron	0.59	0.63	0.60	0.61	0.64	0.66
	Esket	0.67*	0.69	0.71	0.78	0.69*	0.87
	Mirage	0.57*	0.60	0.63	0.64	0.66	0.74
470	Ritmo	0.83*	0.87	0.83*	0.87	0.82*	0.85
	Skalmeje	-	-	-	-	-	-
	Aron	-	-	-	-	-	-
	Esket	-	-	-	-	-	-
	Mirage	-	-	-	-	-	-
500	Ritmo	1.01	1.04	1.05	1.07	1.02	1.04
	Skalmeje	0.99	1.01	1.00	1.01	1.09	1.03
	Aron	-	-	1.00	1.02	1.00	1.04
	Esket	1.03	1.01	1.05*	1.09	1.02*	1.10
	Mirage	-	-	0.94*	1.02	0.96*	1.05
530	Ritmo	1.11*	1.15	1.12	1.15	1.15	1.15
	Skalmeje	1.08	1.09	1.11	1.12	1.09	1.10
	Aron	-	-	1.13	1.13	1.14	1.17
	Esket	1.13	1.17	1.13*	1.18	1.15*	1.23
	Mirage	-	-	1.05*	1.13	1.11*	1.18
560	Ritmo	-	-	-	-	-	-
	Skalmeje	1.08	1.12	1.10*	1.20	1.16	1.20
	Aron	-	-	-	-	-	-
	Esket	1.14*	1.23	1.21	1.27	1.18*	1.34
	Mirage	-	-	-	-	-	-

* Significant differences (ANOVA, $p \leq 0.05$; $n = 4$ for control plants; $n = 5$ for inoculated plants) between control (c) and inoculated (i) leaves for each cultivar and measuring day.

6 References

Agrios GN (2005) Plant Pathology. New Delhi: Elsevier Academic Press, 922 pp.

Belasque Jr J, Gasparoto MCG, Marcassa LG (2008) Detection of mechanical and disease stresses in citrus plants by fluorescence spectroscopy. Applied Optics 47:1922-1926

Berger S, Sinha AK, Roitsch T (2007) Plant physiology meets phytopathology: plant primary metabolism and plant-pathogen interactions. Journal of Experimental Botany 58: 4019-4026

Buschmann C (2007) Variability and application of the chlorophyll fluorescence emission ratio red/far-red of leaves. Photosynthesis Research 92:261-271

Buschmann C, Langsdorf G, Lichtenthaler HK (2009) Fluorescence: the blue, green, red and far-red fluorescence signatures of plant tissues, their multicolour fluorescence imaging and application for agrofood assessment. In: Optical monitoring of fresh and processed agricultural crops, Zude M (Ed.). Boca Raton: CRS Press, Taylor & Francis Group, 272-319

Cerovic ZG, Samson G, Morales F, Tremblay N, Moya I (1999) Ultraviolet-induced fluorescence for plant monitoring: present state and prospects. Agronomie 19:543-578

Chaerle L, Lenk S, Hagenbeek D, Buschmann C, Van Der Straeten D (2007) Multicolour fluorescence imaging for early detection of the hypersensitive reaction to tobacco mosaic virus. Journal of Plant Physiology 164:253-262

Chaerle L and Van Der Straeten D (2000) Imaging techniques and the early detection of plant stress. Trends in Plant Science 5:495-501

German Federal Plant Variety Office [Bundessortenamt] (2008) Beschreibende Sortenliste – Getreide, Mais, Ölfrüchte, Leguminosen und Hackfrüchte außer Kartoffeln. Hannover: Deutscher Landwirtschaftsverlag GmbH

Hu G and Rijkenberg FHJ (1998) Scanning electron microscopy of early infection structure formation by *Puccinia recondita* f. sp. *tritici* on and in susceptible and resistant wheat lines. Mycological Research 102:391-399

Huang S, Vleeshouwers V, Visser RGF, Jacobsen E (2005) An accurate in vitro assay for high-throughput disease testing of *Phytophthora infestans* in potato. Plant Disease 89:1263–1267

Jabs T and Slusarenko AJ (2000) The hypersensitive response. In: Mechanisms of resistance to plant diseases, Slusarenko AJ, Fraser RSS, van Loon LC (Eds.). Dordrecht: Kluwer Academic Publishers, 279-324

Jansen M, Gilmer F, Biskup B, Nagel K, Rascher U, Fischbach A, Briem S, Dreissen G, Tittmann S, Braun S, De Jaeger I, Metzlaff M, Schurr U, Scharr H, Walter A (2009) Simultaneous phenotyping of leaf growth and chlorophyll fluorescence via GROWSCREEN FLUORO allows detection of stress tolerance in *Arabidopsis thaliana* and other rosette plants. Functional Plant Biology 36:902-914

Komura M and Itoh S (2009) Fluorescence measurement by a streak camera in a single-photon-counting mode. Photosynthesis Research 101:19-133

Lang M, Stober F, Lichtenthaler HK (1991) Fluorescence emission spectra of plant leaves and plant constituents. Radiation and Environmental Biophysics 30:333-347

Lenk S, Chaerle L, Pfündel EE, Langsdorf G, Hagenbeek D, Lichtenthaler HK, Van Der Straeten D, Buschmann C (2007) Multispectral fluorescence and reflectance imaging at the leaf level and its possible applications. Journal of Experimental Botany 58:807-814

Lichtenthaler HK (1996) Vegetation stress: an introduction to the stress concept in plants. Journal of Plant Physiology 148:4-14

Lichtenthaler HK and Miehé JA (1997) Fluorescence imaging as a diagnostic tool for plant stress. Trends in Plant Science 2:316-320

Lüdeker W, Dahn H-G, Günther KP (1996) Detection of fungal infection of plants by laser-induced fluorescence: an attempt to use remote sensing. Journal of Plant Physiology 148:579-585

Moerschbacher BM, Noll UM, Gorrichon N, Reisener H-J (1990) Specific inhibition of lignification breaks hypersensitive resistance of wheat to stem rust. Plant Physiology 93:465-470

Morales F, Cerovic ZG, Moya I (1994) Characterization of blue-green fluorescence in the mesophyll of sugar beet (*Beta vulgaris* L.) leaves affected by iron deficiency. Plant Physiology 106:127-133

Pawelec A, Dubourg C, Briard M (2006) Evaluation of carrot resistance to alternaria leaf blight in controlled environments. Plant Pathology 55:68–72

Rost FWD (1995) Autofluorescence in plants, fungi and bacteria. In: Fluorescence microscopy Volume II, Rost FWD (Ed.). Cambridge, New York, Melbourne: Cambridge University Press, 16-39

Schnabel G, Strittmatter G, Noga G (1998) Changes in photosynthetic electron transport in potato cultivars with different field resistance after infection with *Phytophthora infestans*. Journal of Phytopatholgy 146:205-210

Scholes JD and Rolfe SA (2009) Chlorophyll fluorescence imaging as tool for understanding the impact of fungal diseases on plant performance: a phenomics perspective. Functional Plant Biology 36:880-892

Somssich IE and Hahlbrock K (1998) Pathogen defence in plants - a paradigm of biological complexity. Trends in Plant Science 3:86-90

Southerton SG and Deverall BJ (1990a) Changes in phenolic acid levels in wheat leaves expressing resistance to *Puccinia recondita* f. sp. *tritici*. Physiological and Molecular Plant Pathology 37:437-450

Southerton SG and Deverall BJ (1990b) Histochemical and chemical evidence for lignin accumulation during the expression of resistance to leaf rust fungi in wheat. Physiological and Molecular Plant Pathology 36:483-494

Zhang L and Dickinson L (2001) Fluorescence from rust fungi: a simple and effective method to monitor the dynamics of fungal growth *in planta*. Physiological and Molecular Plant Pathology 59:137-141

D Detection of powdery mildew (*Blumeria graminis* f. sp. *tritici*) infection in wheat (*Triticum aestivum*) cultivars by fluorescence spectroscopy

1 Introduction

One of the most important biotic factors limiting wheat production worldwide is powdery mildew infection caused by *B. graminis* f. sp. *tritici* (Liu *et al*. 1999). Early and accurate detection of this fungal disease is necessary to initiate control strategies in time. Recently, new sensors for the fast and non-destructive detection and identification of foliar diseases have been developed. Here, passive and active techniques, such as reflectance and fluorescence procedures, sometimes established as imaging systems, were used to assess the physiological status of the plants (Synková 1997). Hence, by using a combined system for sensing spectral reflection and fluorescence induction, plants infected with *Puccinia striiformis* were discriminated from healthy plants with an accuracy of 95% (Bravo *et al*. 2004). Moreover, the pre-symptomatic detection of fungal diseases, as early as 2 to 3 days after inoculation, was possible using chlorophyll fluorescence measurements under laboratory conditions (Bravo *et al*. 2002).

In addition to the practical importance of sensor-based disease detection, e.g. for optimizing pesticide spray programs, such new technologies allow a better and more objective understanding of genotype-specific reactions to stress. It is widely known that plants respond to pathogen attacks by accumulating specific compounds, such as salicylic acid and phenylpropanoid compounds (e.g., cinnamic acid, stilbens, coumarins, and flavonoids) as key components in plant disease resistance. However, phenolic compounds can also be accumulated as a stress-response in susceptible cultivars (Lenk *et al*. 2007). In addition to papilla formation, lignification, suberin production, accumulation of phytoalexins, and synthesis of pathogenesis-related proteins are common resistance mechanisms in pathogen defence. Indeed, several defence reactions, including signal transduction, seemed to be mediated by linolenic acid and jasmonic acids (Berger *et al*. 2007; Somssich and Hahlbrock 1998). Alternatively, several preformed defence substances, such as phenol derivates, lactones, saponines, and stilbenes are known in various host-pathogen interactions (Agrios 2005).

Depending on the nature of the host-pathogen interaction and the time elapsed from infection to sensing, the pathogen-induced changes in the chemical composition might be

detected non-destructively by using fluorescence techniques. In recent studies evaluating the fluorescence of chlorophyll with a laser-induced fluorometer (LIF), wheat leaves infected with powdery mildew had significantly higher fluorescence ratios only after the appearance of visual symptoms eight to ten days after inoculation; these results were related to the chlorophyll degradation of the infected spots (Kuckenberg *et al*. 2009a). In contrast, an early detection of this fungal infection by means of chlorophyll fluorescence imaging could be accomplished two to three days before visual symptoms became apparent (Kuckenberg *et al*. 2009b). In a resistant barley line, epidermal hypersensitive cell death was detected within 36 h after powdery mildew inoculation by recording the UV autofluorescence using a fluorescence microscope and by the accumulation of phenolic compounds (Swarbrick *et al*. 2006).

UV-induced fluorescence spectroscopy is a well-established system for the detection of physiological and biochemical changes in organisms (Cerovic *et al*. 1999). Recently, its potential to classify the sensitivity level of wheat genotypes for the leaf rust pathogen was shown (Bürling *et al*. 2010). In this context, the spectral information and the great number of possible peak ratios that are allied to determinations of mean fluorescence lifetime provide a sensitive tool for evaluating changes in living plant tissues. In the present work, we therefore hypothesized that the detection of powdery mildew infection on wheat plants shortly after inoculation is possible. Furthermore, we postulated that it would be possible to discriminate between wheat genotypes that are either resistant or susceptible to the powdery mildew pathogen. For these purposes, the combined use of UV-induced fluorescence spectra and the fluorescence lifetime determination were adopted as a non-destructive technique.

2 Materials and Methods

2.1 Plant material

The experiments were conducted in a controlled-environment cabinet simulating a 14 h photoperiod with 200 µmol m^{-2} s^{-1} photosynthetic active radiation (PAR; Philips PL-L 36 W fluorescent lamps, Hamburg, Germany), a day/night temperature of 20/15 ± 2°C and relative humidity of 75/80 ± 10%. For the studies, the winter wheat (*Triticum aestivum* L. emend. Fiori. et Paol.) cultivars Magister and Magnus (powdery mildew susceptible, resistance degree RD = 7 and RD = 6, respectively, according to the descriptive variety list of the German Federal Plant Variety Office [Bundessortenamt] (2008), ranging from 1-9) and Türkis and Esket (mildew resistant, RD = 1 and RD = 2, respectively) were selected. Seeds of each cultivar were sown in individual pots (5 seeds per pot) filled with perlite. Emerging

plants were provided with Hoagland nutrient solution every other day. Twenty days after sowing, when the plants had reached the second-leaf stage, seven pots of each cultivar (four for inoculation, three as control) were selected for the experiment. Powdery mildew inoculation was done on the youngest fully expanded leaf of two plants per pot.

2.2 Inoculation of *Blumeria graminis* f. sp. *tritici*

At the beginning of the experiments, the middle of the leaf, lengthwise, was determined for each single leaf and marked with a felt tip pen. Marked leaves were horizontally fixed before the inoculation with conidia of a non-specific mixture of *B. graminis* f. sp. *tritici* that was produced on wheat without known resistance genes (INRES - Phytomedicine, University of Bonn). For a regular supply of fresh conidia, a set of plants was cultivated separately and infected with powdery mildew. For the inoculation of the experimental plants, conidia were removed with a fine brush and directly applied on the leaf surface of target plants. The application site was 3 x 5 mm and was located on the middle of the leaf half. Twenty-two hours after inoculation (hai), and in a later experiment ten hai, visible conidia were removed by gently blowing and brushing over the leaf surface. Control plants in different pots were handled in the same manner, however without conidia. Experiments were designed to make a pairwise comparison of the response of one resistant and one susceptible cultivar to the powdery mildew inoculation. Hence, the cultivars Magister and Türkis, and Magnus and Esket, were evaluated pairwise.

2.3 Fluorescence measurements

Fluorescence measurements were carried out using a compact fibre-optic fluorescence spectrometer with nanosecond time-resolution provided by the boxcar technique (IOM GmbH, Berlin, Germany). A pulsed N_2-laser (MSG803-TD, LTB Lasertechnik Berlin GmbH, Berlin, Germany) with an emission wavelength of 337 nm and a repetition rate of 20 Hz served as the excitation source. The fibre-optic probe for the detection of fluorescence signals consisted of a central excitation fibre and six surrounding emission fibres, each with a 200 µm diameter. The probe pulse energy was adjusted to be 1-2 µJ with a pulse length of approximately 1 ns resulting in a density of 5.5 x 10^{15} photons per cm^2 and impulse. Fluorescence was recorded with an acousto-optic tunable filter (AOTF) monochromator, which enables a minimal step width of 1 nm, and signals were processed by a photomultiplier (PMT; H5783-01, Hamamatsu, Hamamatsu City, Japan). The sensitivity of the PMT was

adjusted to optimize the signal intensity during the spectral and lifetime measurements. Time resolution was accomplished using a gated integrator with a 2 ns half-width; the position of the gate could be set with an accuracy of 0.1 nanoseconds.

The detection of the fluorescence spectra and the decay data was done on leaves fixed horizontally on a plate with an integrated sample holder. The fibre-optic probe was positioned in a 90° angle to the leaf. Thereby, with the help of a laser-based rangefinder (OptoNCDT 1300, Micro-Epsilon Messtechnik GmbH & Co. KG, Ortenburg, Germany) fixed beside the probe, the distance between the leaf and the probe surface was detected and adjusted for the point of measurement. This alignment of the correct distance was conducted to provide fluorescence intensities in a narrow data range, to provide a minimum of signal intensity and to avoid signal saturation. The spectra and lifetime at selected wavelengths were measured at 21-23°C under ambient light conditions (about 18 µmol m^{-2} s^{-1} PAR) from one to three days after pathogen inoculation (dai) on the inoculation area as described below. Before starting measurements, plants were adapted for 0.5 h to room light and temperature conditions.

For an optimal recording of fluorescence signals, the experimental settings were adjusted for measurements of spectra (SPEC; 370-800 nm), lifetime 1 (LF 1; 410-530 nm), lifetime 2 (LF 2; 560-620 nm), and lifetime 3 (LF 3; 530-560 nm). Common to all measurements was a pulse count of 32, which is the number of laser pulses averaged over every single data point. Spectrally resolved measurements were accomplished at a gate position of 3 ns (in the temporal signal maximum), with a wavelength interval of 2 nm, a distance of 3.95 mm between the probe and the sample, and a PMT gain of 600 Volt. All lifetime measurements (LF 1; LF 2; LF 3) were performed at predefined wavelengths, separated 30 nm from each other within their respective spectral range (e.g. at 410, 440, 470, 500 and 530 nm for LF 1). The step width was set to 0.2 nanoseconds. LF 1 and LF 3 had the same PMT gain of 600 V, while LF 2 was set to 800 Volt. The distance between the probe tip and the sample was adjusted to 4.57 mm for LF 1 and LF 2, and 2.70 mm for LF 3. In order to avoid a time-shift effect within the time-course of a single measuring day alternate measurements on inoculated and non-inoculated leaves were conducted.

2.4 Data processing and statistics

The measured UV-induced fluorescence spectra were processed by Gaussian curve fitting using the freeware Gnuplot, version 4.2, patch level 4 (http://www.gnuplot.info; Fig. 1). Peak position, amplitudes, and half-bandwidth were determined to calculate the ratios of

peak amplitudes, half-bandwidths, and amplitudes-to-half-bandwidths within single peaks. Before curve fitting, the raw data were corrected for the laser energy to remove possible data distortion due to fluctuations of the excitation energy.

In order to analyse the fluorescence decay, the data was deconvoluted using the software DC4 (version 2.0.6.3), by performing a Levenberg-Marquardt fit (IOM GmbH, Berlin, Germany, 2008). The processed experimental data was subjected to analysis of variance using the SPSS statistical package (PASW statistics version 15.0, SPSS Inc., Chicago, USA). For each day, cultivar and evaluation, the means of inoculated and healthy plants were compared by analysis of variance (One-way ANOVA, $p \leq 0.05$). Graphs (Mean ± SD) were drawn with SigmaPlot 8.02 (Systat Software Inc., Richmond, CA, USA) and OriginLab 7.1 SR2 (OriginLab Cooperation, Northhampton, USA).

3 Results

3.1 Pathogen development

The present study focused on the pathogen development and its impact on fluorescence parameters, which were evaluated pairwise between one resistant and one susceptible cultivar. The established pairs were the Magister (RD = 7) and Türkis (RD = 1), and Magnus (RD = 6) and Esket (RD = 2). As a rule, visual evaluations of the pathogen development first revealed small patches of whitish mycelium at four days after inoculation. Both susceptible cultivars, Magnus and Magister, were more affected than the resistant cultivars, Türkis and Esket. During the following days, the patches increased in size due to mycelium growth and development on the susceptible cultivars, whereas patches remained locally restricted on the resistant cultivars.

3.2 Characteristic fluorescence spectra and lifetime

After Gaussian curve fitting, the positions of the fluorescence (F) peaks were determined at 451 nm for the blue peak (B), 522 nm for the green shoulder (G), and 687 nm (R) and 736 nm (FR) for the chlorophyll peaks (Fig. 1). In general, the senescence of leaves during the experimental period from 1 to 3 dai induced a decrease of the F451/F522, F451/F687, F451/F736, F522/F736, and F687/F736 amplitude ratios as was documented for the healthy control (c) leaves of the cultivars Türkis, Magister, Esket, and Magnus (Table 1). However, the magnitude of the change was cultivar-dependent as was shown for the ratio

F522/F687, which was reduced more strongly in the cvs Türkis and Magister than in the cvs Esket and Magnus (Table 1).

The ratios of half-bandwidth (Table 2) that were determined for healthy plants (c) revealed no clear trend of changing values due to leaf senescence. For the amplitude-to-half-bandwidth ratios, it was striking that the values of the blue (F451) and green (F522) peaks decreased in all cultivars over time (Table 3).

The deconvolution of fluorescence decay data showed that one mean lifetime could be generated with greater robustness than using multiple lifetimes. Nevertheless, variations of residuals indicate a bi-exponential function. The mean lifetime of control plants elongated from about 0.6-0.7 ns at 410 nm constantly up to 1.1-1.2 ns between 530 and 560 nm before being shortened to 0.9-1.0 ns at 620 nm (Fig. 2).

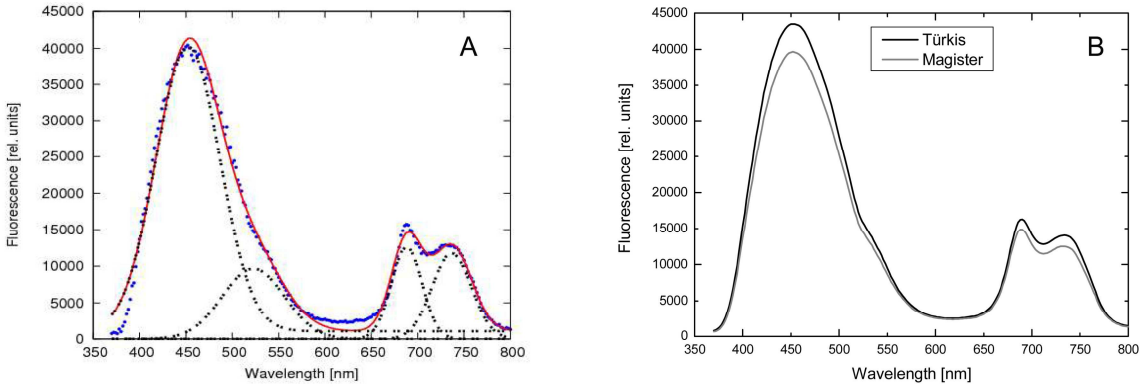

Fig. 1. A) Deconvolution in Gaussian spectral components. Solid circles: measured fluorescence emission spectrum (370-800 nm), solid squares: individual Gaussian spectral components of the fitted spectrum, solid line: fitted spectrum; **B)** Characteristic fluorescence emission spectrum (370-800 nm, smoothed curves) of healthy wheat leaves (excitation at 337 nm) of the cultivars Türkis and Magister.

3.3 Detection of powdery mildew infection

Irrespective of the resistance degree of the cultivar, inoculation of leaves with *B. graminis* induced significant changes in the evaluated fluorescence parameters. As shown in our time-series measurements, the elapsed time from pathogen inoculation until 4 dai significantly impacted both the number of affected parameters and the nominal difference between values measured on control (c) and inoculated (i) leaves. Regarding the spectral characteristic, the most robust parameter was the ratio F451/F522 for both the amplitude (Table 1) and the half-bandwidth (Table 2) ratios.

Table 1. Ratio of amplitudes between fluorescence peaks (F451, F522, F687 and F736) measured on control (c) and inoculated (i) wheat leaves of the cultivars Türkis (RD = 1), Esket (RD = 2), Magister (RD = 7) and Magnus (RD = 6) at 1, 2, 3 and 4 days after inoculation (dai).

		1 dai		2 dai		3 dai		4 dai	
		c	**i**	**c**	**i**	**c**	**i**	**c**	**i**
F451/ F522	Türkis	4.11*	3.58	4.03*	3.41	3.94*	3.31	3.88*	3.23
	Esket	3.78*	3.39	3.73*	3.03	3.71*	2.79	-	-
	Magister	4.04*	3.68	4.03*	3.53	3.99*	3.34	3.95*	3.22
	Magnus	3.73*	3.43	3.72*	3.20	3.72*	3.05	-	-
F451/ F687	Türkis	3.22	2.71	2.90	2.77	2.63	2.62	2.50	2.62
	Esket	2.32	2.01	2.30	2.15	2.26	2.11	-	-
	Magister	3.21	2.83	3.07	2.82	2.86	2.90	2.80*	3.13
	Magnus	2.34*	1.78	2.33	2.17	2.31	2.20	-	-
F451/ F736	Türkis	3.39	3.24	3.03	3.21	2.74	2.96	2.56	2.97
	Esket	2.57	2.26	2.45	2.43	2.35	2.43	-	-
	Magister	3.47	3.43	3.27	3.25	2.96*	3.33	2.85*	3.69
	Magnus	2.69*	2.03	2.53	2.41	2.46	2.51	-	-
F522/ F687	Türkis	0.78	0.76	0.72	0.81	0.67	0.79	0.64*	0.81
	Esket	0.61	0.59	0.61	0.71	0.61*	0.76	-	-
	Magister	0.79	0.77	0.76	0.80	0.72*	0.87	0.71*	0.97
	Magnus	0.63	0.52	0.63	0.68	0.62	0.72	-	-
F522/ F736	Türkis	0.83	0.90	0.75*	0.94	0.70*	0.89	0.66*	0.92
	Esket	0.68	0.67	0.66*	0.80	0.63*	0.87	-	-
	Magister	0.86	0.93	0.81*	0.92	0.74*	1.00	0.72*	1.15
	Magnus	0.72	0.59	0.68	0.76	0.66*	0.82	-	-
F687/ F736	Türkis	1.05*	1.19	1.04*	1.15	1.04*	1.13	1.02*	1.13
	Esket	1.11	1.12	1.07*	1.13	1.04*	1.15	-	-
	Magister	1.08*	1.21	1.07*	1.15	1.03*	1.15	1.02*	1.18
	Magnus	1.15	1.14	1.09	1.11	1.06*	1.14	-	-

* Significant differences (ANOVA, $p \leq 0.05$) between control and inoculated leaves for each cultivar and measuring day (n = 6 for control plants; n = 8 for inoculated plants).

In both cases, the ratio F451/F522 decreased continuously from the first evaluation day until the end of the experiment, but when comparing each day individually, the values were significantly lower in inoculated leaves. For the cv Türkis, the values of F451/F522 decreased from 4.11 (c) to 3.58 (i) at 1 dai, whereas for the cv Magister, the values changed from 4.04 (c) to 3.68 (i) for the same evaluation (Table 1). At this early point of time, changes were also revealed by the half-bandwidth ratio F522/F687 and F522/F736, which showed significantly higher values for inoculated leaves than for control ones in all four cultivars (Table 2). Thereby, modifications were more pronounced in both of the resistant cvs, Türkis and Esket.

Table 2. Ratio of half-bandwidth between fluorescence peaks (F451, F522, F687 and F736) on control (c) and inoculated (i) wheat leaves of the cultivars Türkis (RD = 1), Esket (RD = 2), Magister (RD = 7) and Magnus (RD = 6) at 1, 2, 3 and 4 days after inoculation (dai).

		1 dai		2 dai		3 dai		4 dai	
		c	**i**	**c**	**i**	**c**	**i**	**c**	**i**
F451/ F522	Türkis	1.05*	1.00	1.04*	0.97	1.04*	0.95	1.03*	0.94
	Esket	1.05*	0.98	1.05*	0.94	1.05*	0.89		
	Magister	1.03*	1.00	1.03*	0.98	1.02*	0.96	1.01*	0.93
	Magnus	1.05	1.04	1.05*	1.01	1.05*	0.99		
F451/ F687	Türkis	2.10	2.11	2.08	2.08	2.08	2.08	2.07	2.07
	Esket	2.07	2.07	2.07*	2.05	2.06*	2.03		
	Magister	2.09*	2.10	2.07	2.07	2.07	2.06	2.06	2.04
	Magnus	2.07*	2.09	2.06	2.06	2.06	2.06		
F451/ F736	Türkis	1.65	1.65	1.63	1.64	1.63	1.64	1.62*	1.64
	Esket	1.61	1.61	1.61	1.61	1.61	1.61		
	Magister	1.63	1.64	1.63	1.63	1.62	1.63	1.62*	1.65
	Magnus	1.61	1.61	1.60	1.61	1.61	1.61		
F522/ F687	Türkis	2.01*	2.11	2.00*	2.15	2.01*	2.18	2.01*	2.20
	Esket	1.98*	2.12	1.98*	2.19	1.96*	2.29		
	Magister	2.02*	2.09	2.02*	2.12	2.04*	2.15	2.05*	2.20
	Magnus	1.98*	2.02	1.96*	2.04	1.96*	2.08		
F522/ F736	Türkis	1.58*	1.65	1.57*	1.70	1.57*	1.72	1.57*	1.75
	Esket	1.54*	1.65	1.54*	1.72	1.53*	1.82		
	Magister	1.58*	1.63	1.59*	1.67	1.60*	1.71	1.61*	1.77
	Magnus	1.54	1.56	1.52*	1.59	1.53*	1.63		
F687/ F736	Türkis	0.79	0.78	0.78	0.79	0.78	0.79	0.78*	0.79
	Esket	0.78	0.78	0.78	0.79	0.78*	0.79		
	Magister	0.78	0.78	0.78	0.79	0.78*	0.79	0.79*	0.81
	Magnus	0.78*	0.77	0.78	0.78	0.78	0.78		

* Significant differences (ANOVA, $p \leq 0.05$) between control and inoculated leaves for each cultivar and measuring day (n = 6 for control plants; n = 8 for inoculated plants).

A direct comparison between Esket (RD = 2) and Magnus (RD = 6) indicated an increase of F522/F687 from 1.98 (c) to 2.12 (i) for Esket, and from 1.98 (c) to 2.02 (i) for Magnus (Table 2). As indicated by the ratio F522/F736, the difference between the control and inoculated leaves was significant, e.g., for the cv Türkis, increasing from 1.58 (c) to 1.65 (i). One day later, the amplitude ratios F522/F736 and F687/F736 showed increased values in all four cultivars for the inoculated leaves; in the case of Türkis, from 0.75 (c) to 0.94 (i), and 1.04 (c) to 1.15 (i), respectively. The described modifications at 1 and 2 dai were consistent during the consecutive days until the end of the measurements.

In Table 3, ratios of amplitudes-to-half-bandwidth for each single peak are presented. Although there were statistical differences at single comparisons between inoculated and non-inoculated plants, none of the evaluated parameters gave reliable indications for a potential differentiation between diseased and healthy plants.

Table 3. Ratio of amplitude-to-half-bandwidth from fluorescence (F451, F522, F687 and F736) on control (c) and inoculated (i) wheat leaves of the cultivars Türkis (RD = 1), Esket (RD = 2), Magister (RD = 7) and Magnus (RD = 6) at 1, 2, 3 and 4 days after inoculation (dai).

		1 dai		2 dai		3 dai		4 dai	
		c	**i**	**c**	**i**	**c**	**i**	**c**	**i**
F451	Türkis	1238*	1115	1111	1041	1061	1006	1021	959
	Esket	1148*	1023	1078*	963	1060*	943		
	Magister	1134*	1051	1069*	963	1020	995	982	996
	Magnus	1137	1126	1086	1182	1071*	1202		
F522	Türkis	315	311	287	296	279	290	271	280
	Esket	318	296	303	298	300	301		
	Magister	291	287	272	267	260*	286	250*	288
	Magnus	319	340	308*	37	303*	391		
F687	Türkis	816	886	812	801	847	812	857	771
	Esket	1042	1066	991	931	980	920		
	Magister	745	784	727	710	741	709	725	656
	Magnus	1028*	1329	984*	1132	969*	1135		
F736	Türkis	611	580	610	550	638	570	655*	542
	Esket	733	740	724	648	737	637		
	Magister	540	506	535	485	562*	490	560*	449
	Magnus	700*	903	703	794	713	782		

* Significant differences (ANOVA, $p \leq 0.05$) between control and inoculated leaves for each cultivar and measuring day (n = 6 for control plants; n = 8 for inoculated plants).

Fluorescence lifetime measurements (Fig. 2) revealed clear modifications of inoculated leaves with regard to control leaves, irrespective of the resistance degree of the cultivar. The overall tendency observed was a more or less pronounced elongation of lifetime for all selected wavelengths. Mildew resistant and susceptible cultivars showed early responses to the pathogen attack, which could be measured as early as one day after inoculation. At this time, clear differences between control and inoculated leaves of the cvs Magister and Türkis could be detected at 500, 530, 560, 590, and 620 nm.

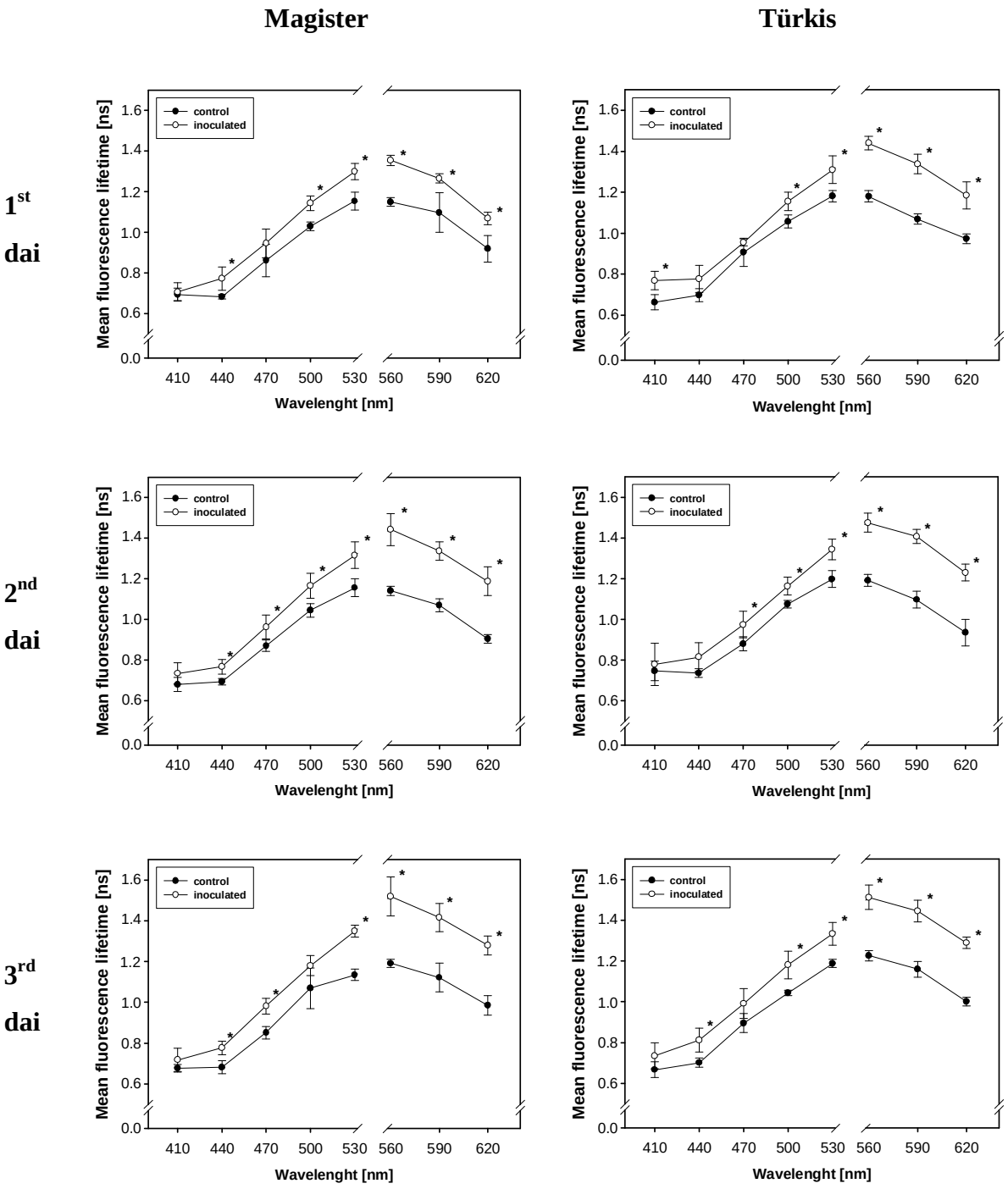

Fig. 2. Mean fluorescence lifetime at selected wavelengths between 410 and 620 nm for control and inoculated leaves of Magister (left, RD = 7) and Türkis (right, RD = 1), respectively at 1, 2, and 3 days after inoculation (dai). Measurements from 410-530 nm and from 560-620 nm were conducted with different settings as described in the materials and methods. * Values indicate mean ± SD; significant differences (ANOVA, $p \leq 0.05$) between control ($n = 4$) and inoculated ($n = 5$) leaves for each cultivar and measuring day.

Changes were most pronounced in the range from 560 to 620 nm. This is described by values of 1.35 ns (i) and 1.15 ns (c) and 1.34 ns (i) and 1.07 ns (c) for Magister (560 nm) and Türkis (590 nm), respectively. The significance between the control and the powdery mildew inoculated leaves in the spectral range from 500 to 620 nm remained unchanged during the following two days. Measurements at selected wavelengths (500, 530, 560 nm) in the cvs Magnus and Esket at 1 and 2 dai confirmed these findings (Table 4).

Table 4. Mean fluorescence lifetime at the selected wavelength for control and inoculated leaves of Magnus (RD = 6) and Esket (RD = 2) at 1 and 2 days after inoculation (dai).

		1 dai		2 dai	
		control	**inoculated**	**control**	**inoculated**
500 nm	Magnus	0.98*	1.18	1.04*	1.15
	Esket	1.02*	1.19	1.01*	1.16
530 nm	Magnus	1.09*	1.33	1.13*	1.30
	Esket	1.09*	1.30	1.13*	1.31
560 nm	Magnus	1.13*	1.42	1.19*	1.43
	Esket	1.12*	1.36	1.17*	1.44

* Significant differences (ANOVA, $p \leq 0.05$) between control and inoculated leaves for each cultivar and measuring day ($n = 4$ for control plants; $n = 5$ for inoculated plants).

3.4 Early changes of fluorescence due to pathogen establishment

Lifetime fluorescence measurements at 530 and 560 nm, conducted for the four cultivars from ten to twelve hours after pathogen inoculation, indicated a longer mean lifetime in inoculated leaves compared to control leaves. The intensity of modification depended on the cultivar and the measured wavelength (Fig. 3). A direct comparison of the susceptible cv Magister (A) and the resistant cv Türkis (B) showed that the lifetime at 530 nm was significantly increased from 1.02 ns and 1.04 ns in control leaves to 1.07 ns and 1.10 ns in inoculated ones, respectively. The magnitude of modification was more pronounced in the resistant than in the susceptible cultivar. Similarly, determinations at 560 nm showed a longer lifetime in inoculated leaves than in control leaves. The results observed for Magister and Türkis were confirmed in the experiment comparing the other sensitive (Magnus, Fig. 3C) and resistant (Esket, Fig. 3D) cultivars. In this case, the values increased from 1.03 ns (c) to 1.07 ns (i) for Magnus and significantly increased from 0.98 ns (c) to 1.01 ns (i) for Esket.

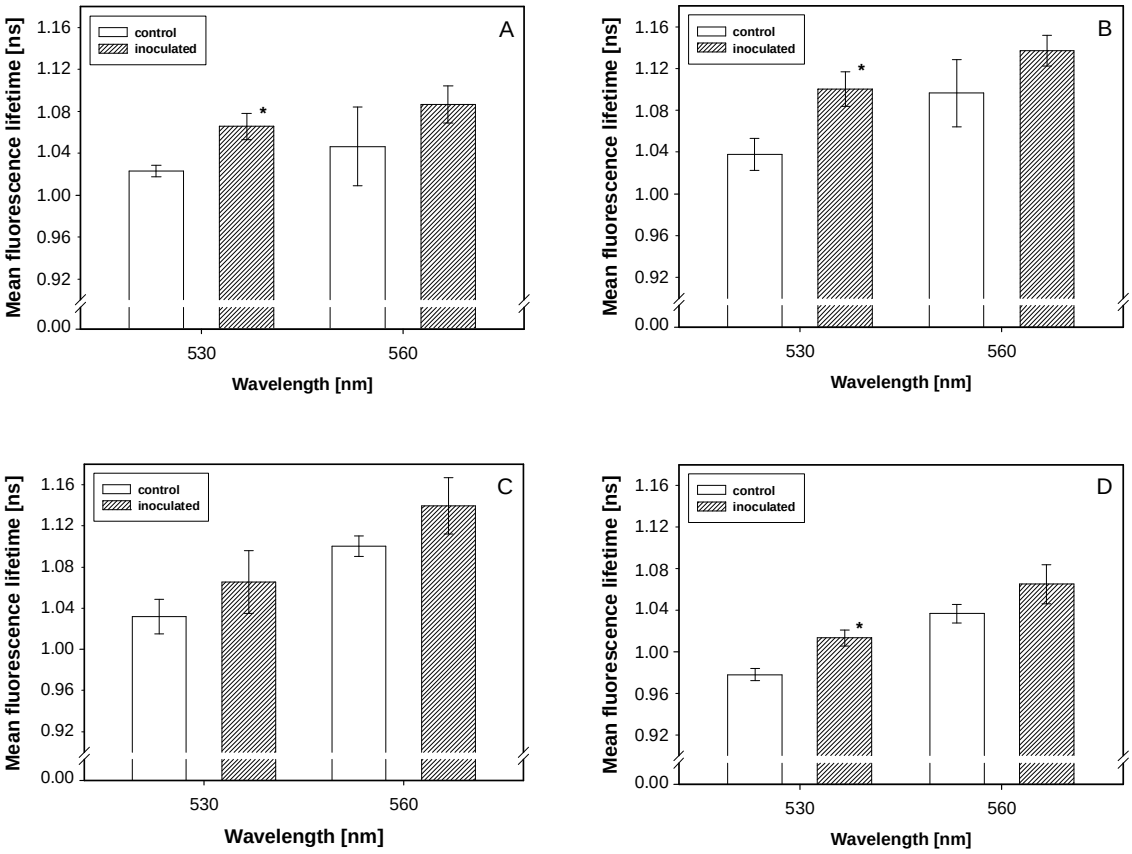

Fig. 3. Mean fluorescence lifetime at 530 nm and 560 nm for control and inoculated leaves of **A)** Magister (RD = 7), **B)** Türkis (RD = 1), **C)** Magnus (RD = 6), and **D)** Esket (RD = 2) at ten to twelve hours after inoculation (hai). Values indicate mean ± SD (n = 3). * Significant differences (ANOVA, $p \leq 0.05$) between control and inoculated leaves for each cultivar and measuring day.

4 Discussion

In our studies, we demonstrate that an early, pre-symptomatic detection of *B. graminis* infection on wheat plants is possible. Previous studies have shown the identification of powdery mildew 2 to 3 days after inoculation (Bravo *et al*. 2002), and with our approach, this time can be reduced to 1 dai or less. Irrespective of the resistance degree of the cultivar to the pathogen, the amplitude ratio F451/F522 was the most appropriate parameter to reveal pre-symptomatic pathogen infection as early as one day after inoculation. Moreover, F451/F522, F522/F687, and F522/F736 for the half-bandwidth ratios are also appropriate parameters to detect the fungal development. The mean lifetime was significantly longer in inoculated leaves as compared to control leaves in the spectral range between 410 nm and 620 nm,

whereupon the most pronounced differences were observed in the range of 500-620 nm. Furthermore, significant changes in the fluorescence mean lifetime were detected ten to twelve hours after first host-pathogen interaction.

As shown earlier, based on the F440/F520 ratio after UV excitation, it has been possible to detect powdery mildew in grapevines three days after inoculation (Bélanger *et al*. 2008). In our experiments, all tested cultivars revealed a reduction of the F451/F522 amplitudes and half-bandwidths as early as one day after inoculation (Tables 1 and 2). In accordance with the observations of Lüdeker *et al*. (1996), alterations might be induced by the increase of F520 due to the blue/green fluorescence band of the fungi, or the produced intercellular substances, which emit blue-green fluorescence. Von Röpenack (1998) reported that the maximum penetration frequency of powdery mildew fungus in a resistant cultivar was less than 0.1%, whereas in the susceptible cultivar, penetration was about 60%. The same authors observed a strong correlation between the accumulation of *p*-coumaroyl-hydroxyagmatine and the onset of penetration in the susceptible cultivars.

As indicated by the chlorophyll fluorescence, the increase of the F687/F736 amplitude ratio in the four cultivars by 1 dai (Table 1) might be caused by a reduced chlorophyll content, as similarly detected in inoculated leaves by means of reflectance measurements long before visible changes have occurred (West *et al*. 2003). Allen (1942) stated that the chlorophyll content of wheat leaves that are heavily inoculated with mildew decreased from the first day after inoculation due to a rapid degradation of this molecule. Further pathogen-triggered modifications were the increase of the ratios F522/F687 and F522/F736 for the half-bandwidth (Table 2) and F522/F736 for the amplitudes (Table 1). Presumably, the changes in F451/F522 and F687/F736 ratios are related to alterations in phenolic composition and chlorophyll concentration, respectively. Alternatively, modifications of F522/F687 and F522/F736 might reflect changes in both phenolic composition and chlorophyll degradation.

For the four wheat cultivars evaluated in our experiments, a clear elongation of mean lifetime due to pathogen development was registered between 410 nm and 620 nm. Mean fluorescence lifetime is an averaged value that is composed of several fluorophores with distinct lifetimes (Cerovic *et al*. 1999). The synthesis of new compounds in the tissue might result in the elongation or shortening of the mean lifetime, depending on the lifetime of the accumulated compound. Changes to the pH-value or the localization of substances in the cell/ cell compartments can also cause changes to the fluorescence lifetime. Our results on the fluorescence lifetime measurements revealed a general tendency towards a longer mean lifetime in the inoculated plants compared to the control plants (Fig. 2). In the compatible and

incompatible interaction between barley and powdery mildew, an increase of polyamine concentration has been observed one to three days after inoculation (Cowley and Walters 2002). As has been shown for a resistant barley genotype, epidermal hypersensitive cell death was induced within 24 h after powdery mildew inoculation and was associated with the accumulation of phenolic compounds (Swarbrick *et al*. 2006).

The successful identification of *B. graminis* infection at 1 dai in the two susceptible and two resistant wheat cultivars selected for our experiments were the basis for additional experiments addressing *B. graminis* detection some hours after inoculation. In this approach, changes in fluorescence, as a general reference to the pathogen-host interaction, were evaluated during a time period of ten to twelve hours after inoculation (hai). Even at this early point of time after inoculation, clear changes in the mean lifetime could be detected. Thereby, the magnitude of modifications could be a suitable basis for the differentiation between susceptible and resistant cultivars (Fig. 3). As described elsewhere, the first twelve hours of pathogen infection are characterized by the contact of spores with the leaf surface, the development of a primary germ tube, appressorial germ tube and appressorium and the first papilla defence (Thordal-Christensen *et al*. 2000). Upon contact with the pathogen, signalling substances like salicylic acid and jasmonic acid are produced by epidermal cells to initiate defence mechanisms (Berger *et al*. 2007). Several of the newly synthesized and accumulated substances like phenols and phenol derivates emit fluorescence when excited with UV light. Resistant plants respond more rapidly and more vigorously to pathogens than do susceptible plants (Taiz and Zeiger 2007). Von Röpenack (1998) observed that a differential accumulation of *p*-coumaroylagmatine was induced 2 h earlier, and at higher amounts, in the resistant line when compared to the susceptible one. The basic response of two phenolic compounds in resistant and susceptible lines was the same, but the dynamics and amount of substance formation were different (von Röpenack *et al*. 1998). Moreover, papilla, which contain, amongst others, phenols, were about 50% thicker in the resistant line when compared to the non-resistant line (Jorgensen 1992). Doll *et al*. (1994) evaluated the contribution of phenolic compounds in different barley varieties expressing partial resistance against powdery mildew. They found a large quantitative variation in the amount of nine phenolic components. This might also be a reason for the non-differentiation between the response of resistant and susceptible genotypes to powdery mildew by means of fluorescence spectroscopy in our studies.

5 Conclusions

UV-induced measurements of spectral characteristics and the determination of fluorescence lifetime are suitable approaches to detect powdery mildew (*B. graminis*) one to three days after inoculation. Specific ratios of amplitudes and of half-bandwidths can be determined as best suited for reliable and robust information. Furthermore, the mean lifetime was significantly increased in inoculated leaves when compared to control leaves, with the most pronounced differences observed in the range of 500 nm to 620 nm. Based on the changes in mean fluorescence lifetime, it is possible to reveal physiological and biochemical reactions ten to twelve hours after the initial pathogen-host interaction. Based on our results, it was not possible to discriminate between susceptible and resistant wheat cultivars. However, lifetime measurements shortly after pathogen inoculation indicate the potential of fluorescence spectroscopy as a complementary tool for screening new genotypes with unknown degrees of resistance to the pathogen.

6 References

Agrios GN (2005) Plant Pathology. New Delhi: Elsevier Academic Press, 922 pp.

Allen PJ (1942) Changes in the metabolism of wheat leaves induced by infection with powdery mildew. American Journal of Botany 29:425-435

Berger S, Sinha AK, Roitsch T (2007) Plant physiology meets phytopathology: plant primary metabolism and plant-pathogen interactions. Journal of Experimental Botany 58:4019-4026

Bravo C, Moshou D, Oberti R, West J, McCartney A, Bodria L, Ramon H (2002) Detection of foliar disease in the field by the fusion of measurements made by optical sensors. St. Joseph, Michigan: American Society of Agricultural and Biological Engineers, ASAE, Paper number 023087. 2002

Bravo C, Moshou D, Oberti R, West J, McCartney A, Bodria L, Ramon H (2004) Foliar disease detection in the field using optical sensor fusion. Agricultural Engineering International: the CIGR Journal of Scientific Research and Development, 6

Bürling K, Hunsche M, Noga G, Pfeifer L, Damerow L (2010) UV-induced fluorescence spectra and lifetime determination for detection of leaf rust (*Puccinia triticina*) in susceptible and resistant wheat (*Triticum aestivum*) cultivars. Functional Plant Biology (under evaluation)

Bélanger M-C, Roger J-M, Cartolaro P, Viau AA, Bellon-Maurel V (2008) Detection of

powdery mildew in grapevine using remotely sensed UV-induced fluorescence. International Journal of Remote Sensing 29:1707-1724

Cerovic ZG, Samson G, Morales F, Tremblay N, Moya I (1999) Ultraviolet-induced fluorescence for plant monitoring: present state and prospects. Agronomie 19:543-578

Cowley T and Walters DR (2002) Polyamine metabolism in an incompatible interaction between barley and the powdery mildew fungus, *Blumeria graminis* f. sp. *hordei*. Journal of Phytopathology 150:581-586

Doll H, Holm U, Sogaard B, Bay H (1994) Phenolic compounds in barley varieties with different degree of partial resistance against powdery mildew. Acta Horticulturae 381:576-582

Jorgensen JH (1992) Discovery, characterization and exploitation of *Mlo* powdery mildew resistance in barley. Euphytica 63:141-152

Kuckenberg J, Tartachnyk I, Noga G (2009a) Detection and differentiation of nitrogen-deficiency, powdery mildew and leaf rust at wheat leaf and canopy level by laser-induced chlorophyll fluorescence. Biosystems Engineering 103:121–128

Kuckenberg J, Tartachnyk I, Noga G (2009b) Temporal and spatial changes of chlorophyll fluorescence as a basis for early and precise detection of leaf rust and powdery mildew infections in wheat leaves. Precision Agriculture 10:34-44

Lenk S, Chaerle L, Pfündel EE, Langsdorf G, Hagenbeek D, Lichtenthaler HK, Van Der Straeten D, Buschmann C (2007) Multispectral fluorescence and reflectance imaging at the leaf level and its possible applications. Journal of Experimental Botany 58:807-814

Liu Z, Sun Q, Ni Z, Yang T (1999) Development of SCAR markers linked to the *Pm10* gene conferring resistance to powdery mildew in common wheat. Plant Breeding 118:215-219

Lüdeker W, Dahn H-G, Günther KP (1996) Detection of fungal infection of plants by laser-induced fluorescence: an attempt to use remote sensing. Journal of Plant Physiology 148:579-585

Somssich IE and Hahlbrock K (1998) Pathogen defence in plants - a paradigm of biological complexity. Trends in Plant Science 3:86-90

Synková H (1997) Vegetation stress. Biologia Plantarum 40:448

Swarbrick PJ, Schulze-Lefert P, Scholes JD (2006) Metabolic consequences of susceptibility and resistance (race specific and broad spectrum) in barley leaves challenged with powdery mildew. Plant, Cell and Environment 29:1061-1076

Taiz L and Zeiger E (2007) Plant Physiology. Berlin, Heidelberg: Springer, 770 pp.

Thordal-Christensen H, Gregersen PL, Messmer M (2000) The barley/*Blumeria* (Syn. Erysiphe) *graminis* interaction. In: Mechanisms of resistance to plant diseases, Slusarenko AJ, Fraser RSS, van Loon LC (Eds.). Dordrecht: Kluwer Academic Publishers, 77-100

von Röpenack E, Parr A, Schulze-Lefert P (1998) Structural analysis and dynamics of soluble and cell wall-bound phenolics in a broad spectrum resistance to the powdery mildew fungus in barley. The Journal of Biological Chemistry 273:9013-9022

West J, Bravo C, Oberti R, Lemaire D, Moshou D, McCartney HA (2003) The potential of optical canopy measurement for targeted control of field crop diseases. Annual Review of Phytopathology 41:593-614

E Blue-green and chlorophyll fluorescence for differentiation between nitrogen deficiency and pathogen infection in winter wheat

1 Introduction

The incidence of diseases and deficiency of nutrients representing biotic and abiotic stresses, respectively, are the limiting factors for crop production worldwide. As estimated, the potential of yield loss of wheat due to fungal pathogens might amount 15% under specific conditions (Oerke and Dehne 2004). During its life cycle, wheat plants are often infected by the biotrophic fungi *Puccinia triticina* and *Blumeria graminis* f. sp. *tritici*, causing leaf rust and powdery mildew, respectively. On the other hand, nitrogen is a key element in the plant nutrition (Marschner 2002), and its adequate supply is the most important nutritional process a farmer can manage in cultivated crops (McMurtrey III *et al*. 1994).

In recent years, with advanced technology sensing of stress-induced alterations of metabolism and crop physiology became more and more of interest to detect modifications at early stages before extensive plant damage occurs. For this purpose, several non-destructive approaches, e.g. fluorescence, reflectance, and thermal-imaging measurements, have been evaluated and adopted for the fast and early detection of individual stresses, such as diseases (e.g. Bodria *et al*. 2002; Bravo *et al*. 2003; Franke and Menz 2007; Kuckenberg *et al*. 2009a; Lindenthal *et al*. 2005) and mineral deficiency, especially the nitrogen status of plants (e.g. Bredemeier *et al*. 2003; Buschmann 2007; Schächtl *et al*. 2005; Subhash and Mohanan 1994; Tartachnyk and Rademacher 2003). Besides promising results, the specificity of the measuring system and the particularities of the experiments have to be considered when evaluating or comparing suitable techniques. As recently shown, the chlorophyll fluorescence imaging technique proved to be more sensitive than the thermal imaging for early detection of pathogen infection and nutrient deficiency (Chaerle *et al*. 2007a). Thereby, both nitrogen deficiency and pathogen infection are accompanied by a decrease in chlorophyll content (Tartachnyk and Rademacher 2003).

In general, a good detection of stress can be achieved when evaluating biotic and abiotic stresses as single factors. However, it is not unusual that several stresses influence the plant physiology simultaneously. Besides considerable advances, a reliable discrimination between biotic and abiotic stresses by using non-destructive techniques remains a challenge. Tartachnyk *et al*. (2006) showed that a discrimination between strong N-deficiency and pathogen infection at advanced stages can be accomplished on basis of fluorescence peak

ratio F690/F730. However, as shown for a cross-validation analysis of chlorophyll fluorescence, diseased leaves could be misrecognised as N-deficiency and vice versa, whereas the classification was improved when in addition the standard deviation of the mean was considered as a parameter for discrimination (Kuckenberg *et al*. 2009b). Unfortunately these conclusions were based on pathogen infection and N-deficiency evaluated on different leaves, whereas research studying both stressors concomitantly on the same plants are scarce.

When exposed to stresses, specific pigments and other molecules might be synthesized, accumulated or degraded, having an indirect or direct influence on the fluorescence signature. In general, nitrogen deficiency leads to less chlorophyll in the tissues (Ciompi *et al*. 1996). As shown in other experiments, nitrate availability influences not only the chlorophyll concentration but also phenol and lignin production which are reduced in wheat shoot by high nitrate levels (Brown *et al*. 1984). When infected with fungal pathogens, plants might accumulate specific compounds such as salicylic acid and phenylpropanoid compounds (e.g. cinnamic acid, stilbens, coumarins and flavonoids) as the most important substances in plant disease resistance (Chaerle *et al*. 2007b; Lenk *et al*. 2007). Accordingly, the fluorescence in the blue-green spectral range might yield promising results since it has been proven to be very sensitive to single stress events reflecting amongst others accumulation of secondary metabolites (Buschmann *et al*. 2009; Cerovic *et al*. 1999; Lichtenthaler and Miehé 1997). However, the suitability of the fluorescence outcome in the blue, green, and yellow spectral range for discriminating stressors is not yet proven. Therefore we hypothesized that a differentiation between wheat plant's physiological reaction due to N-deficiency and leaf rust (*Puccinia triticina*) as well as N-deficiency and powdery mildew (*Blumeria graminis* f. sp. *tritici*) might be accomplished by means of UV-induced fluorescence spectral measurements in the blue, green and yellow range (370 to 620 nm) in addition to the chlorophyll fluorescence (640 to 800 nm). Thereby we focused on a slight N-deficiency and the early stages of pathogen infection, justifying the need of sensors to detect pre-symptomatic stress signals. Of main interest is the basic suitability of combined spectral information by evaluation of several fluorescence ratios for consideration in future field experiments requiring more complex and developed detection systems.

2 Material and Methods

2.1 Plant material

Experiments were conducted in a controlled-environment cabinet simulating a 14 h photoperiod with 200 µmol m^{-2} s^{-1} photosynthetic active radiation (PAR; Philips PL-L 36 W fluorescent lamps, Hamburg, Germany), day/night temperature of 20/15 ± 2°C and relative humidity of 75/80 ± 10%. Winter wheat (*Triticum aestivum* L. emend. Fiori. et Paol.) seeds of the leaf rust (LR) and powdery mildew (PM) susceptible cultivar Ritmo were sown in individual pots (5 seeds per pot) filled with perlite. According to the descriptive variety list of the German Federal Plant Variety Office [Bundessortenamt] (2008), Ritmo is classified with a resistance degree (RD) of 8 for leaf rust and RD = 5 for powdery mildew, in a classification range from one (resistant) to nine (susceptible). Inoculation of single leaves with either leaf rust or powdery mildew was accomplished on the second fully developed leaf, twenty days after sowing. Experiments with combined nitrogen supply and leaf rust or powdery mildew inoculation were conducted separately and repeated at least twice. Accordingly, the experimental setup was as follows: a) N-full-supply [N+]; b) N-deficiency [N-]; c) N-full-supply + pathogen [N+/LR] or [N+/PM]; d) N-deficiency + pathogen [N-/LR] or [N-/PM]. In each experiment, number of replications was n = 12 for the nitrogen treatments, and n = 16 for the nitrogen + pathogen treatments. Pathogen inoculation was done on two plants per pot.

2.2 Fertilization and chlorophyll determination

Emerging plants were provided with either a standard or a modified Hoagland nutrient solution; the first one contained all mineral nutrients for optimal plant growth and development, while the second one was adjusted to induce nitrogen deficiency. For this purpose, several pre-experiments with defined amounts of nitrogen were conducted in order to find the appropriate N-concentration to induce a slight N-deficit which is not evident by visual observation. The full nitrogen supply solution (N+) contained 1 M $Ca(NO_3)_2*4H_2O$, 0.5 M $(NH_4)H_2PO_4$, and 0.66 M KNO_3 whereas the N-deficiency solution contained 0.5 M KH_2PO_4, 1 M KCl, 0.5 M $Ca(NO_3)_2*4H_2O$, and 0.1 M $(NH_4)_2SO_4$. Consequently, the deficiency solution (N-) contained 40% of the N-amount of the standard solution. The content of micronutrients was similar in both fertilization solutions.

Leaves in the same developmental stage as those used in the main experiments were sampled and the nitrogen status was evaluated non-destructively with the SPAD 502 (Konika Minolta, Langenhagen, Germany) equipment on adaxial leaf sides by measuring red (~ 650

nm) and infra-red (~ 940 nm) light transmission. From the same leaves chlorophyll content was extracted from 1 cm^2 leaf pieces with dimethyl sulfoxide (DMSO) and analytically determined as described elsewhere (Blanke 1992). The absorbance of extracts was evaluated at 665 nm (A665) and 647 nm (A647) with a UV-VIS spectrophotometer (Lambda 5, Perkin-Elmer, Massachusetts, USA). Total chlorophyll (Chl*t*) concentration was calculated on fresh-weight basis according to the equation: Chl*t* = 17.9 x A647 + 8.08 x A665.

2.3 Pathogen inoculation

2.3.1 Inoculation of *Puccinia triticina*

Inoculation was done with a non-specific mixture of *Puccinia triticina* spores produced on wheat without known resistance genes (INRES - Phytomedicine, University of Bonn). Before each experiment, fresh *P. triticina* spores were suspended in a solution of distilled water + Tween 20 (0.01% w/v; Merck-Schuchardt, Hohenbrunn, Germany). The spore concentration was estimated microscopically with a Fuchs-Rosenthal counting chamber and adjusted to 10 000 spores per millilitre. On each leaf, the middle of the leaf length was marked on the adaxial side with a felt tip pen, and seven 6 µl droplets of spore suspension were applied in a row on one leaf half. Prior to the application, leaves were fixed horizontally on a sample holder to prevent droplet run-off. During the inoculation period (22 h), plants were maintained in the climate chamber at almost saturated atmosphere ensured by a plastic cover. Thereafter, the plastic cover was removed and the leaves were released from their horizontal fixation. Plants of the groups without pathogen inoculation were handled similarly but treated with water droplets + Tween 20 (0.01% w/v). Fluorescence measurements were done on the central of the seven droplets. The development of disease spots was evaluated visually over the experimental period *in situ* and on digital photographs taken in parallel to the fluorescence readings.

2.3.2 Inoculation of *Blumeria graminis*

Similarly as described for the inoculation of leaf rust, the target leaves were selected and the middle of leaf length was marked with a felt tip pen. Marked leaves were horizontally fixed before inoculation with conidia of a non-specific mixture of *Blumeria graminis* f. sp. *tritici* produced on wheat without known resistance genes (INRES - Phytomedicine, University of Bonn). Stock plants inoculated with the pathogen ensured the supply of fresh conidia when needed. For inoculation of experimental plants, conidia were carefully removed

from the stock plants with a fine brush and directly applied on the leaf surface of the target plants. Application site (3 x 5 mm) was located at the leaf length middle in the centre of a leaf half. Twenty-two hours after inoculation (hai), visible conidia were removed by gently blowing and brushing over leaf surface. Leaves of the plant groups N+ and N- were handled in a similar way without conidia.

2.4 Fluorescence measurements

Fluorescence measurements were carried out using a compact fibre-optic fluorescence spectrometer with nanosecond time resolution and employing the boxcar technique (IOM GmbH, Berlin, Germany). A pulsed N_2-laser (MNL100, LTB Lasertechnik Berlin GmbH, Berlin, Germany) with an emission wavelength of 337 nm and a repetition rate of 20 Hz served as the excitation source. The fibre-optic probe for detection of fluorescence signals consisted of a central excitation fibre and six surrounding emission fibres, each with a 200 µm diameter. The pulse energy at the probe exit was adjusted to be in the range of 1.5-3.0 µJ with a pulse length of approximately 2.5 ns resulting in a density of 7.5-15 x 10^{15} photons per cm^2 and pulse. Fluorescence was recorded with an acousto-optic tunable filter (AOTF) monochromator, which enables a minimal step width of 1 nm. A photomultiplier (PMT; H5783-01, Hamamatsu, Hamamatsu City, Japan) was used as detector. The sensitivity of the PMT was adjusted in order to optimize the signal intensity during the spectral measurements. Time resolution was accomplished using a gated integrator with a 2 ns half-width; positioning of the gate allowed an accuracy of 0.1 nanoseconds.

Detection of fluorescence spectra was done on leaves fixed horizontally on a plate with integrated sample holder. The fibre-optic probe was positioned at a 90° angle to the leaf. By employing a laser-based rangefinder (OptoNCDT 1300, Micro-Epsilon Messtechnik GmbH & Co. KG, Ortenburg, Germany) fixed beside the probe, the distance between leaf and probe surface was adjusted to 3.95 mm at the point of measurement. The standard distance enabled fluorescence intensities in a narrow data range, providing a minimum of signal intensity and avoiding signal saturation. Spectra were measured at 21-23°C under ambient light conditions (about 18 µmol m^{-2} s^{-1} PAR) at two to four days after pathogen inoculation (dai) for leaf rust experiments, and 1 to 3 dai for powdery mildew experiments. Prior to fluorescence measurements plants were adapted for 0.5 h to room conditions. For optimization of fluorescence signals, equipment settings were adjusted as follows. Spectral analysis was accomplished at a wavelength interval of 2 nm between 370 and 800 nm with a

gate position of 5 nanoseconds (in the temporal signal maximum). Measurements were done with a pulse count of 32, which is the number of laser pulses averaged for each single data point. The PMT sensitivity was set to 600 Volt. Fluorescence peaks were determined at 451 nm (blue, B), 522 nm (green, G), 689 nm (red, R), and 737 nm (far-red, FR). In order to avoid a time-shift effect within the time-course of a single measuring day alternate measurements on inoculated and non-inoculated leaves were conducted.

2.5 Data processing and statistics

The measured UV-induced fluorescence spectra were processed by Gaussian curve fitting using the freeware Gnuplot, version 4.2 patchlevel 4 (http://www.gnuplot.info). Position, amplitudes as well as half-bandwidth (*hbw*) of peaks were determined to calculate the ratios between amplitudes, half-bandwidths, and amplitudes-to-half-bandwidths (*) for individual peaks. The processed experimental data were subjected to statistical analysis using the SPSS package (PASW statistics version 18.0, SPSS Inc., Chicago, USA). The relation between SPAD and chlorophyll content was established with a linear regression. For each day and evaluation group, the means were compared by One-way ANOVA ($p \leq 0.05$) and means separated with the Duncan's multiple range test. Graphs (Mean ± SD) were drawn with SigmaPlot 8.02 (Systat Software Inc., Richmond, CA, USA).

3 Results

3.1 Validation of N-deficiency

The chlorophyll content of plant treatments with N+ and N- was evaluated to give proof that the N- treatment group is under nitrogen deficiency even if visual symptoms were not evident. On basis of SPAD-values and chlorophyll extraction, a linear function expressed as Chl [µg g^{-1} FW] = 53.34 * SPAD – 248.024 (R^2 = 0.93) was established (Fig. 1). On average, leaf chlorophyll concentration of N+ plants was 2311 µg g^{-1} FW whereas the leaves of the N- treatment group had 1698 µg g^{-1} FW. Besides this significant difference, the visual assessment of N-deficiency leaves revealed no distinct stress symptoms (Fig. 2A).

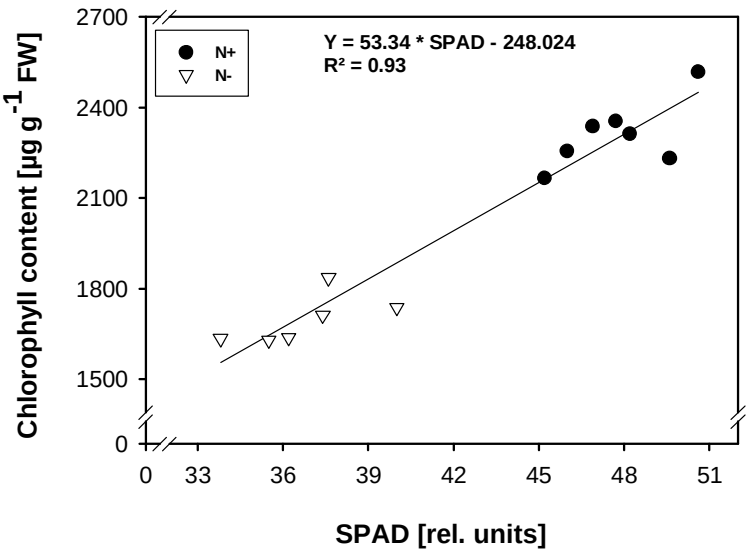

Fig. 1. Correlation between SPAD values and chlorophyll content of wheat leaves as affected by two levels of nitrogen supply ($n \geq 6$).

3.2 Combined nitrogen deficiency and leaf rust infection

Visual evaluations of leaf rust development indicated small and loom chlorotic spots 4 dai (days after inoculation) on the adaxial leaf lamina (Fig. 2B) in both nitrogen full supply (N+) and nitrogen deficient (N-) leaves. Two days later (6 dai), small red-brown pustules appeared on leaf surface and became larger and more distinct in the following days. After 8 dai disease symptoms were evident (Fig. 2B).

As shown in Table 1, several of the examined fluorescence ratios enable a reliable discrimination between healthy and inoculated leaves from 2 to 4 dai, irrespective of nitrogen fertilization. Thereby, amplitude ratios of B/R, B/FR, G/R and G/FR were significantly higher in inoculated than in non-inoculated leaves. Two days after inoculation, values for B/R were 2.98 and 3.01 for N+ and N-, and 3.53 and 3.37 for N+/LR and N-/LR, respectively (Table 1). In a similar trend, values of the G/R ratio were 0.77 and 0.80 for N+ and N- and 0.96 for both nitrogen variants inoculated with the leaf rust pathogen. In addition, the pathogen inoculation reduced the B/G_*hbw* and increased the G/FR_*hbw* and R/FR_*hbw* ratios (Table 1). Of all evaluated amplitude-to-half-bandwidth ratios, a clear difference between the treatment groups was registered for the FR* peak showing values of 923 (N+), 920 (N-), 796 (N+/LR) and 788 (N-/LR) at two days after inoculation (Table 1). As observed, the difference between healthy and inoculated leaves became slightly larger during 3 days of measurements as indicated by values of the amplitude ratio B/R (Table 1).

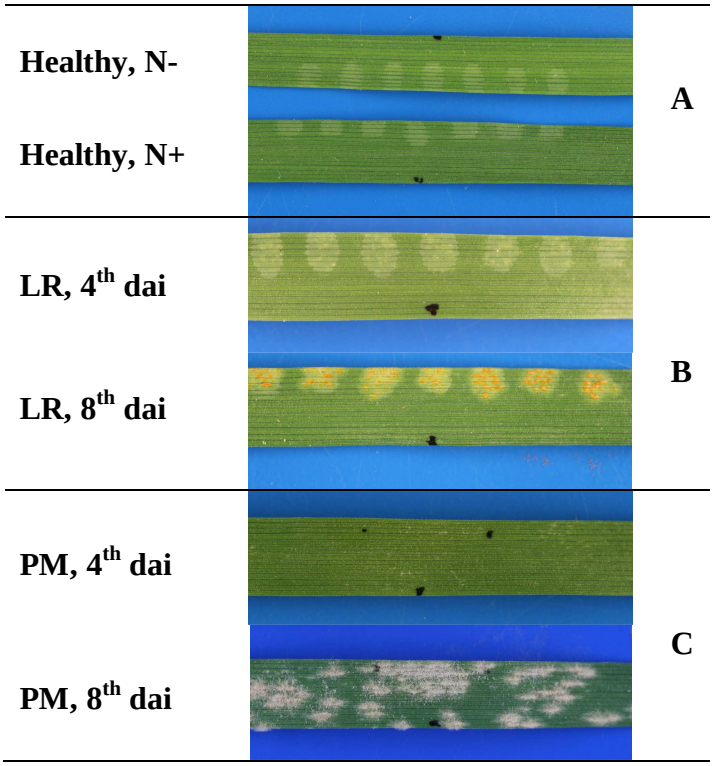

Fig. 2. Digital photographs of wheat leaves affected by abiotic or biotic stress factors: **A)** influence of nitrogen fertilization, N-full-supply (N+) and N-deficiency (N-); **B)** leaves infected by leaf rust, 4 and 8 days after inoculation (dai); **C)** infection of powdery mildew at 4 and 8 days after inoculation.

In order to distinguish between the four experimental groups, two fluorescence ratios could be considered as promising parameters. On all the three measuring days (2 to 4 dai) the amplitude ratio B/G was significantly different between the four groups (Fig. 3A). At the 2nd dai, leaves of N+ plants had highest values (3.89), followed by N- (3.75), N+/LR (3.68), and N-/LR (3.50) (Fig. 3A). In all treatments values decreased over time due to leaf senescence and at the 4th dai, one day before first visible symptoms appeared, ratios reached 3.64 for N+, 3.50 for N-, 2.93 for N+/LR and 2.77 for N-/LR (Fig. 3A). Consequently, the difference between N+ and N- as well as between N+/LR and N-/LR remained the same, but the difference between inoculated and non-inoculated leaves became larger. Measurements of the chlorophyll fluorescence in the R and FR peaks indicate slightly higher amplitude ratio R/FR in inoculated (N+/LR, 0.99; N-/LR, 1.04) than in non-inoculated (N+, 0.94; N-, 0.96) leaves two days after inoculation (Fig. 3B). In the time-course development values for N+ and N- remained almost constant while for the inoculated leaves showed a strong increase (Fig. 3B).

Table 1. Influence of nitrogen supply (N+, full supply; N-, 40% of full supply) and leaf rust (LR) inoculation on selected fluorescence ratios, determined from 2 to 4 days after inoculation (dai).

Fluorescence ratio	Experimental group	2 dai	3 dai	4 dai
B/R	N+	2.98 a	2.55 a	2.24 a
	N+/LR	3.53 b	3.09 b	2.91 b
	N-	3.01 a	2.55 a	2.29 a
	N-/LR	3.37 b	3.04 b	3.00 b
B/FR	N+	2.81 a	2.34 a	2.06 a
	N+/LR	3.50 b	3.22 b	3.38 b
	N-	2.90 a	2.44 a	2.20 a
	N-/LR	3.49 b	3.37 b	3.80 b
G/R	N+	0.77 a	0.68 a	0.62 a
	N+/LR	0.96 b	0.93 b	1.00 b
	N-	0.80 a	0.71 a	0.65 a
	N-/LR	0.96 b	0.97 b	1.09 b
G/FR	N+	0.72 a	0.62 a	0.57 a
	N+/LR	0.95 b	0.97 b	1.17 b
	N-	0.77 a	0.67 a	0.63 a
	N-/LR	1.00 b	1.07 b	1.39 b
B/G_*hbw*	N+	1.07 b	1.06 b	1.05 b
	N+/LR	1.06 a	1.03 a	1.01 a
	N-	1.08 b	1.06 b	1.06 b
	N-/LR	1.06 a	1.03 a	1.01 a
G/FR_*hbw*	N+	1.52 a	1.52 a	1.53 a
	N+/LR	1.55 b	1.58 b	1.59 b
	N-	1.51 a	1.52 a	1.52 a
	N-/LR	1.54 b	1.56 b	1.58 b
R/FR_*hbw*	N+	0.79 a	0.78 a	0.78 a
	N+/LR	0.80 b	0.79 b	0.79 b
	N-	0.79 a	0.79 a	0.78 a
	N-/LR	0.79 b	0.79 b	0.79 b
FR*	N+	923 b	956 b	975 b
	N+/LR	796 a	784 a	739 a
	N-	920 b	933 b	941 b
	N-/LR	788 a	753 a	694 a

Means of the fluorescence parameters for each evaluation day followed by the same letter do not differ significantly according to Duncan's multiple range test ($p \leq 0.05$; $n = 12$ for N+ and N-; $n = 16$ for N+/LR and N-/LR). *hbw* = half-bandwidth, * = amplitude-to-half-bandwidth ratio.

3.3 Combined nitrogen deficiency and powdery mildew infection

Visual evaluations of the powdery mildew development revealed first small patches of whitish mycelium on leaf surface at four days after inoculation (Fig. 2C). During the following days the patches increased in size, and further new mycelium was formed. As the results of fluorescence measurements show, irrespective of nitrogen level only a small number of the evaluated fluorescence ratios are suited to discriminate between healthy and inoculated leaves (Table 2). During the 3 day period of measurements the half-bandwidth ratios B/G, G/R and G/FR revealed constant differences between inoculated and non-inoculated leaves. As shown for the B/G_*hbw* at 1 dai, powdery mildew lowered the ratio to 1.00 (N+/PM) and 0.99 (N-/PM) as compared to 1.07 in the non-inoculated leaves (Table 2). In contrast, ratios of G/R_*hbw* and G/FR_*hbw* were higher in *B. graminis* inoculated leaves as compared to non-inoculated leaves. The G/R_*hbw* ratio for N+ and N- leaves at 1 dai were of 1.95 and 1.94 respectively, contrasting to 2.08 and 2.09 in the inoculated leaves (Table 2). During the following two days the difference between healthy and inoculated leaves became larger and one day ahead of first visible infection symptoms (3 dai) the G/R_*hbw* ratio raised to 1.97 for both N+ and N-, 2.19 for N+/PM and 2.16 for N-/PM (Table 2).

Table 2. Impact of nitrogen supply (N+, full supply; N-, 40% of full supply) and powdery mildew (PM) inoculation on selected fluorescence half-bandwidth ratios, determined from 1 to 3 days after inoculation (dai).

Fluorescence ratio	Experimental group	1 dai	2 dai	3 dai
B/G_*hbw*	N+	1.07 b	1.06 b	1.05 b
	N+/PM	1.00 a	0.95 a	0.94 a
	N-	1.07 b	1.05 b	1.04 b
	N-/PM	0.99 a	0.96 a	0.94 a
G/R_*hbw*	N+	1.95 a	1.97 a	1.97 a
	N+/PM	2.08 b	2.16 b	2.19 b
	N-	1.94 a	1.97 a	1.97 a
	N-/PM	2.09 b	2.14 b	2.16 b
G/FR_*hbw*	N+	1.51 a	1.52 a	1.52 a
	N+/PM	1.60 b	1.68 b	1.70 b
	N-	1.51 a	1.52 a	1.53 a
	N-/PM	1.61 b	1.67 b	1.69 b

Means of the fluorescence ratios for each evaluation day followed by the same letter do not differ significantly according to Duncan's multiple range test ($p \leq 0.05$; $n = 12$ for N+ and N-; $n = 16$ for N+/LR and N-/LR). *hbw* = half-bandwidth.

Figures 3C and 3D display the time-course development of the B/G and R/FR amplitude ratios of the four experimental groups (N+, N-, N+/PM, N-/PM). During the whole evaluated period, plants supplied with adequate nitrogen showed the highest values of the B/G ratio, followed by the N- group, N+/PM, and finally N-/PM. On the first measuring day (1 dai) amplitude ratios of B/G for N+ and N- were of 3.73 and 3.55 respectively, whereas N+/PM and N-/PM leaves indicated significantly lower values of 3.19 and 3.06, respectively (Fig. 3C). During the following two days values decreased in all experimental groups but the difference between inoculated and non-inoculated leaves remained almost constant. On the last evaluation day (3 dai) values on N+ and N- were 3.48 and 3.31 and for inoculated ones N+/PM and N-/PM 2.76 and 2.66, respectively (Fig. 3D).

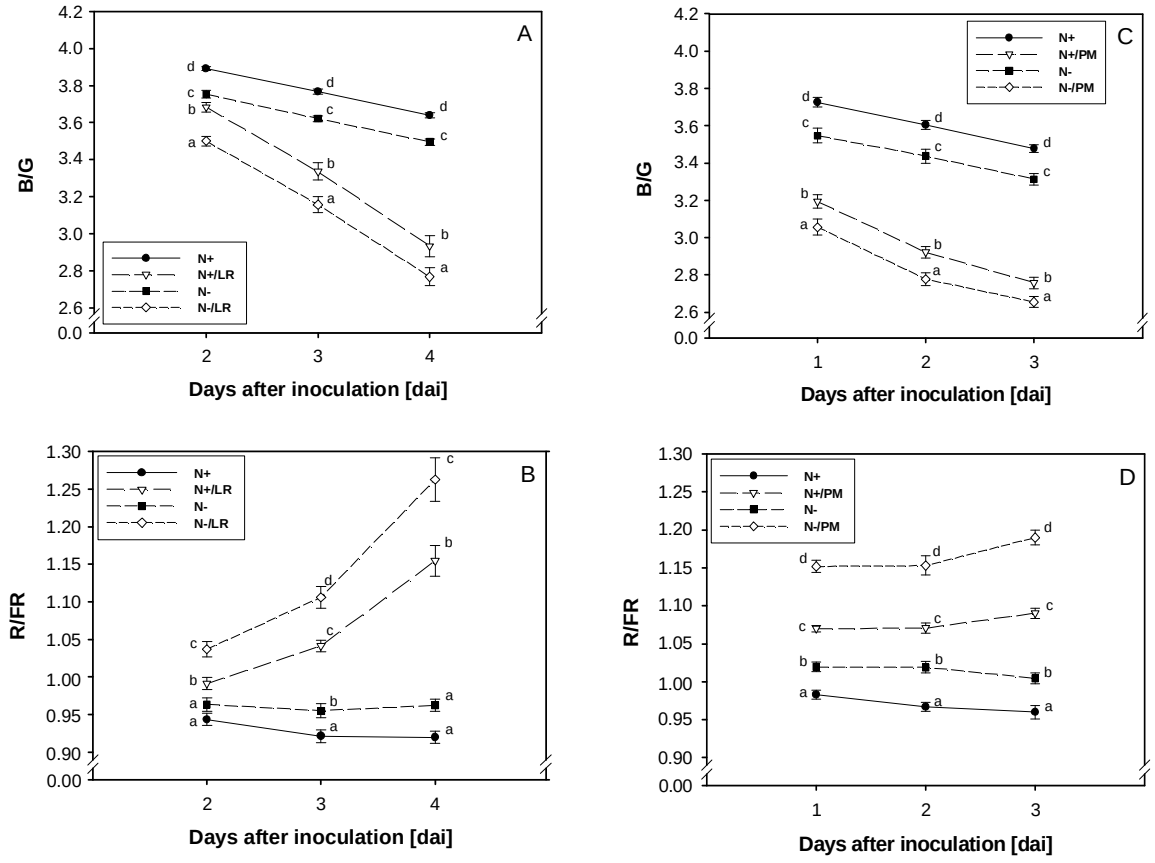

Fig. 3. Influence of nitrogen supply (N+, full supply; N-, 40% of full supply) and disease development on the ratios of fluorescence amplitudes B/G and R/FR. **A-B)** leaf rust (LR) infection measured from 2 to 4 days after inoculation (dai; left); **C-D)** powdery mildew (PM) infection, measured from 1 to 3 days after inoculation (dai; right). Means (± SD) of the experimental groups (within each evaluation day) followed by the same letter do not differ statistically according to Duncan's multiple range test ($p \leq 0.05$; $n = 12$ for N+ and N-; $n = 16$ for the other treatment groups).

Similarly, values of the ratio R/FR on healthy leaves remained on a comparable level whereas infected leaves showed a significant increase. Already at 1 dai significant differences between treatment groups were noticed, and values were of 0.98 and 1.02 for N+ and N-, and 1.07 and 1.15 for N+/PM and N-/PM (Fig. 3D). At 3 dai values for N+ and N- were still at 0.96 and 1.00, whereas the groups N+/PM and N-/PM indicated ratios of 1.09 and 1.19, respectively (Fig. 3D).

4 Discussion

The objective of the current study was to evaluate the feasibility of the spectral resolved fluorescence for detection of a simultaneous occurrence of slight N deficiency and pathogen infection at a pre-symptomatic stage. Based on the fluorescence peaks in the blue, green, red and far-red regions, ratios of amplitudes, half-bandwidths, and amplitude-to-half-bandwidths were established. The outcome is that a large number of fluorescence ratios might be considered for detection and differentiation between the stressors. Besides the early detection of leaf rust and powdery mildew infection and slight nitrogen deficiency by means of chlorophyll fluorescence, the amplitude ratio R/FR is also suited for detection of both factors occuring simultaneously on the same leaves. Moreover, the blue-green fluorescence amplitude ratio (B/G) shows the more precise results when distinguishing between the four experimental groups N+, N-, N+/pathogen, and N-/pathogen. As observed in both pathosystems, leaf rust and powdery mildew, the difference between values of the healthy and inoculated plants became larger in the time-course of the infection development.

It is well known that wheat plants grown under reduced N-supply exhibit lower chlorophyll levels as compared to plants grown under full N-supply (Cartelat *et al*. 2005). Our results reveal a reduction of chlorophyll content (Fig. 1) and an associated increase of the R/FR fluorescence ratio (Fig. 3), which is an inverse indicator of the chlorophyll content (Buschmann 2007). Thereby, a high and negative correlation coefficient (r^2 = -0.86) between the chlorophyll content and the amplitude ratio R/FR was established (*data not shown*). Moreover, our analyses show a high and positive correlation coefficient (r^2 = 0.90) between the chlorophyll content and the B/G amplitude ratio (*data not shown*). Lichtenthaler *et al*. (1996) associated a decrease in the F440/F520 ratio with the change of chlorophyll content per leaf area whereas the increase of blue fluorescence with decreasing chlorophyll and carotenoid content was discussed in terms of reduced re-absorption effects.

Experiments with barley and wheat grown under N-deficiency revealed close relations between the accumulation of phenolic metabolites as well as changes of chlorophyll content, and modifications in UV-induced fluorescence signature (Cartelat *et al.* 2005; Mercure *et al.* 2004). As consequence of lower N-supply in barley, the amount of total soluble phenolic compounds and the blue-green fluorescence increased (Mercure *et al*. 2004). In our study, the B/G fluorescence amplitude ratio decreased with less N-supply (Fig. 3). This is in accordance with Bélanger *et al*. (2006), who pointed out that the ratio F440/F520 revealed differences between potato plants fertilized with several nitrogen levels. In our study, the decrease of B/G values for plants grown under N-deficient conditions is explained by a combination of small increase in blue fluorescence (2-3%) and a more pronounced increase in green fluorescence (6-7%) (*data not shown*).

General associations of the relationship between nitrogen status and fungal infection consider that higher N-supply increases the susceptibility of cereals to pathogens such as mildew and rusts (Walters and Bingham 2007). Alternatively, low nitrogen levels were associated with higher amounts of phenols and reduced disease intensity (Cartelat *et al*. 2005) as phenols are known to play an important role in disease resistance (e.g. Herms and Mattson 1992; Nicholson and Hammerschmidt 1992; Vermerris and Nicholson 2006). Besides, the synthesis and accumulation of such compounds depends on the time scale. As shown, slightly increased levels of bound and unbound hydroxycinnamic acid due to powdery mildew infection under low and medium N-supply were measured already 20 h after inoculation (Sander and Heitefuss 1998). In the present studies with leaf rust and powdery mildew, the differences in the amplitude ratio B/G between healthy and infected leaves became larger when infection was further developed (Fig. 3). Nevertheless, the difference between N-/pathogen and N+/pathogen leaves remained at the same level. As observed in our studies, absolute intensities of rust infected leaves increased on average from 4% (dai 2) to 23% (dai 4) for the blue and from 11% (dai 2) to 55% (dai 4) for the green fluorescence as compared to the non-inoculated tissue, irrespective of nitrogen supply (*data not shown*).

Alternatively, re-absorption effects of blue fluorescence light by chlorophyll (Lang *et al*. 1991), as well as a possible shielding effect of the excitation light by phenolics located in the epidermis (Chaerle and Van Der Straeten 2000) should be considered. The observed increase of the amplitude ratio R/FR in our experiments (Fig. 3) indicates a decrease in chlorophyll content in plants inoculated with leaf rust or powdery mildew (Buschmann 2007), which is in accordance with Lorentzen and Jensen (1989) and Owera *et al.* (1981).

As reported by several authors (Heisel *et al*. 1996; McMurtrey III *et al*. 1994; Mercure *et al*. 2004), of several computed fluorescence ratios the F440/F685, F440/F740, F525/F685 and F740/F685 revealed differences between maize plants fertilized with 100% or with 75% or less nitrogen. Thereby, the ratios F440/F690 and F440/F740 indicated to be more sensitive to nutrient deficiencies than the F690/F740 ratio (Heisel *et al*. 1996; Lichtenthaler *et al*. 1997). Our results did not confirm this for plants grown under N-deficiency for a comparatively very short period. These fluorescence parameters seem to be more suited to reveal early pathogen infection irrespective of the nitrogen status of the plants, as proven for amplitude and half-bandwidth ratios in the leaf rust experiment (Table 1), and for half-bandwidth ratios in the powdery mildew trials (Table 2). Thereby, in the experiment with leaf rust, especially the amplitude ratios G/R and G/FR as well as the FR* amplitude-to-half-bandwidth ratio revealed a strong effect of pathogen infection during two to four days after inoculation (Table 2). Nevertheless, changes in these ratios in response to nitrogen deficiency are expected under progressed and more pronounced limitations as compared to the slight deficiency conditions in our experiment.

Comparing both leaf rust and powdery mildew pathosystems, the difference between infected and healthy leaves for the parameters B/G and R/FR amplitude ratio were smaller for leaf rust than powdery mildew (Fig. 3). In addition, the time-course development of the fluorescence signals was more pronounced for leaf rust. Nevertheless, both fluorescence parameters enable a differentiation among the experimental groups N+, N-, N+/LR or PM, and N-/LR or PM. Proceeding, improved statistics and raw data analysis under consideration of classification algorithms such as Decision Trees, Naive Bayes, Artificial Neural Networks, Logistic Regression and Support Vector Machines (SVMs) might render a more precise classification. Preliminary results indicate that SVMs yield a precise discrimination of healthy and infected leaves (Römer *et al*. 2010). Ongoing studies will clarify if such data evaluation tools can support and improve a robust differentiation between simultaneous occurring of biotic and abiotic stresses.

5 Conclusions

The fluorescence signature measured between 370 and 800 nm is a useful tool when addressing the challenge of discrimination between biotic and abiotic stress factors. The focus on blue-green fluorescence yields important additional information for a more precise discrimination as compared to previous approaches with chlorophyll fluorescence. The

amplitude ratio B/G as well as R/FR revealed to be well suited to distinguish among N–full-supply, N-deficiency, N-full-supply + pathogen, and N-deficiency + pathogen. Besides, several fluorescence ratios enabled an early detection of leaf rust or powdery mildew infection irrespective of the plants' nitrogen status.

6 References

Bélanger M-C, Viau A, Samson G, Chamberland M (2006) Near-field fluorescence measurements for nutrient deficiencies detection on potatoes (*Solanum tuberosum* L.): effects of the angle of view. International Journal of Remote Sensing 27:4181-4198

Blanke MM (1992) Determination of chlorophyll using DMSO. Wein-Wissenschaft 47:32-35

Bodria L, Fiala M, Oberti R, Naldi E (2002) Chlorophyll fluorescence sensing for early detection of crop´s diseases symptoms. In: Proceedings ASAE Annual International Meeting and CIGR XVth World Congress, 2002, (pp. 1-15). St. Joseph, Michigan: American Society of Agricultural and Biological Engineers

Bravo C, Moshou D, West J, McCartney A, Ramon H (2003) Early disease detection in wheat fields using spectral reflectance. Biosystems Engineering 84:137-145

Bredemeier C, Schmidhalter U, Stafford J, Werner A (2003) Non-contacting chlorophyll fluorescence sensing for site-specific nitrogen fertilization in wheat and maize. In: Precision Agriculture, Stafford JV and Werner A (Eds.). Wageningen: Wageningen Academic Publishers, 103-108

Brown P, Graham R, Nicholas D (1984) The effects of managanese and nitrate supply on the levels of phenolics and lignin in young wheat plants. Plant and Soil 81:437-440

Buschmann C (2007) Variability and application of the chlorophyll fluorescence emission ratio red/far-red of leaves. Photosynthesis Research 92:261-271

Buschmann C, Langsdorf G, Lichtenthaler HK (2009) Fluorescence: the blue, green, red and far-red fluorescence signatures of plant tissues, their multicolour fluorescence imaging and application for agrofood assessment. In: Optical monitoring of fresh and processed agricultural crops, Zude M (Ed.). Boca Raton: CRS Press, Taylor & Francis Group, 272-319

Cartelat A, Cerovic ZG, Goulas Y, Meyer S, Lelarge C, Prioul J, Barbottin A, Jeuffroy M, Gate P, Agati G (2005) Optically assessed contents of leaf polyphenolics and chlorophyll as indicators of nitrogen deficiency in wheat (*Triticum aestivum* L.). Field Crops Research 91:35-49

Cerovic ZG, Samson G, Morales F, Tremblay N, Moya I (1999) Ultraviolet-induced fluorescence for plant monitoring: present state and prospects. Agronomie 19:543-578

Chaerle L, Hagenbeek D, Vanrobaeys X, Van der Straeten D (2007a) Early detection of nutrient and biotic stress in *Phaseolus vulgaris*. International Journal of Remote Sensing 28:3479-3492

Chaerle L, Lenk S, Hagenbeek D, Buschmann C, Van Der Straeten D (2007b) Multicolour fluorescence imaging for early detection of the hypersensitive reaction to tobacco mosaic virus. Journal of Plant Physiology 164:253-262

Chaerle L and Van Der Straeten D (2000) Imaging techniques and the early detection of plant stress. Trends in Plant Science 5:495-501

Ciompi S, Gentili E, Guidi L, Soldatini GF (1996) The effect of nitrogen deficiency on leaf gas exchange and chlorophyll fluorescence parameters in sunflower. Plant Science 118:177-184

Franke J and Menz G (2007) Multi-temporal wheat disease detection by multi-spectral remote sensing. Precision Agriculture 8:161-172

German Federal Plant Variety Office [Bundessortenamt] (2008) Beschreibende Sortenliste – Getreide, Mais, Ölfrüchte, Leguminosen und Hackfrüchte außer Kartoffeln. Hannover: Deutscher Landwirtschaftsverlag GmbH

Heisel F, Sowinska M, Miehé JA, Lang M, Lichtenthler HK (1996) Detection of nutrient deficiencies of maize by laser induced fluorescence imaging. Journal of Plant Physiology 148:622-631

Herms D and Mattson W (1992) The dilemma of plants: to grow or defend. The Quarterly Review of Biology 67:283–335

Kuckenberg J, Tartachnyk I, Noga G (2009a) Temporal and spatial changes of chlorophyll fluorescence as a basis for early and precise detection of leaf rust and powdery mildew infections in wheat leaves. Precision Agriculture 10:34-44

Kuckenberg J, Tartachnyk I, Noga G (2009b) Detection and differentiation of nitrogen-deficiency, powdery mildew and leaf rust at wheat leaf and canopy level by laser-induced chlorophyll fluorescence. Biosystems Engineering 103:121-128

Lang M, Stober F, Lichtenthaler HK (1991) Fluorescence emission spectra of plant leaves and plant constituents. Radiation and Environmental Biophysics 30:333-347

Lenk S, Chaerle L, Pfündel EE, Langsdorf G, Hagenbeek D, Lichtenthaler HK, Van Der Straeten D, Buschmann C (2007) Multispectral fluorescence and reflectance imaging at the leaf level and its possible applications. Journal of Experimental Botany 58:807-

814

Lichtenthaler HK (1996) Vegetation stress: an introduction to the stress concept in plants. Journal of Plant Physiology 148:4-14

Lichtenthaler HK and Miehé JA (1997) Fluorescence imaging as a diagnostic tool for plant stress. Trends in Plant Science 2:316-320

Lichtenthaler HK, Subhash N, Wenzel O, Miehé JA (1997) Laser-induced imaging of blue/red and blue/far-red fluorescence ratios, F440/F690 and F440/F740, as a means of early stress detection in plants. Geoscience and Remote Sensing, 1997. IGARSS '97. Remote Sensing - A Scientific Vision for Sustainable Development, 1997 IEEE International 4:1799-1801

Lindenthal M, Steiner U, Dehne H-W, Oerke E-C (2005) Effect of downy mildew development on transpiration of cucumber leaves visualized by digital infrared thermography. Phytopathology 95:233-240

Lorentzen B and Jensen A (1989) Changes in leaf spectral properties induced in barley by cereal powdery mildew. Remote Sensing of Environment 27:201-209

Marschner H (2002) Mineral nutrition of plants. London, San Diego (California): Elsevier Academic Press, 889 pp.

McMurtrey III J, Chappelle E, Kim M, Meisinger J (1994) Distinguishing nitrogen fertilization levels in field corn (*Zea mays* L.) with actively induced fluorescence and passive reflectance measurements. Remote Sensing of Environment 47:36-44

Mercure S, Daoust B, Samson G (2004) Causal relationship between growth inhibition, accumulation of phenolic metabolites, and changes of UV-induced fluorescences in nitrogen-deficient barley plants. Botany 82:815-821

Nicholson R and Hammerschmidt R (1992) Phenolic compounds and their role in disease resistance. Annual Review of Phytopathology 30:369-389

Oerke E-C and Dehne H-W (2004) Safeguarding production-losses in major crops and the role of crop protection. Crop Protection 23:275-285

Owera S, Farrar J, Whitbread R (1981) Growth and photosynthesis in barley infected with brown rust. Physiological Plant Pathology 18:79-90

Römer C, Bürling K, Rumpf T, Hunsche M, Noga G, Plümer L (2010) Early identification of leaf rust on wheat leaves with robust fitting of hyperspectral signatures. In: Proceedings of the 10th International Conference on Precision Agriculture. Denver, USA

Sander J and Heitefuss R (1998) Suceptibility to *Erysiphe graminis* f. sp *tritici* and phenolic

acid content of wheat as influenced by different levels of nitrogen fertilization. Journal of Phytopathology 146:495-507

Schächtl J, Huber G, Maidl F, Sticksel E, Schulz J, Haschberger P (2005) Laser-induced chlorophyll fluorescence measurements for detecting the nitrogen status of wheat (*Triticum aestivum* L.) canopies. Precision Agriculture 6:143-156

Subhash N and Mohanan C (1994) Laser-induced red chlorophyll fluorescence signatures as nutrient stress indicator in rice plants. Remote Sensing of Environment 47:45-50

Tartachnyk I and Rademacher I (2003) Estimation of nitrogen deficiency of sugar beet and wheat using parameters of laser induced and pulse amplitude modulated chlorophyll fluorescence. Journal of Applied Botany 77:61-67

Tartachnyk I, Rademacher I, Kühbauch W (2006) Distinguishing nitrogen deficiency and fungal infection of winter wheat by laser-induced fluorescence. Precision Agriculture 7:281-293

Vermerris W and Nicholson R (2006) The role of phenols in plant defence. In: Phenolic compound biochemistry, Vermerris W and Nicholson R (Eds.). Dordrecht: Springer, 222-234

Walters DR and Bingham IJ (2007) Influence of nutrition on disease development caused by fungal pathogens: implications for plant disease control. Annals of Applied Biology 151:307–324

F Summary and Conclusion

The key objective of the present thesis was to early assess physiological modifications of wheat plants due to biotic and abiotic stresses by means of non-destructive fluorescence measurement techniques. Thereby the focus was the physiological response of the plant rather than development of sensors for field applications; experiments were conducted under laboratory conditions and examinations done at leaf level. Two biotrophic fungi, *Puccinia triticina* and *Blumeria graminis*, which are of economical importance in wheat production, as well as nitrogen deficiency as the most significant factor in terms of nutrient management, were selected for representative studies. The first chapter addressed the hypothesiz that the PAM-fluorescence imaging technique enables a discrimination of susceptible and resistant wheat (*Triticum aestivum* L.) cultivars to the leaf rust pathogen *Puccinia triticina*. In these studies two inoculation methods under consideration of the spore density were tested in order to evaluate the response of susceptible and resistant genotypes on the basis of fluorescence readings. Furthermore, the masking effect of fungal inoculum on chlorophyll fluorescence parameters was assessed. With the same purpose, differentiation of susceptible and resistant cultivars, the UV-induced fluorescence spectra between 350 and 820 nm and the lifetime of fluorophores at selected wavelengths were examined. Similar studies aiming at the early detection and differentiation of genotypes having distinct resistance degrees to powdery mildew (*Blumeria graminis*) were conducted. In a last step, the challenge of the differentiation between stresses caused by pathogen infection (*Puccinia triticina* or *Blumeria graminis*) and N-deficiency occurring simultaneously was highlighted by UV-induced fluorescence spectral measurements. The results obtained and outlined in the single chapters can be summarized as follows:

1. Experiments with the PAM-imaging system showed that amongst the evaluated chlorophyll fluorescence parameters, the quantum yield of non-regulated energy dissipation in PSII (Y(NO)) is the most promising parameter for screening wheat plants for leaf rust resistance. Measurements revealed a stronger pathogen-triggered increase of the Y(NO) values in the susceptible cultivar Dekan than in the resistant cultivar Retro. Thereby, the most appropriate time for a reliable differentiation between was two days after inoculation, when changes in leaf optical properties are negligible and differences between inoculated and control leaves are large. Preliminary experiments with spore densities of up to 20 000 spores per ml in case of

fast fluorescence kinetic parameters, and up to 100 000 spores per ml in case of slow fluorescence kinetic parameters, revealed that changes in the fluorescence signals were not related to physical masking.

2. The assessment of fluorescence lifetime and UV-induced spectra were adopted for the detection of leaf rust (*Puccinia triticina*) in resistant wheat cultivars Esket, Mirage, and Retro in comparison to the susceptible cultivars Dekan, Ritmo, Skalmeje, and Aron. A combination of spectral and lifetime characteristics revealed pre-symptomatic alterations of fluorescence indicating changes in the content of chlorophyll and secondary metabolites. Thereby, the determination of the B/G amplitude ratio seemed to be the most appropriate parameter for early detection of fungal infection, whereupon it decreased in inoculated compared to control leaves. Furthermore, discrimination between resistant and susceptible cultivars to the leaf rust pathogen might be feasible by monitoring the amplitude ratio of B/R fluorescence at three days after inoculation. As additional parameters, mean lifetime at 440 nm, 500 nm and 530 nm should be considered; for these parameters the difference between control and inoculated leaves was significantly more pronounced in the resistant cultivars.

3. UV-induced spectral signature as well as mean fluorescence lifetime are suitable approaches for sensing powdery mildew (*Blumeria graminis*) as early as one day after inoculation. The decreased amplitude ratio B/G as well as the increased G/R and G/FR half-bandwidth ratios in inoculated as compared to control leaves, were appropriate parameters to detect fungal development. In addition, the increased mean lifetime in inoculated leaves in the wavelength range of 500-620 nm may enable a distinction between healthy and diseased leaves. Additional experiments revealed increased mean lifetime of the green fluorescence as early as ten to twelve hours after the first host-pathogen interaction.

4. Fluorescence intensity measured between 370 and 800 nm provided to be a useful tool to address the challenge of discrimination between nitrogen deficiency and fungal diseases. Precisely, the amplitude ratio R/FR was suited for early detection, and gives a basis for discrimination between N-full-supply, N-deficiency, N-full-supply + pathogen and N-deficiency + pathogen. In addition, the blue-green fluorescence yielded important information targeting a possible discrimination between the

evaluated multiple stress factors. Besides, several more fluorescence amplitude ratios and half-bandwidth ratios for leaf rust as well as half-bandwidth ratios for powdery mildew were found to be applicable for early detection of both leaf rust and powdery mildew infection, irrespective of the nitrogen status of the plants.

In summary, the results obtained in our studies indicate the potential of fluorescence techniques for sensing biotic and abiotic stresses in *Triticum aestivum* L. In addition, specific parameters could be identified for evaluations of the sensitivity of genotypes to leaf rust and powdery mildew. Nevertheless, in order to establish an accurate and reliable evaluation protocol, a higher number of cultivars with distinct resistance degrees should be investigated. Thereby, a future goal should be to establish a scale as basis for differentiation among genotypes with different levels of resistance or susceptibility. Ideally, such a system should work independently of being in need for measuring control plants as reference. Moreover, changes in the chemical composition of infected leaves should be correlated with the non-invasive signals and would support the interpretation of the modified fluorescence ratios, especially in the blue-green spectral range. Proceeding, improved statistics and raw data analysis would support an even more precise classification. With future perspectives, new mathematical algorithms and further developments in sensor technology could enable fast and robust determination of complex fluorescence parameters to be implemented in screening systems with a high throughput.

Acknowledgement

I wish to express my gratitude to Prof. Dr. G. Noga for giving me the chance to work on this interesting topic and for integrating me in his research group. Moreover, many thanks for his support and guidance during my studies and for supporting my research trip to the 'Equipe Biospectroscopie Végétale (CNRS)' of Dr. Zoran G. Cerovic, 'Département Ecophysiologie Végétale, Laboratoire Ecologie Systématique Evolution', at the 'Université Paris-Sud 11' in Orsay, France.

I am very grateful to PD Dr. E.-C. Oerke for his willingness to act as my co-referee and for his outstanding efforts and contributions as speaker of the DFG research training group 722.

Special thanks to PD Dr. U. Rascher for his willingness to act as my third referee.

I am greatly thankful to my colleague Dr. M. Hunsche for his willingness to act as my instructor and for the close and friendly collaboration. Furthermore, I thank him for his continuous and highly competent assistance during the preparation of this thesis.

Many thanks to Dr. L. Pfeifer, IOM Co., for his advice on the laserfluoroscope measurements, and for critically reviewing the chapter on fluorescence theory.

The continuous interest and readiness for in-depth discussions of PD Dr. Claus Buschmann, Karlsruhe Institute of Technology, was always highly appreciated.

I thank all the staff members of the Department of Horticulture and the Department of Phytomedicine of the University of Bonn for their cooperation and help in conducting the experiments.

Finally, I would like to thank my family and my friend Lothar for their continuous support and encouragement.

Last but not least, these studies would not have been possible without the generous financial support of the German Research Foundation (DFG-Graduiertenkolleg 722), which is highly acknowledged.